Meteoritics & Planetary Science 37, 1451–1490 (2002)
Available online at http://www.uark.edu/meteor

Invited Review

The CR chondrite clan: Implications for early solar system processes

ALEXANDER N. KROT[1]*, ANDERS MEIBOM[2], MICHAEL K. WEISBERG[3,4] AND KLAUS KEIL[1]

[1]Hawai'i Institute of Geophysics and Planetology, School of Ocean and Earth Science and Technology, University of Hawai'i at Manoa, Honolulu, Hawai'i 96822, USA
[2]Geological and Environmental Sciences, 320 Lomita Mall, Stanford University, California 94305-2115, USA
[3]Department of Physical Sciences, Kingsborough College of the City University of New York, Brooklyn, New York 11235, USA
[4]Department of Earth and Planetary Sciences, American Museum of Natural History, New York, New York 10024, USA
*Correspondence author's e-mail address: sasha@higp.hawaii.edu

(Received 2002 January 9; accepted in revised form 2002 July 22)

Abstract–In this paper, we review the mineralogy and chemistry of calcium-aluminum-rich inclusions (CAIs), chondrules, FeNi-metal, and fine-grained materials of the CR chondrite clan, including CR, CH, and the metal-rich CB chondrites Queen Alexandra Range 94411, Hammadah al Hamra 237, Bencubbin, Gujba, and Weatherford. The members of the CR chondrite clan are among the most pristine early solar system materials, which largely escaped thermal processing in an asteroidal setting (Bencubbin, Weatherford, and Gujba may be exceptions) and provide important constraints on the solar nebula models. These constraints include (1) multiplicity of CAI formation; (2) formation of CAIs and chondrules in spatially separated nebular regions; (3) formation of CAIs in gaseous reservoir(s) having ^{16}O-rich isotopic compositions; chondrules appear to have formed in the presence of ^{16}O-poor nebular gas; (4) isolation of CAIs and chondrules from nebular gas at various ambient temperatures; (5) heterogeneous distribution of ^{26}Al in the solar nebula; and (6) absence of matrix material in the regions of CAI and chondrule formation.

TABLE OF CONTENTS

Prelude preprint MS#4722

INTRODUCTION

Chondritic meteorites (chondrites) are the most ancient rocks formed in our solar system, providing unique opportunities to constrain physical and chemical processes that were active in the accretionary disk (solar nebula) surrounding the nascent Sun ~4.57 Ga ago. Chondrites are mixtures of four components including: calcium-aluminum-rich inclusions (CAIs), chondrules, FeNi-metal, and fine-grained matrix material. A primary goal of the chondrite studies is to understand the evolution of the solar nebula and the accretion of asteroids and planets.

In this paper, we review the mineralogy, petrography and isotopic properties of CAIs, chondrules, FeNi-metal, and fine-grained materials of the CR chondrite clan, including CR chondrites, CH chondrites, and the metal-rich CB chondrites Queen Alexandra Range (QUE) 94411, Hammadah al Hamra (HH) 237, Bencubbin, Gujba, and Weatherford. We infer (1) that the members of the CR chondrite clan are among the most pristine early solar system materials, which largely escaped thermal processing in an asteroidal setting (Bencubbin, Weatherford, and Gujba may be exceptions). (2) Many CR clan chondritic components preserve nebular records of their formation essentially unchanged and provide important constraints on the solar nebula models.

The outline of the paper is as follows. We introduce the different members of the CR clan and describe their bulk mineralogical, petrographic, and chemical properties. The mineralogical, petrographic, and isotopic properties of the individual chondritic components are described in separate sections, which are divided into subsections on CR chondrites, CH chondrites, Bencubbin/Gujba/Weatherford (CB_a) and QUE 94411/HH 237 (CB_b) meteorites. Sections on CAIs and chondrules + FeNi-metal end with a summary of the most significant observations and a brief discussion of their implications for the solar nebula models. In the final discussion, we summarize the major constraints on the solar nebula models from the CR clan chondritic components.

PETROGRAPHY, MINERALOGY, AND BULK CHEMISTRY OF THE CR CHONDRITE CLAN

The CR clan was established by Weisberg *et al.* (1995) and includes five kinds of carbonaceous chondrites: (1) **c**arbonaceous **R**enazzo-like (CR) group, (2) **c**arbonaceous **h**igh-metal (CH) group, (3) **c**arbonaceous **B**encubbin-like, subgroup **a** (CB_a) meteorites (*i.e.*, Bencubbin, Gujba, and Weatherford), (4) **c**arbonaceous **B**encubbin-like, subgroup **b** (CB_b) meteorites (*i.e.*, HH 237 and QUE 94411 paired with QUE 94627), and (5) Lewis Cliff (LEW) 85332 (Table 1). Conventionally a chondrite group is defined as a minimum of five unpaired chondrites having similar mineralogy, petrography, bulk isotopic properties, and bulk chemical compositions in major, non-volatile elements. The term "clan" is a higher order of

TABLE 1. List of meteorites in the CR clan.

CR group	CH group	Bencubbin-like grouplet	CH-like grouplet	Ungrouped
Renazzo	Acfer 182§	Bencubbin	HH 237	LEW 85332
Al Rais	ALH 85085	Gujba	QUE 94411$	–
El Djouf 001*	PAT 91546	Weatherford	–	–
Kaidun†	PCA 91328#	–	–	–
Temple Bar	PCA 91452#	–	–	–
EET 87770‡	PCA 91467#	–	–	–
GRA 95229	RKPA 92435	–	–	–
GRO 95577 (CR1)	–	–	–	–
MAC 87320	–	–	–	–
PCA 91082	–	–	–	–
Y-790112	–	–	–	–
Y-791498	–	–	–	–
Y-793495	–	–	–	–
Y-8449	–	–	–	–

Abbreviations: ALH = Allan Hills, EET = Elephant Moraine, GRA = Graves Nunataks, GRO = Grosvenor Mountains, HH = Hammadah al Hamra, LEW = Lewis Cliff, MAC = MacAlpine Hills, PAT = Patuxent Range, PCA = Pecora Escarpment, QUE = Queen Alexandra Range, RKPA = Reckling Peak, Y = Yamato.

*Paired with nine Acfer meteorites (Bischoff *et al.*, 1993a).

†Complex chondritic breccia (Clayton *et al.*, 1994).

‡Paired with 40 other EET meteorites (*Antarctic Meteorite Newsletter*, 1989, 1994).

§Paired with Acfer 207 and 214.

#Pairing of some (or all) of these meteorites is uncertain.

$Paired with QUE 94627 (*Antarctic Meteorite Newsletter*, 1996).

classification than "group" and was originally defined by Kallemeyn and Wasson (1981) to denote chondrite groups that were believed to have formed in a narrow range of heliocentric distances, as indicated by similar isotopic and petrologic properties. In this paper, this term is used for chondrites that have chemical, mineralogical and isotopic similarities that suggest a petrogenetic kinship, but have petrologic and/or bulk chemical characteristics that challenge a group relationship (Weisberg *et al.*, 1995).

The CR clan chondrites are considered carbonaceous because their whole-rock elemental abundances and oxygen-isotopic compositions are similar to those of the carbonaceous (CO, CK, CV, CM) chondrites: their mean refractory lithophile/Mg abundance ratios relative to CI chondrites are ≥1 (Fig. 1) and their bulk oxygen-isotopic compositions plot below the terrestrial fractionation line (Fig. 2). In contrast, the mean refractory lithophile/Mg abundance ratios relative to CI chondrites in ordinary (H, L, LL) and enstatite (EH, EL) chondrites are <1.0 and their bulk oxygen-isotopic compositions plot above (H, L, LL) or along (EH, EL) the terrestrial fractionation line (Clayton, 1993; Clayton and Mayeda, 1999; Weisberg *et al.*, 1993, 1995, 2001).

Members of the CR clan have the following similar characteristics: (1) they are metal-rich and metal abundances vary widely among them (Figs. 3 and 4). (2) FeNi-metal has a broad compositional range and is characterized by an approximately solar Co/Ni ratio (Fig. 5). (3) They are highly depleted in moderately volatile lithophile elements; the depletions correlate with increasing volatility (Fig. 1). (4) Their bulk oxygen-isotopic compositions plot on or near the CR-mixing line on a three-isotope diagram (Fig. 2). (5) Their bulk nitrogen-isotopic compositions have large positive anomalies in $\delta^{15}N$ (Fig. 6). (6) Most of their anhydrous mafic silicates are Mg-rich (Fa and Fs <4 mol%). (7) They contain heavily hydrated matrix and/or matrix lumps composed of serpentine, saponite, prismatic sulfides, framboidal and platelet magnetites, and carbonates.

The CR chondrites, first recognized by McSween (1977), are a group of 14 meteorites and their paired samples (Table 1) (*e.g.*, Bischoff *et al.*, 1993a; Weisberg *et al.*, 1993; Ichikawa and Ikeda, 1994; Kallemeyn *et al.*, 1994; Noguchi, 1994). Most of the CR chondrites are petrologic type 2 and generally contain abundant hydrous silicates, carbonates, and magnetite (Weisberg and Prinz, 1991; Weisberg *et al.*, 1993). Grosvenor Mountains (GRO) 95577 contains no anhydrous silicates and is classified as CR1 (Weisberg and Prinz, 2000). The Kaidun meteorite is a complex chondrite breccia that appears to be mainly CR chondrite, but also contains clasts of enstatite, ordinary, and several carbonaceous chondrite groups (Ivanov, 1989; Clayton *et al.*, 1994). Although hydrously altered, the CR chondrites are considered to be highly primitive meteorites because their refractory lithophile/Mg abundance ratios relative to CI chondrites are ~1.0 (Fig. 1) and because the CR chondrite components show no evidence for thermal or shock metamorphism.

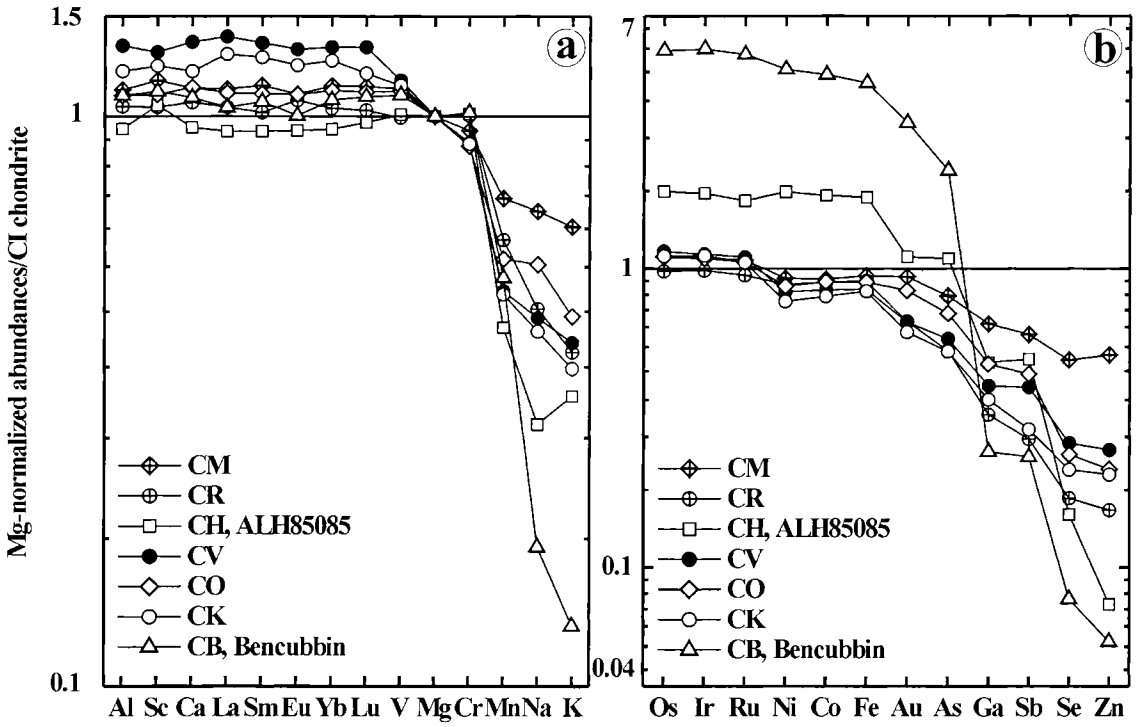

FIG. 1. Magnesium- and CI-normalized bulk lithophile (a) and siderophile (b) element abundances of the carbonaceous chondrite groups. The CR, CH (ALH 85085), and CB (Bencubbin) have CI-like abundances of refractory and normal lithophile elements and are highly depleted in moderately volatile lithophile elements such as Mn, Na, and K. The CH and CB chondrites are highly enriched in refractory and normal siderophile elements and depleted in moderately volatile siderophile elements (data from Kallemeyn and Wasson (1981, 1982, 1985), Kallemeyn *et al.* (1978, 1991, 1994), and Weisberg *et al.* (2001)).

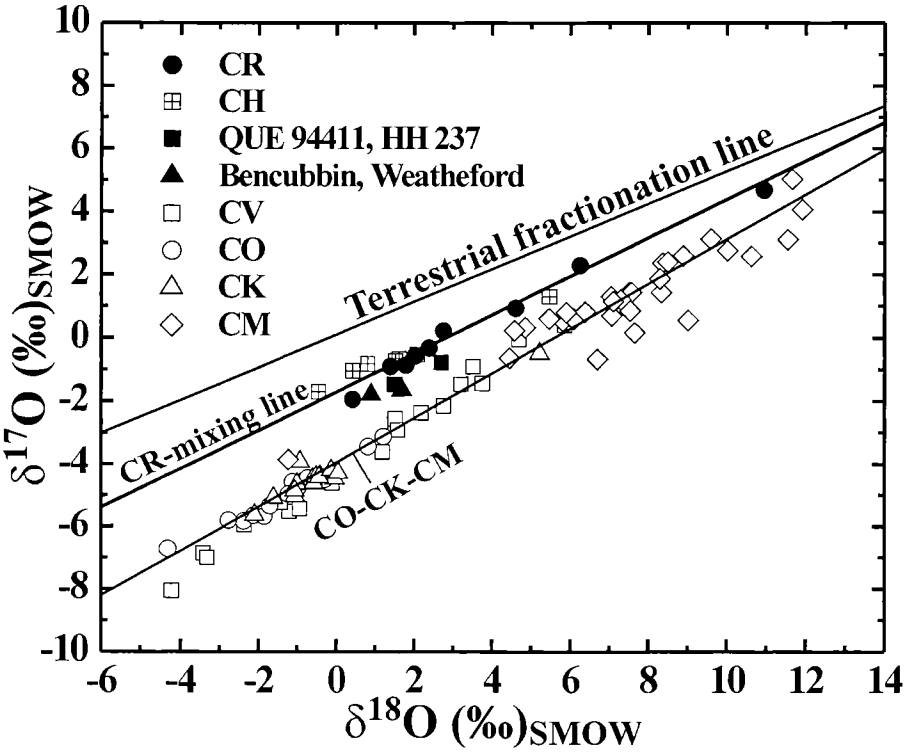

FIG. 2. Bulk oxygen-isotopic compositions of the major carbonaceous chondrite groups. The Bencubbin, Weatherford, Hammadah al Hamra 237, QUE 94411, CR and CH chondrites define a unique CR-mixing line (data from Clayton and Mayeda, 1999).

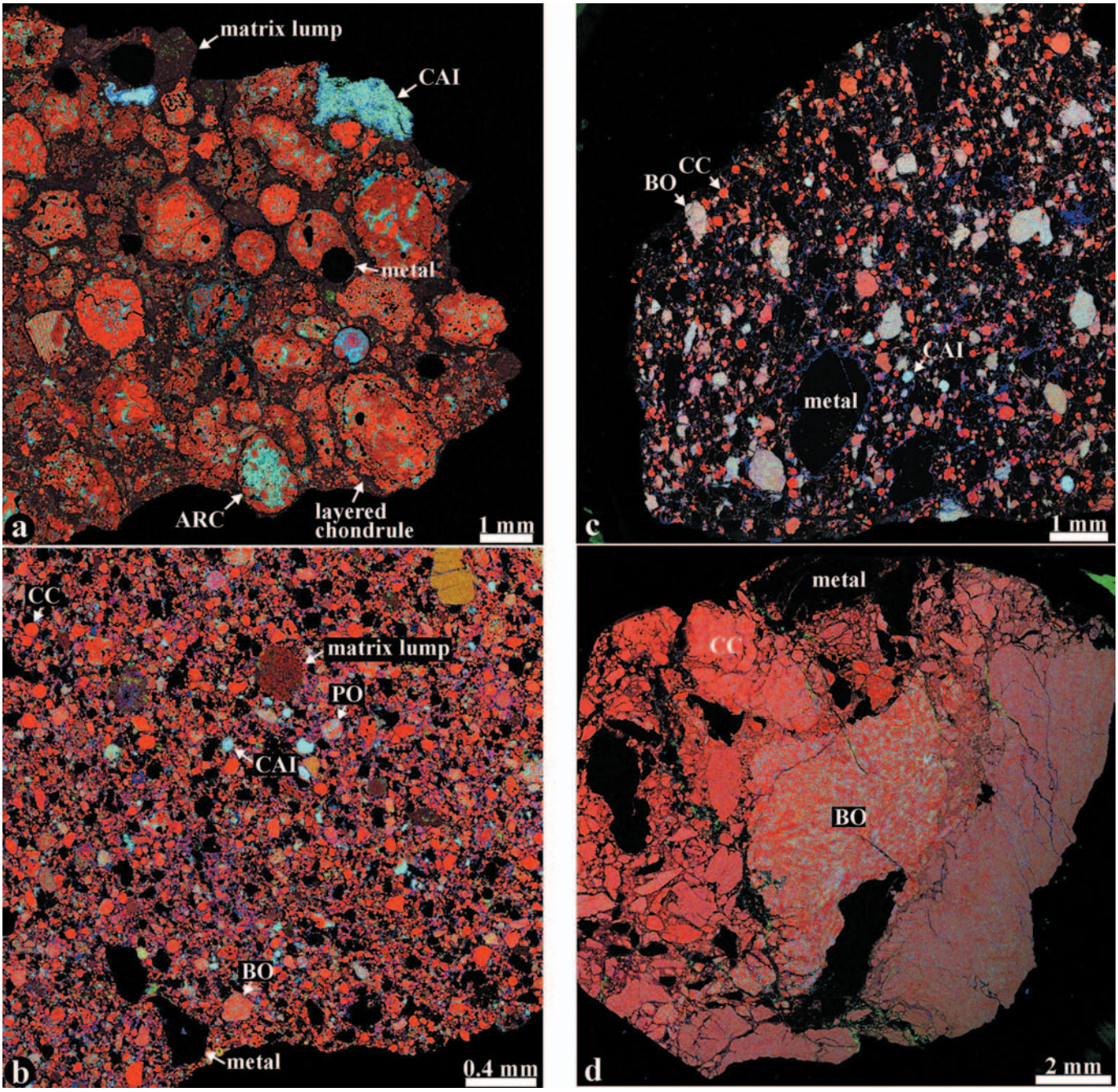

FIG. 3. Combined x-ray elemental maps in Mg (red), Ca (green) and Al Kα (blue) of the CR chondrite PCA 91082 (a), CH chondrite PAT 91546 (b), QUE 94627 (c) and Bencubbin (d). The same color mixing scheme is used in Figs. 12, 14 and 16. PCA 91082 (a) contains metal-rich porphyritic chondrules, rare calcium-aluminum-rich inclusions (CAI) and anorthite-rich chondrules (ARC), and matrix lumps. Many chondrules show layering. PAT 91546 (b) consists of tiny chondrules having barred olivine (BO), cryptocrystalline (CC), and porphyritic (PO) textures, FeNi-metal, CAIs, and matrix lumps; metal largely occurs outside chondrules. QUE 94627 (c) consists of FeNi-metal, BO and CC chondrules, and rare CAIs; metal occurs exclusively outside chondrules. (d) Bencubbin consists of fragmented FeNi-metal grains, BO and CC chondrules; CAIs are absent.

The CH chondrite group consists of seven meteorites (Table 1); some of the Antarctic CH chondrites might be paired (Grossman *et al.*, 1988; Scott, 1988; Weisberg *et al.*, 1988; Wasson and Kallemeyn, 1990; Bischoff *et al.*, 1993b; Prinz and Weisberg, 1992; Prinz *et al.*, 1994). When Allan Hills (ALH) 85085 was first described, it sparked much controversy because of its high metal abundance (~20 vol%), small chondrule sizes (average diameter ~20 μm), dominance of cryptocrystalline (CC) chondrules, and lack of matrix surrounding chondrules (Figs. 3b and 4b) (Grossman *et al.*,

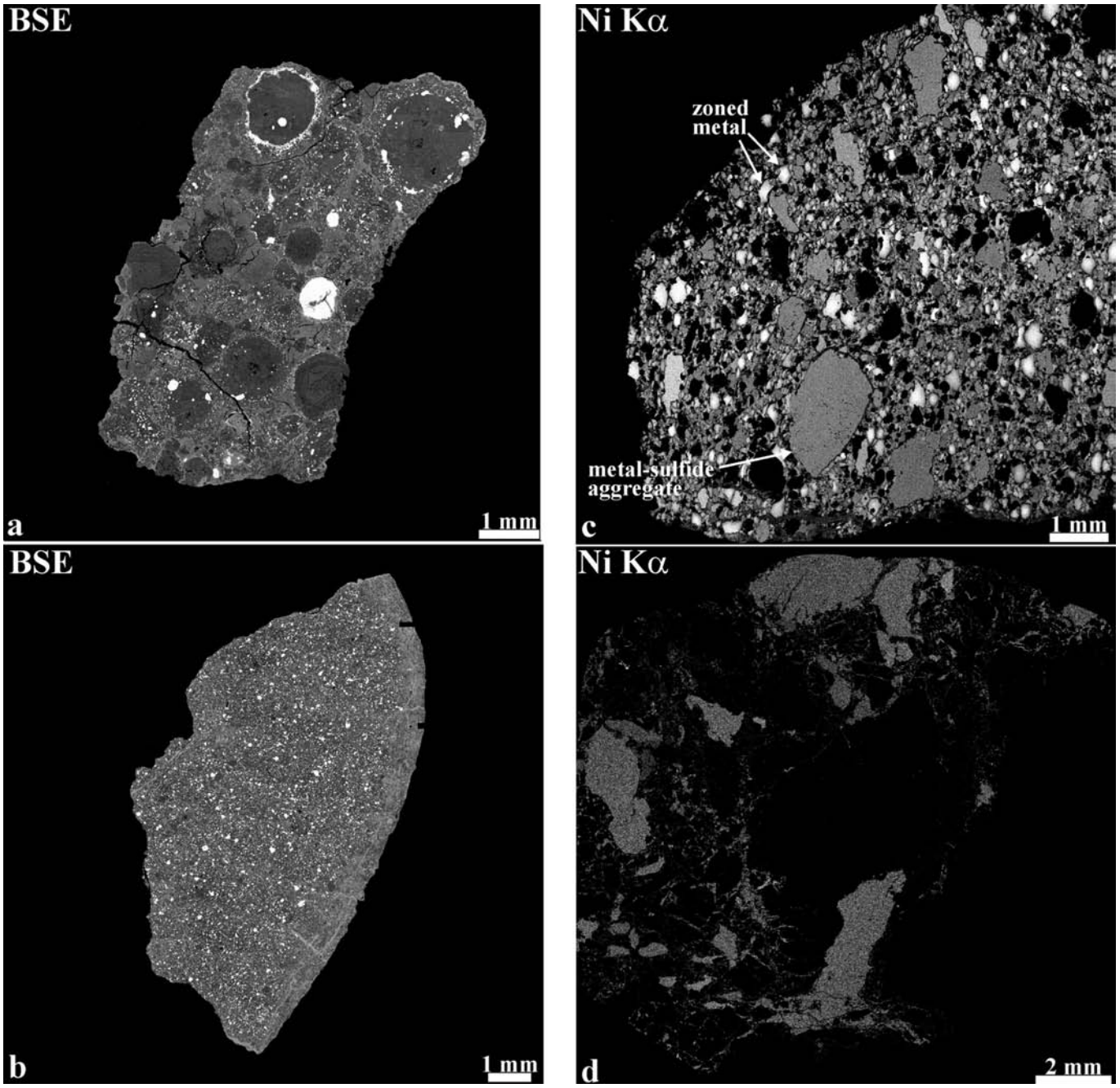

FIG. 4. Backscattered electron (BSE) images (a, b) and x-ray elemental maps in Ni Kα (c, d) of the CR chondrite PCA 91082 (a), CH chondrite PCA 91467 (b), QUE 94627 (c) and Bencubbin (d). (a) FeNi-metal occurs as nodules in chondrules, igneous rims around chondrules and in the matrix. (b) FeNi-metal occurs largely as irregularly shaped grains outside chondrules. (c) FeNi-metal occurs exclusively outside chondrules; ~20% of all metal grains are compositionally zoned, with cores enriched in Ni relative to edges. Some of the zoned metal grains contain silicate inclusions. Metal–sulfide aggregates are compositionally uniform. (d) Most FeNi-metal grains are fragmented and texturally similar to metal–sulfide aggregates in QUE 94627.

1988; Scott, 1988; Weisberg *et al.*, 1988). These unusual characteristics led Wasson and Kallemeyn (1990) to suggest that the CH chondrites are modified "subchondritic" meteorites formed as a result of a highly energetic asteroidal collision(s) leaving doubt as to the pristine nature of these meteorites. More recently, it has been argued that refractory inclusions, chondrules, and zoned metal grains in these meteorites are in fact pristine nebular products (Meibom *et al.*, 1999a,b, 2000a,b, 2001, unpubl. data; Petaev *et al.*, 1999, 2000; Weisberg and Prinz, 1999; Weisberg *et al.*, 2001; McKeegan *et al.*, 2002).

The Bencubbin, Weatherford and Gujba meteorites are characterized by even higher metal abundances (about 40–

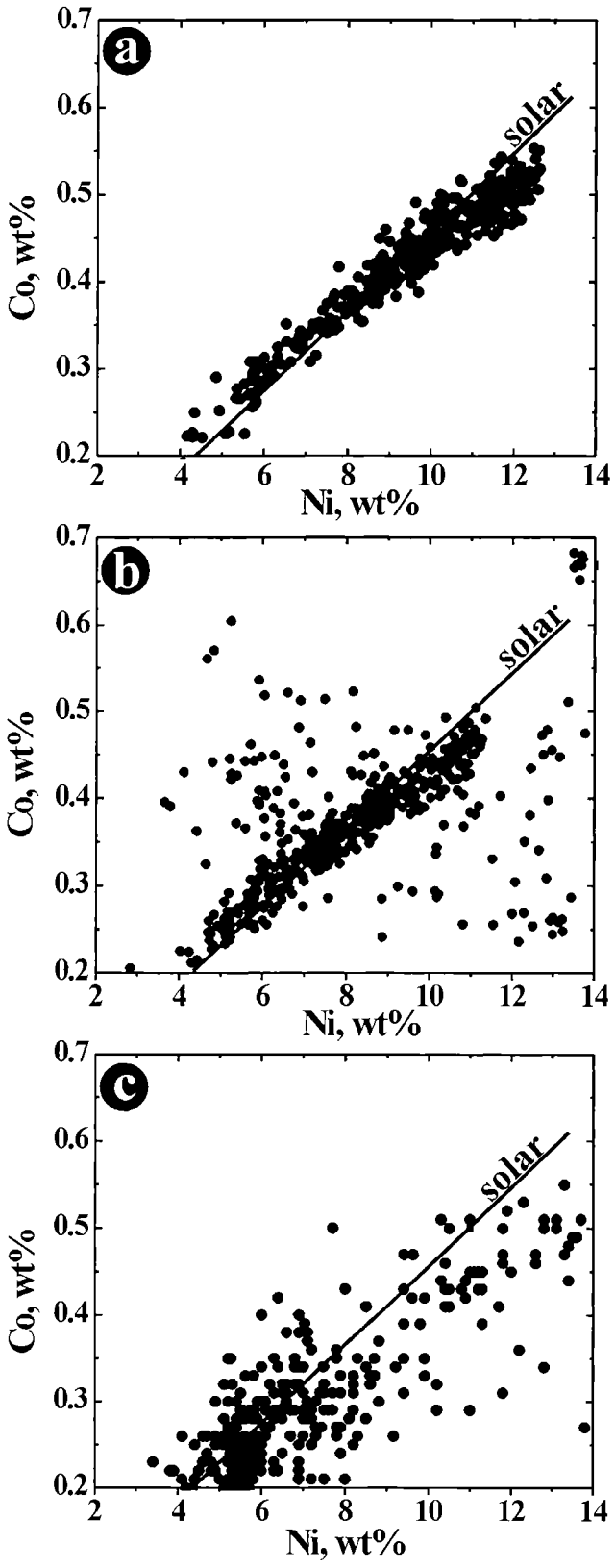

FIG. 5. Concentrations of Ni *vs.* Co in metal grains from Hammadah 237 and QUE 94411 (a), CH (b) and CR (c) chondrites.

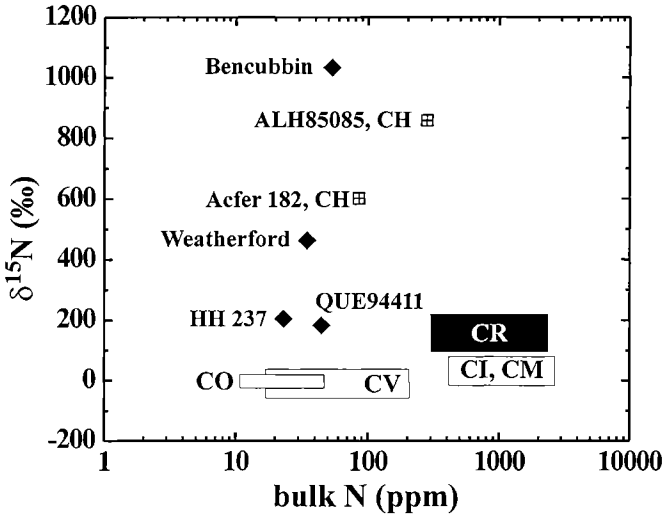

FIG. 6. Bulk concentrations of N *vs.* $\delta^{15}N$ in carbonaceous chondrites. The Bencubbin, Weatherford, HH 237, QUE 94411, CR chondrites and CH chondrites are enriched in $\delta^{15}N$ compared to other chondrite groups (data from Kerridge (1985), Franchi *et al.* (1986), Keeling *et al.* (1987), Grady and Pillinger (1990), Ash and Pillinger (1992), Sugiura *et al.* (2000), and Weisberg *et al.* (2001)).

60 vol%) (Lovering, 1962; Mason and Nelen, 1968; Kallemeyn *et al.*, 1978; Newsom and Drake, 1979; Weisberg *et al.*, 1990, 2001; Prinz *et al.*, 1993a; Rubin *et al.*, 2001). Silicates are present in the form of large barred olivine (BO) and CC chondrules (Weisberg *et al.*, 1990). Both metal and chondrules occur as centimeter-sized, angular to rounded fragments (Figs. 3d and 4d). Interstitial to the clasts is silicate-metal melt material, which is presumably shock-produced (Ramdohr, 1973; Meibom *et al.*, 2000c). Newsom and Drake (1979) referred to Bencubbin as a shock-welded breccia. In addition to the large metal and silicate fragments, a small percentage of exotic chondrite clasts are found in Bencubbin and Weatherford. These include ordinary and R (Rumuruti-like) chondrites and an unusual dark (carbonaceous chondritic) inclusion (Simpson and Murray, 1932; Lovering, 1962; McCall, 1968; Kallemeyn *et al.*, 1978; Weisberg *et al.*, 1990; Prinz *et al.*, 1993a).

More recently, two very metal-rich chondrites (~70 vol% metal), HH 237 and QUE 94411 (Figs. 3c and 4c), paired with QUE 94627, have been found (Righter and Chabot, 1998; Zipfel *et al.*, 1998; Weisberg *et al.*, 2001). Similar to CH chondrites, these meteorites contain CAIs, chemically zoned metal grains, and rare heavily hydrated matrix lumps (Meibom *et al.*, 2000b; Greshake *et al.*, 2002; Weisberg *et al.*, 2001; Krot *et al.*, 2001a). However, they are more similar to Bencubbin, Gujba and Weatherford, in that they contain more than 70 vol% metal, their chondrules are mostly BO and CC textures (chondrule sizes are intermediate between those in CH chondrites and Bencubbin, Gujba, and Weatherford) and their bulk oxygen-isotopic compositions are very similar to those of Bencubbin, Weatherford and Gujba.

Weisberg *et al.* (2001) grouped together QUE 94411, HH 237, Bencubbin, Gujba, and Weatherford and called them the CB chondrite group. These authors, however, admitted that there are significant mineralogical and petrographic differences between QUE 94411/HH 237 and Bencubbin/Gujba/Weatherford and subdivided them into CB_a (Bencubbin, Gujba, and Weatherford) and CB_b (HH 237 and QUE 94411) subgroups. Other authors (*e.g.*, Bischoff, 2001, pers. comm.) questioned this classification. Since the genetic relationship between these subgroups remains unclear (*e.g.*, Campbell *et al.*, 2002), in this paper, we describe chondritic components in Bencubbin/Gujba/Weatherford (CB_a) and QUE 94411/HH 237 (CB_b) separately.

Lewis Cliff 85332 is a unique, metal-rich type 3 carbonaceous chondrite breccia with chemical, oxygen-isotopic and petrographic characteritics similar to those of the CR chondrites (Rubin and Kallemeyn, 1990; Prinz *et al.*, 1992, 1993b; Weisberg *et al.*, 1995; Brearley, 1997). It has a high abundance of heavily hydrated matrix (~30 vol%), anhydrous chondrules and CAIs, and CR-like refractory lithophile element abundance ratios. Relative to the CR chondrites, however, it has smaller chondrules and higher abundances of Mn and most volatile siderophile elements. LEW 85332 is not discussed in this paper.

MINERALOGY, PETROGRAPHY AND CHEMISTRY OF THE CR CLAN CHONDRITIC COMPONENTS

Refractory Inclusions

Calcium-Aluminum-Rich Inclusions in CH Chondrites

Mineralogy and Petrography–Refractory inclusions in CH chondrites were largely studied in two meteorites, ALH 85085 and Acfer 182 (Grossman *et al.*, 1988; MacPherson *et al.*, 1989; Bischoff *et al.*, 1993b; Prinz and Weisberg, 1992; Kimura *et al.*, 1993; Weber *et al.*, 1995a; Krot *et al.*, 1999a,b). Preliminary results on mineralogy of CAIs from Pecora Escarpment (PCA) 91467 suggest that they are similar to those from ALH 85085 (Weber *et al.*, 1995b).

The modal abundance of CAIs in CH chondrites is <1 vol%. CAIs in ALH 85085 are much smaller (5–80 μm) than those in Acfer 182 (up to 450 μm). Most ALH 85085 CAIs are spherical in shape; many Acfer 182 CAIs are irregularly shaped. Based on the mineralogy, the CH CAIs can be divided into grossite-rich, hibonite-rich, spinel-rich, melilite-rich, pyroxene-rich, and perovskite-rich (Figs. 7 and 8) (Grossman *et al.*, 1988; MacPherson *et al.*, 1989; Bischoff *et al.*, 1993b; Kimura *et al.*, 1993; Krot *et al.*, 1999a,b). The grossite-rich and melilite-rich CAIs dominate in Acfer 182; spinel-hibonite-rich, melilite-rich and grossite-rich inclusions dominate in ALH 85085. The pyroxene-rich CAIs can be divided into two types: (1) unrimmed spherules with ±hibonite, ±grossite, ±melilite, ±spinel and (2) spinel-bearing spherules surrounded by forsterite rims (Fig. 8). Concentrations of Al and Ti in pyroxenes within an individuals spherule are highly variable and do not exhibit a concentric pattern (Fig. 8).

Many of the ALH 85085 CAIs are surrounded by a double layer of gehlenitic melilite and diopside or a single layer of diopside; spinel and hibonite are very rare in these rims (Kimura *et al.*, 1993). In contrast, rims around the Acfer 182 CAIs are more complex and, in addition to pyroxene, commonly include an inner layer of spinel ±hibonite; the outermost layer of forsterite is present around most pyroxene ±spinel spherules and around some of the melilite-rich CAIs (Krot *et al.*, 1999b). Secondary alteration minerals, such as nepheline, sodalite, or grossular are absent in the CH CAIs; anorthite is very rare.

Mineral Chemistry–Melilite is Na-free and åkermanite-poor ($Åk_{1-29}$). Grossite has nearly end-member composition ($CaAl_4O_7$). Hibonite has low concentrations of MgO (0.7–2 wt%) and TiO_2 (1.5–3.1 wt%). Forsterite ($Fa_{<1}$) contains high abundances of CaO (0.5–0.6 wt%). Spinel is Mg-rich (Mg/(Mg + Fe) > 0.98) and Cr_2O_3-poor (<1 wt%). Pyroxenes show significant compositional variations within an individual inclusion (1.4–19 wt% MgO, 2.4–40.3 wt% Al_2O_3, 0.1–11 wt% TiO_2, 24.5–53.7 wt% SiO_2). In contrast to pyroxenes in CAIs from other carbonaceous chondrites, those in CH CAIs show no correlation between Al_2O_3 and TiO_2 (Fig. 9a). The compositional variations of pyroxenes are largely due to the substitution $Mg^{(VI)} + Si^{(IV)} \rightarrow Al^{(IV)} + Al^{(VI)}$ suggesting the presence of Ca-Tschermakite component ($CaAl_2SiO_6$) (Fig. 9b).

Trace Element and Isotope Chemistry–Most CH CAIs have volatility fractionated, refractory depleted group II-related trace element patterns, suggestive of a condensation origin (MacPherson *et al.*, 1989; Kimura *et al.*, 1993; Weber *et al.*, 1995a; Ireland and Fegley, 2001). Ultrarefractory rare earth element (REE) patterns and group III-related trace element patterns, indicative of condensation or distillation origin (Ireland and Fegley, 2001), are less common. Calcium and Ti in most CAIs have normal isotopic compositions; exceptions are four CAIs with small nonlinear ^{48}Ca excesses in the range of 4–12‰ (Weber *et al.*, 1995a). Most CH CAIs show no evidence for mass-dependent fractionation of Mg isotopes ($\Delta^{25}Mg < 5$‰/amu); one exception is a CAI with ultrarefractory REE pattern, which has $\Delta^{25}Mg \approx 19$‰/amu (MacPherson *et al.*, 1989). Only 3 out of 13 analyzed CAIs in ALH 85085 and 1 out of 18 analyzed CAIs in Acfer 182 show excesses of ^{26}Mg ($^{26}Mg^*$) corresponding to $(^{26}Al/^{27}Al)_0 \approx 5 \times 10^{-5}$, one has ~$2 \times 10^{-6}$; others show no detectable $^{26}Mg^*$ (Weber *et al.*, 1995a).

Oxygen isotopes were only measured in one ALH 85085 CAI that showed ^{16}O excesses of ~50‰ in all minerals (spinel, perovskite, hibonite, grossite, melilite) except the Al-diopside rim, which has O-isotopic composition close to terrestrial fractionation line (Kimura *et al.*, 1993). Twenty-two CAIs from Acfer 182 studied by McKeegan *et al.* (2002) show bimodal distribution of O-isotopic composition along a mixing line of slope equal 1.02 ± 0.03 on the three-isotope plot (Fig. 10a). The most refractory inclusions composed of grossite, hibonite, spinel, perovskite, and melilite are enriched

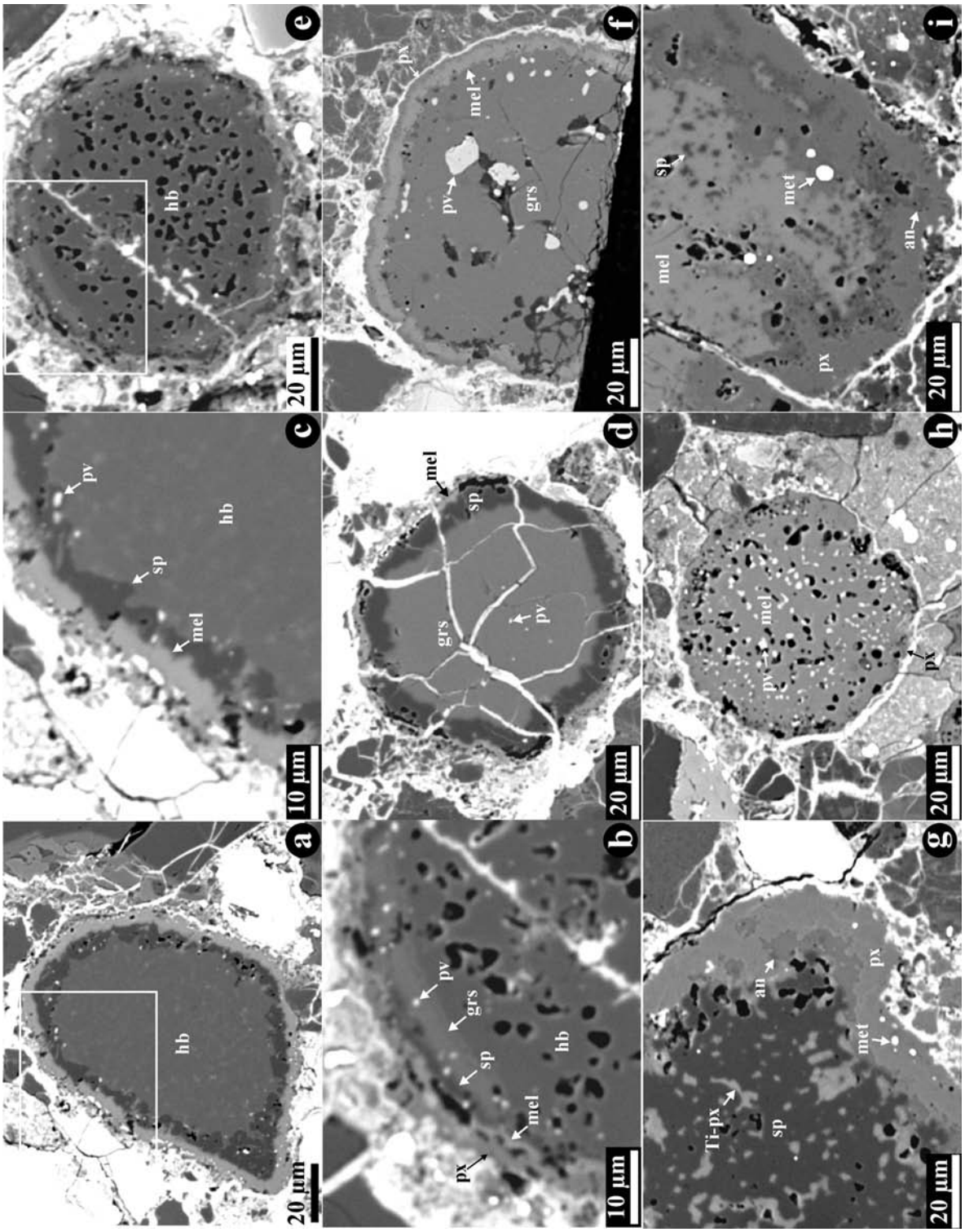

FIG. 7. BSE images of the refractory inclusions from the CH chondrite Acfer 182. (a, b) Compact-type hibonite (hb) CAI surrounded by a Wark–Lovering rim sequence composed of spinel (sp) and melilite (mel); perovskite (pv) is minor. (c, d) Fluffy-type hibonite CAI surrounded by a Wark–Lovering rim sequence composed of grossite (grs), spinel, melilite, and Al-diopside (px); perovskite is minor. (e) Compact-type grossite CAI surrounded by the spinel and melilite rims; perovskite is minor. (f) Compact-type grossite CAI surrounded by the melilite and Al-diopside rims; perovskite is minor. (g) Spinel-Al,Ti-diopside (Ti-px) CAI surrounded by the anorthite (an) and Al-diopside rims; the rim contains tiny nodules of FeNi-metal (met). (h) Melilite spherule containing numerous inclusions of perovskite and surrounded by a thin Al-diopside rim. (i) Melilite-rich CAI surrounded by the anorthite and Al-diopside rims; the rim contains small FeNi-metal nodules.

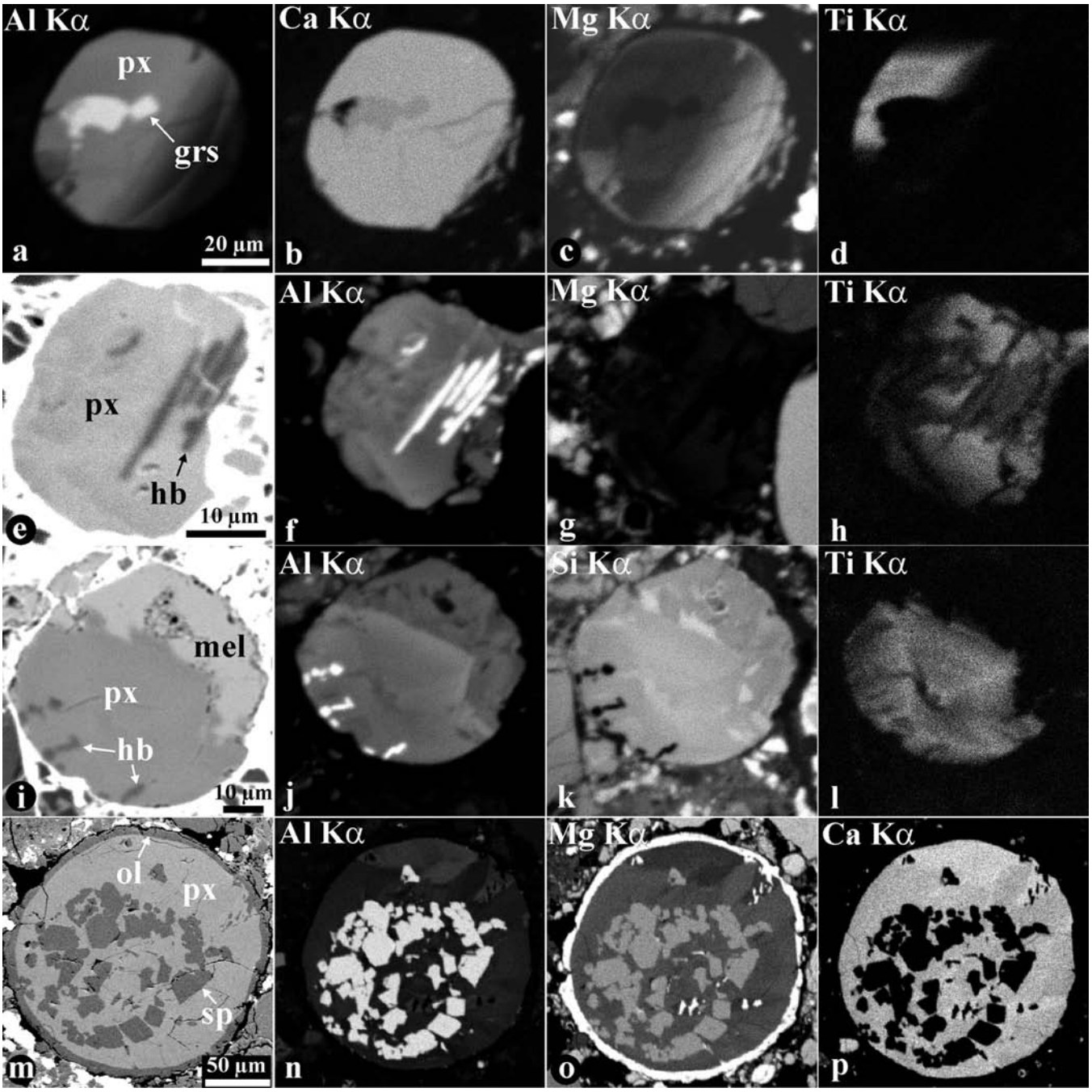

FIG. 8. BSE images (e, i, m) and x-ray elemental maps in Al (a, f, j, n), Ca (b, p), Mg (c, g, o), Ti (d, h, l) and Si Kα (k) of the pyroxene-rich spherules from the CH chondrites Acfer 182 (a–l) and PAT 91546 (m–p). Spherules associated with grossite (a–d), hibonite (e–h) and melilite (i–l) are unrimmed; spherule associated with spinel (m–p) is surrounded by a forsterite (ol) rim. The concentrations of Al and Ti in pyroxenes within an individual spherule are highly variable and do not exhibit a concentric pattern.

in ^{16}O; Al-diopside rims around these CAIs, pyroxene-spinel CAIs and two melilite-rich CAIs surrounded by a forsterite layer are ^{16}O-poor. In general, and in contrast to CAIs in CV chondrites (*e.g.*, Clayton *et al.*, 1977; Clayton, 1993; Yurimoto *et al.*, 1998; Young and Russell, 1998), oxygen-isotopic compositions within individual CH CAIs are rather homogeneous (Fig. 10b).

Calcium-Aluminum-Rich Inclusions in CR chondrites

Mineralogy and Petrography–Refractory inclusions in CR chondrites are rare (<1 vol%); they are typically small (10–300 μm) and irregularly shaped (Weisberg *et al.*, 1993; Bischoff *et al.*, 1993a; Weber and Bischoff, 1994, 1997; Weber *et al.*, 1995a; Weber, 1996; Marhas *et al.*, 2001). Based on mineralogy, they can be divided into grossite-rich, fluffy and compact melilite-

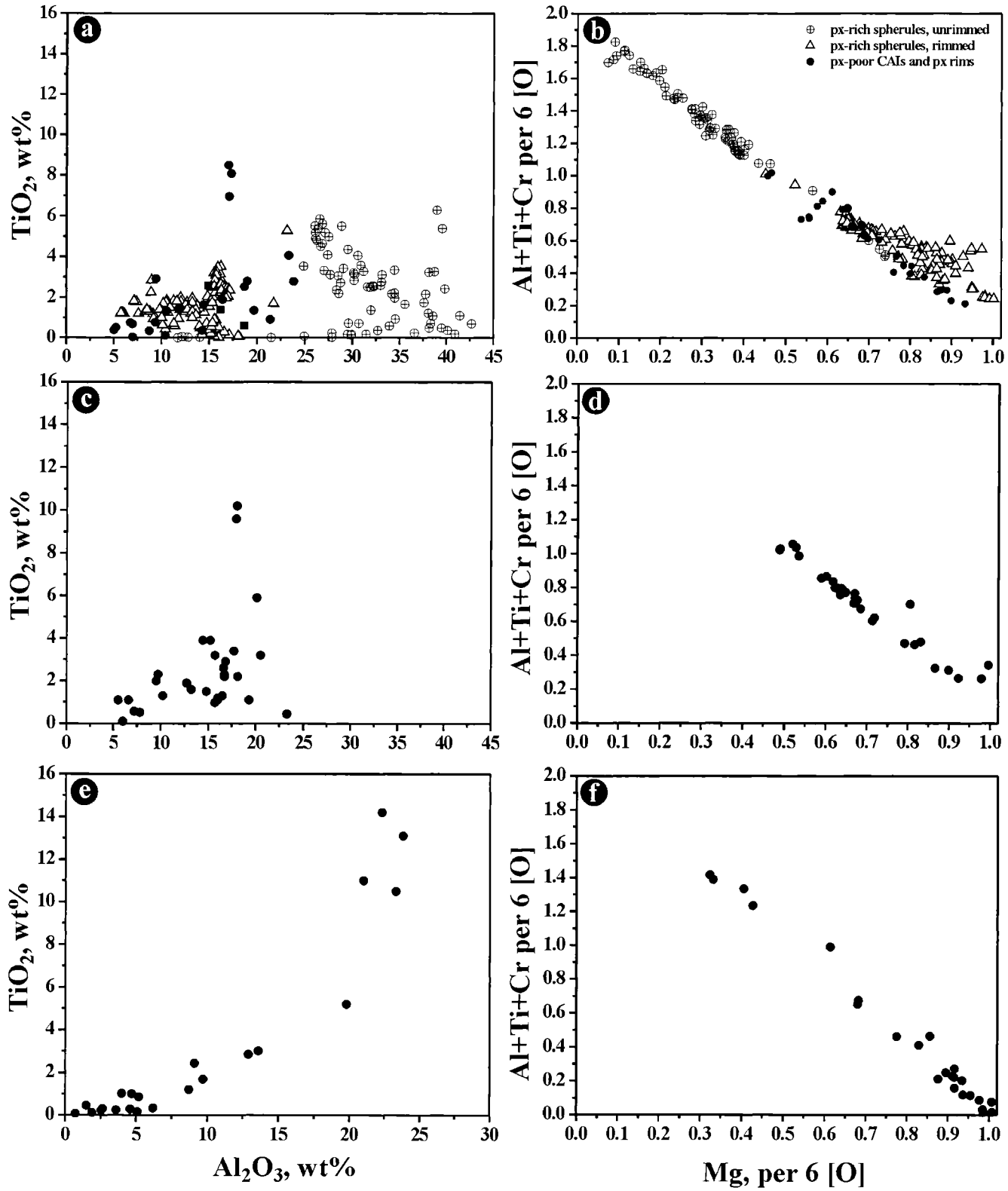

FIG. 9. Concentrations of Al_2O_3 (wt%) *vs.* TiO_2 (wt%) (a, c, d) and Mg (number of atoms per 6 oxygens) *vs.* Al + Ti + Cr (number of atoms per 6 oxygens) in pyroxenes of refractory inclusions from the CH chondrites (a, b), CR chondrites (c, d), HH 237 and QUE 94411 (e, f).

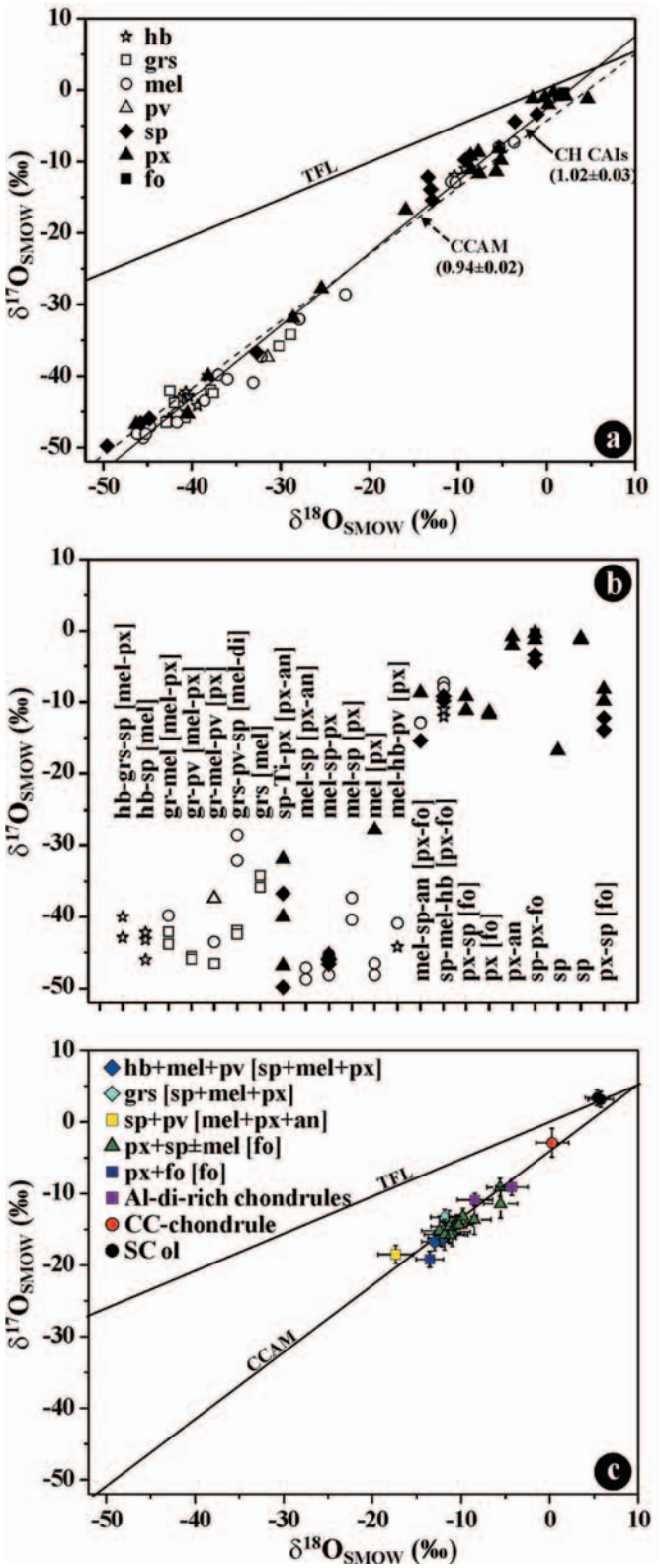

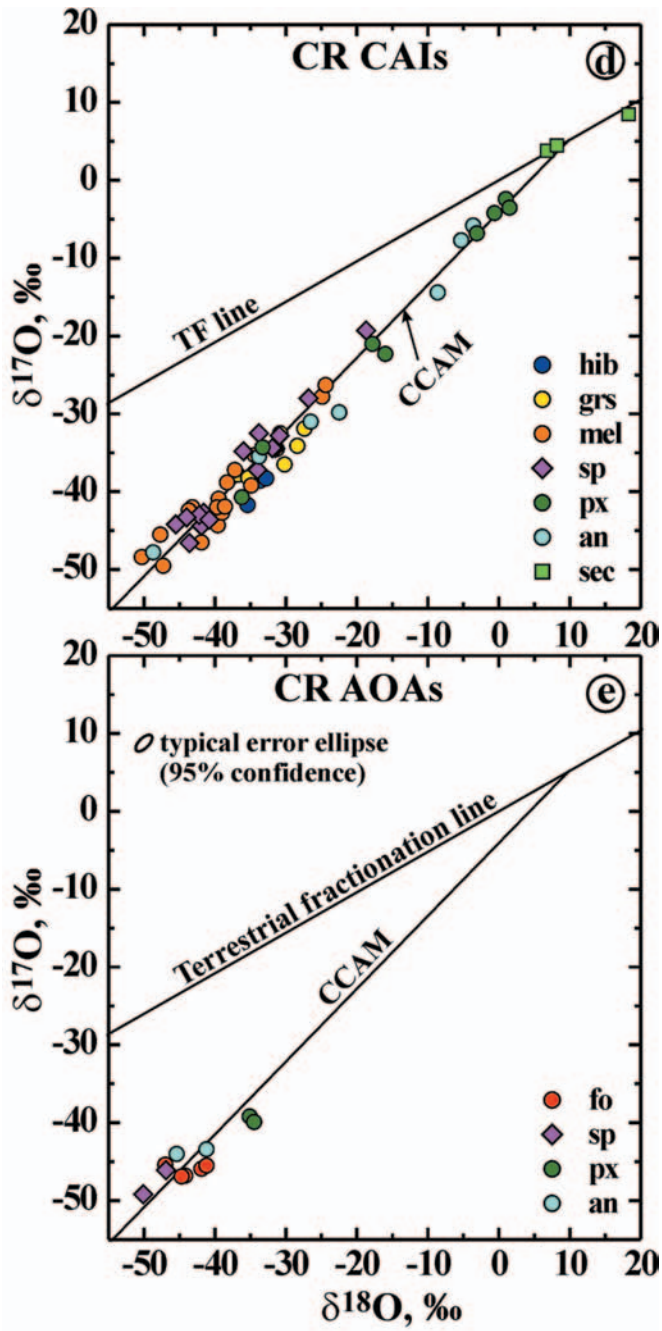

FIG. 10. Oxygen-isotopic compositions of hibonite, grossite, melilite, perovskite, spinel, pyroxene and forsterite in refractory inclusions from the CH chondrites Acfer 182 and PAT 91546 (a, b) (after McKeegan *et al.*, 2002), HH 237 and QUE 94411 (c) (after Krot *et al.*, 2001b) and CR chondrites (d, e) (after Aléon *et al.*, 2002). The CH CAIs (a, b) plot along a mixing line of slope equal 1.02 ± 0.03 which is different from the carbonaceous chondrite anhydrous mineral (CCAM) mixing line of slope 0.94 ± 0.02. Most of the refractory inclusions composed of grossite, hibonite, spinel, perovskite and melilite are enriched in ^{16}O; Al-diopside rims around these CAIs, pyroxene-spinel spherules and two melilite-rich CAIs surrounded by forsterite rims are ^{16}O-poor. The HH 237 and QUE 94111 CAIs (c) are ^{16}O-poor. Oxygen-isotopic compositions within individual CAIs are rather homogeneous. Rim mineralogy is listed in parentheses. AOAs and most CAIs in CR chondrites (d, e) are uniformly ^{16}O-enriched.

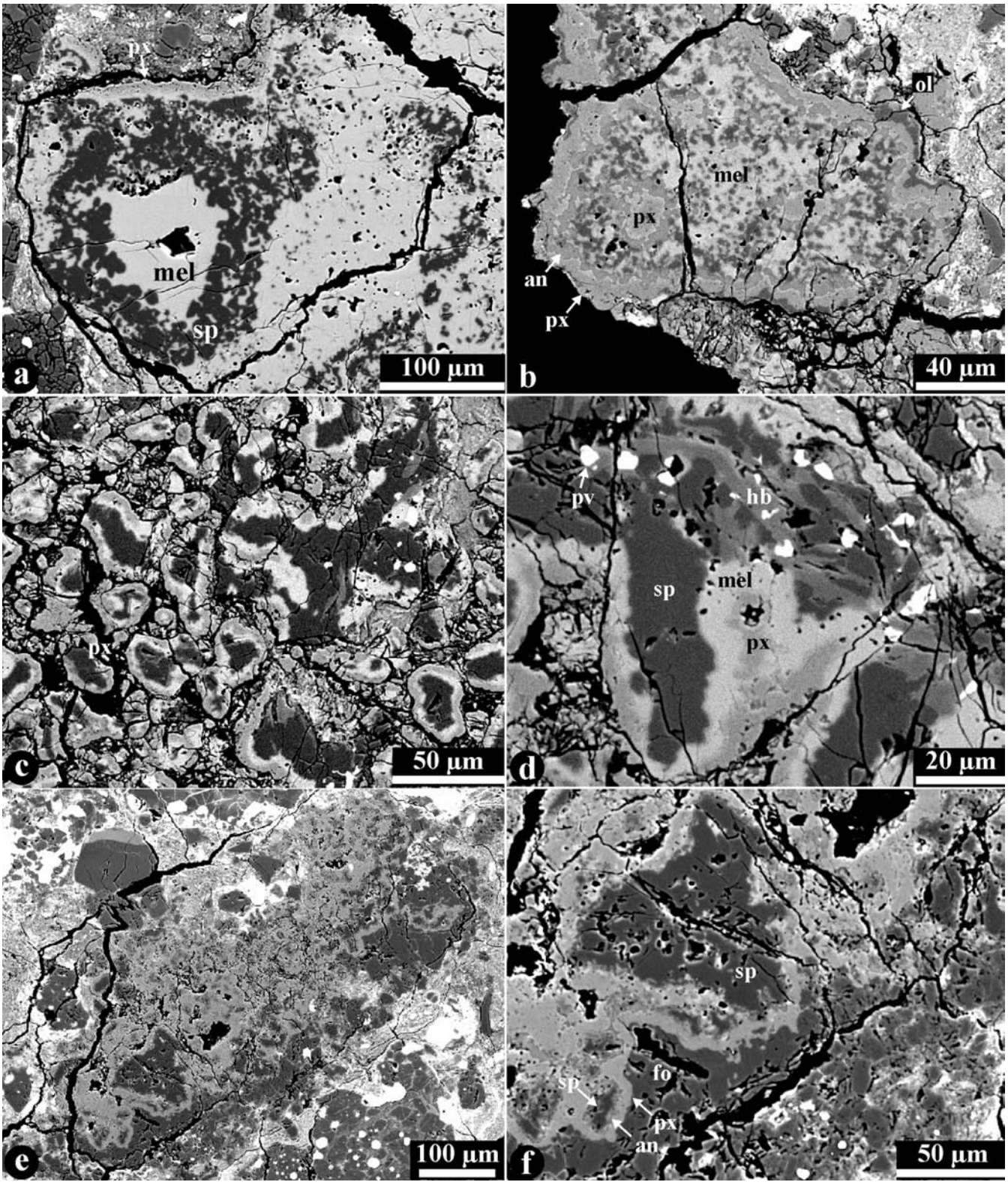

FIG. 11. BSE images of the refractory inclusions from the CR chondrites GRA 95529 (a), PCA 91082 (b-d) and EET 87747 (e, f). (a) Melilite-rich CAI surrounded by Al-diopside rim. (b) Melilite-spinel-anorthite CAI surrounded by the rims of anorthite, Al-diopside and forsterite; anorthite in the core replaces melilite. (c, d) A multicored CAI consisting of spinel-hibonite-perovskite cores surrounded by the rims of melilite and Al-diopside. (e, f) Amoeboid olivine aggregate containing a refractory component composed of spinel, Al-diopside and anorthite.

rich (type A); anorthite-rich, spinel-pyroxene aggregates; and amoeboid olivine aggregates (AOAs). The melilite-rich CAIs, spinel-pyroxene aggregates, and AOAs dominate; grossite-rich and hibonite-rich CAIs are very rare (Fig. 11).

The melilite-rich CAIs have cores composed of melilite, spinel, ±hibonite, and ±perovskite; the cores are surrounded by layers of ±spinel, ±anorthite, pyroxene, and ±forsterite (Fig. 11a). In most melilite-rich CAIs, anorthite replaces melilite (Fig. 11b); igneous, lath-shaped anorthite is found in exceptionally rare type B-like CAIs (Weber and Bischoff, 1997; Marhas *et al.*, 2001). In the spinel-pyroxene aggregates, melilite is commonly observed between spinel ±hibonite core and pyroxene rim (Fig. 11c,d). Grossite-rich CAIs have compact grossite cores surrounded by the spinel and melilite rims. AOAs consist of forsterite and refractory component composed of spinel, anorthite, and Al-diopside; anorthite typically occurs between spinel and Al-diopside.

Secondary minerals such as nepheline and sodalite are absent in the CR CAIs (Weber and Bischoff, 1997; Marhas *et al.*, 2001), although Renazzo and Al Rais CAIs contain secondary calcite and phyllosilicates (Weisberg *et al.*, 2002, unpubl. data; Krot *et al.*, 2002a; Aléon *et al.*, 2002).

Mineral Chemistry–Hibonite is relatively MgO-rich (2.6–3.3 wt%). Spinel is FeO-poor (<0.4 wt%). Melilite is Na-free and åkermanite-poor ($Åk_{5-35}$); the åkermanite content increases in the order grossite-rich, melilite-rich, spinel-pyroxene-rich, and anorthite-rich CAIs (Weber and Bischoff, 1997). Pyroxenes are Mn- and Cr-free and show significant variations in Al_2O_3 (0.4–23 wt%) and TiO_2 (0–14 wt%) concentrations (Fig. 9c,d). Plagioclase is nearly end-member anorthite. AOAs contain two types of olivine: one fluoresces blue and the other fluoresces red; both olivine types are nearly pure forsterites ($Fa_{0.2-0.5}$), but red olivines contain more MnO (0.2–0.6 wt% *vs.* <0.2 wt%) and Cr_2O_3 (0.2–0.4 wt% *vs.* <0.2 wt%) than the blue olivines.

Trace Element and Isotope Chemistry–Trace element data of the CR CAIs are very limited (Weisberg *et al.*, 2002, unpubl. data). Pyroxene of a spinel-pyroxene aggregate has essentially flat REE patterns (about 20–40 × CI) except strong negative Eu and Yb anomalies. Melilite of a compact type A CAI is enriched in light REEs (La ≈ 10 × CI; Lu ≈ 4 × CI) and exhibits a large positive Eu anomaly. Melilite of a fluffy type A CAI exhibits a light REE enriched pattern (La ≈ (20–50) × CI; Lu ≈ (5–15) × CI); REE abundances in anorthite are similar to the least enriched melilite; Al-diopside has the lowest REE abundances with an identical pattern to melilite, but with La ≈ 16 × CI. Both melilite (F_{Mg} = –7.3‰/amu) and Al-diopside (F_{Mg} = –4.2‰/amu) exhibit isotopic fractionation favoring the lighter isotopes (Weisberg *et al.*, 2002, unpubl. data).

All four grossite-rich CAIs analyzed so far show the presence of $^{26}Mg^*$ corresponding to an initial $^{26}Al/^{27}Al$ ratio of ~5×10^{-5} (Weber *et al.*, 1995a; Marhas *et al.*, 2001). Three out of six type A CAIs show the presence of $^{26}Mg^*$ which is consistent with the canonical $^{26}Al/^{27}Al$ ratio within experimental uncertainty; the low Al/Mg ratio (<10) in melilites from the other type A CAIs made it difficult to search for $^{26}Mg^*$; type B CAI showed no detectable $^{26}Mg^*$ (Marhas *et al.*, 2001).

In situ ion microprobe analyses of oxygen-isotope compositions of 27 CAIs and AOAs from 7 CR chondrites (Fig. 10d,e) have been recently reported by Aléon *et al.* (2002). Most of the CR CAIs are ^{16}O-rich ($\Delta^{17}O$ of hibonite, melilite, spinel, pyroxene, and anorthite less than –22‰) and isotopically homogeneous within 3–4‰. Likewise, forsterite, spinel, anorthite, and pyroxene in AOAs have nearly identical, ^{16}O-rich compositions (–24‰ < $\Delta^{17}O$ < 20‰). In contrast, CAIs which show petrographic evidence for extensive melting are not as ^{16}O-rich ($\Delta^{17}O$ > –18‰). Secondary alteration minerals (phyllosilicates?) replacing ^{16}O-rich melilite in melilite-rich CAIs plot along the terrestrial fractionation line (Fig. 10d,e).

Calcium-Aluminum-Rich Inclusions in Hammadah al Hamra 237 and Queen Alexandra Range 94411

Mineralogy and Petrography–As in the CR and CH chondrites, refractory inclusions in QUE 94411 and HH 237 is a minor (<1 vol%) constituent (Zipfel *et al.*, 1998; Krot *et al.*, 2001b,c; Weisberg *et al.*, 2001). Most of these CAIs are compact, irregularly shaped objects (about 50–400 μm); fluffy inclusions are very rare. Based on mineralogy, the refractory inclusions can be divided into hibonite-rich, grossite-rich, pyroxene-rich, forsterite-bearing, spinel-pyroxene aggregates, and AOAs (Fig. 12). The pyroxene-rich and forsterite-bearing CAIs are the dominant types of refractory inclusions. Modal abundances of pyroxene, spinel, melilite, and forsterite in these CAIs vary within a wide range; anorthite is virtually absent. Most CAIs are surrounded by monomineralic forsterite rims; one of the hibonite-rich CAIs is surrounded by a Wark–Lovering rim sequence composed of spinel, pyroxene and forsterite. Secondary nepheline and sodalite are absent.

Mineral Chemistry–Hibonite is MgO-poor (<1 wt%). Spinel is poor in FeO (<1.2 wt%), Cr_2O_3 (0.1–0.6 wt%) and V_2O_3 (<0.8 wt%). Melilite is Na-free and shows a large range in åkermanite content ($Åk_{5-78}$); the highest Åk-content was found in a forsterite-bearing CAI. Pyroxenes are poor in MnO and Cr_2O_3 (<0.15 wt%) and show significant variations in Al_2O_3 (5–23 wt%) and TiO_2 (0–10 wt%) concentrations (Fig. 9e,f). Plagioclase is nearly pure anorthite. Forsterite ($Fa_{<1.5}$) is rich in CaO (0.5–1.5 wt%).

Trace Element and Isotope Chemistry–Trace element data of the CAIs from HH 237 and QUE 94411 are very limited (Russell *et al.*, 2000a). Two pyroxene-rich CAIs have unfractionated, group I, REE patterns at ~10 × CI and a negative Eu anomaly. A hibonite-rich CAI (Fig. 12a,b) has REE at ~100 × CI and exhibits negative anomalies in Ce, Eu and Yb.

Hibonite, grossite, melilite, spinel, and pyroxene in eight CAIs studied from HH 237 and QUE 94411 have relatively heavy O-isotopic compositions with $\Delta^{17}O$ ranging from –6 to –10‰ (Fig. 10c) (Krot *et al.*, 2001b,c). Variations in O-isotopic compositions of different minerals within an individual CAI are small (<2–3‰).

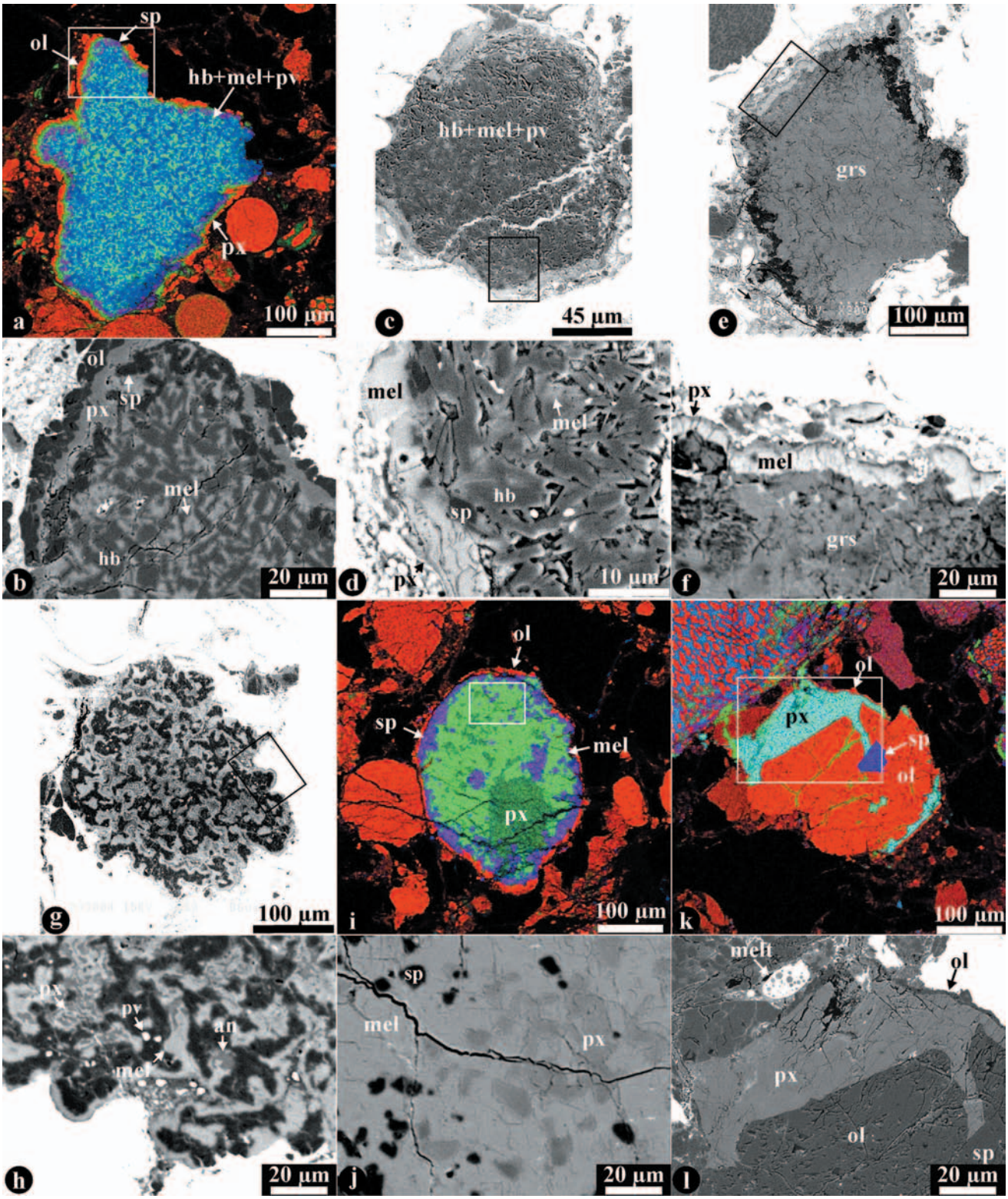

FIG. 12. Combined x-ray elemental maps (a, i, k) and BSE images (b–g, h, j, l) of the CAIs from the HH 237 and QUE 94411. (a, b) Hibonite-melilite CAI surrounded by a Wark–Lovering rim sequence composed of spinel, Al-diopside, and forsterite; perovskite is minor. (c, d) Hibonite-melilite CAI surrounded by the melilite and Al-diopside rims; perovskite is minor. (e, f) Compact-type grossite CAI surrounded by the melilite and Al-diopside rims; spinel and perovskite are minor. (g, h) A multicored CAI consisting of spinel-perovskite cores surrounded by the layers of melilite, anorthite and Al-diopside. (i, j) Melilite-spinel-pyroxene surrounded by forsterite rim. (k, l) Forsterite-pyroxene-spinel CAI surrounded by forsterite rim.

No Al-Mg-isotope studies of CAIs from HH 237 and QUE 94411 have been reported yet.

Calcium-Aluminum-Rich Inclusions in Bencubbin, Gujba, and Weatherford

No CAIs have been identified in Bencubbin and Weatherford. The large size of the components in these meteorites (several millimeters to centimeter-sized) combined with the low abundance of refractory inclusions in CR clan chondrites may make them extremely difficult to find, if present. However, refractory rich inclusions were found in Gujba (Weisberg *et al.*, 2002). They contain Ca-pyroxene, forsterite, anorthite and Mg-spinel, similar to some of the inclusions in HH 237 and QUE 94411 (Krot *et al.*, 2001b,c).

Discussion (I)

Comparison of Calcium-Aluminum-Rich Inclusions from the CR Clan: Evidence for Isolation of Calcium-Aluminum-Rich Inclusions from Nebular Gas at Various Ambient Temperatures–There are mineralogical differences between CAIs from CR and CH chondrites, and QUE 94411/HH 237. The CH CAIs are tiny and very refractory with grossite, hibonite, spinel, melilite, and Al,Ti-diopside as the major minerals. Anorthite-bearing CAIs are exceptionally rare; AOAs are absent. Most CH CAIs are covered by either a double mineral layer (an interior melilite and an outer pyroxene) or a single layer of pyroxene; forsterite rims are rare.

The CR CAIs are less refractory on average than those from CH chondrites; spinel-pyroxene aggregates, melilite-rich CAIs, and AOAs are the dominant types. Anorthite replacing melilite is common in most CR CAIs. The Wark–Lovering rim sequence around CR CAIs typically consist of spinel, ±melilite, ±anorthite, and pyroxene; forsterite layers are rare.

The CAIs in HH 237 and QUE 94411 are also less refractory on average than those in CH chondrites; grossite-rich and hibonite-rich CAIs are rare. However, compared to the CR CAIs, those in HH 237 and QUE 94411 are dominantly pyroxene-rich, typically surrounded by monomineralic forsterite rims and contain virtually no anorthite; AOAs are exceptionally rare.

It was suggested that these differences could have resulted from isolation of the CR clan refractory inclusions from the nebular gas at various temperatures (Weber and Bischoff, 1994, 1997; Krot *et al.*, 2001c). The very refractory nature and nearly complete absence of the relatively low-temperature condensates, such as anorthite and forsterite, in the CH CAIs may indicate these inclusions were removed from the CAI-forming region(s) prior to condensation of these minerals. The less refractory nature of the CAIs in QUE 94411, HH 237, Gujba and CR chondrites and common presence of forsterite in and around CAIs in QUE 94411/HH 237 and secondary anorthite in CR CAIs suggest that these inclusions were removed from the CAI-forming region(s) at lower temperatures (Fig. 13).

Comparison of CR Clan Calcium-Aluminum-Rich Inclusions to Inclusions from Other Groups: Evidence for

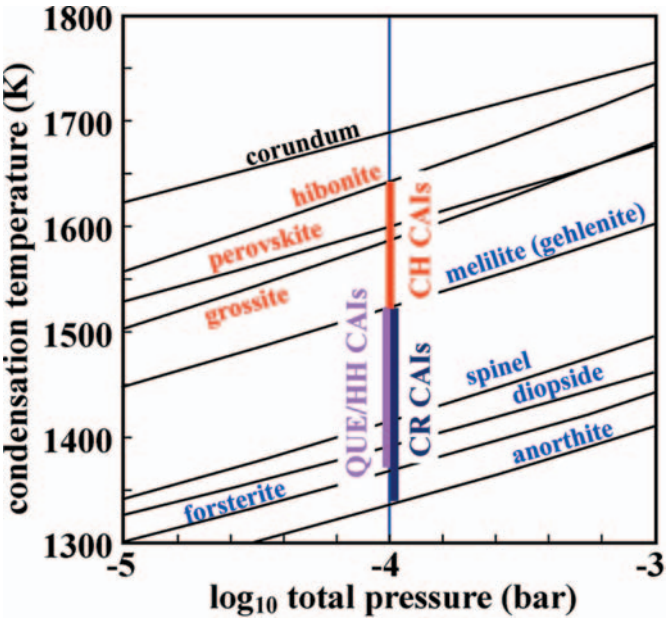

FIG. 13. Condensation temperatures as a function of total pressure for refractory minerals in CAIs (from Ireland and Fegley, 2001). Vertical lines show temperature intervals of minerals in CAIs from CH, CR and QUE 94411 and HH 237 chondrites.

Multiplicity of Calcium-Aluminum-Rich Inclusions Formation–A comparison of CAIs from the CR chondrite clan to those from other chondrite groups shows that all inclusion types existing in the former occur in at least one of the other carbonaceous chondrite groups (*i.e.*, CV, CM, CO, or CK) (Table 2). However, the relative proportions of CAI types are different in different chondrite groups. In addition, there are mineralogical and isotopic differences between CAIs from different chondrite groups. These include (1) the low abundance of secondary minerals in the CR clan CAIs, such as nepheline, sodalite, hedenbergite, wollastonite, andradite, phyllosilicates, and carbonates, commonly observed in the CV, CO and CM CAIs (MacPherson *et al.*, 1988; Russell *et al.*, 2000a); (2) the occurrence of grossite, which is rare to absent in CAIs from other chondrite groups; (3) lack of $^{26}Mg^*$ in most grossite-rich and hibonite-rich CAIs in CH chondrites; (4) relatively uniform oxygen-isotopic compositions of CAIs in QUE 94411, HH 237, CR and CH chondrites; (5) the presence of type B CAIs almost exclusively in CV chondrites; and (6) the common presence of isotopically anomalous platy hibonites (PLACs) only in CM chondrites.

The fact that each chondrite group has a distinct population of refractory inclusions may suggest that there were multiple episodes of CAI formation in the nebula, each characterized by a distinct set of physical–chemical conditions (*e.g.*, dust/gas ratio, peak heating temperature, cooling rate, ambient temperature, isolation temperature, number of recyclings).

Implications for the Oxygen-Isotopic Composition of the Solar Nebula Gas–The oxygen-isotopic compositions of individual minerals from CH CAIs are best fit by a line with a

TABLE 2. Types of CAIs associated with chondrite groups.

CAI type	CH	CR	QUE 94411, HH 237	CV	CO	CM	CK	OC	EC
Melilite-rich (type A)	common	common	common	common	common	rare	–	rare	–
Al,Ti-px-rich (type B)	–	rare	rare	common	–	–	rare	–	–
Amoeboid olivine aggregates	–	common	rare	common	common	common	common	–	–
Forsterite-bearing CAIs	–	–	rare	rare	–	–	–	–	–
Spinel ± pyroxene-rich	common	common	common	common	common	common	rare	rare	rare
Hibonite ± spinel-rich	common	rare	common	common	common	common	–	rare	rare
Grossite-rich	common	rare	rare	–	rare	–	–	–	–
Pyroxene-rich spherules	common	–	common	–	rare	rare	–	–	rare

Modified from MacPherson *et al.* (1988). Additional data: CH, Weber and Bischoff (1994), Kimura *et al.* (1993); CO, Greenwood *et al.*(1992), Russell *et al.* (1998); CM, MacPherson *et al.* (1983, 1984), Simon *et al.* (1994); CR, Weisberg and Prinz (1990), Weisberg *et al.* (1993), Kallemeyn *et al.* (1994), Weber and Bischoff (1997); CK, McSween (1977), MacPherson and Delaney (1985), Kallemeyn *et al.* (1991), Keller (1992), Noguchi (1993); EC, Bischoff *et al.* (1985), Guan *et al.* (2000), Fagan *et al.* (2000); QUE 94411, HH 237, Krot *et al.* (2001b).
Abbreviations: QUE = Queen Alexandra Range, HH = Hammadah al Hamra.

slope equal 1.02 ± 0.03, which is distinct from the carbonaceous chondrite anhydrous mixing (CCAM) line determined from Allende CAIs (Fig. 10a). Thus, the CH data provide the first definite observation of isotopic mixing along a pure ^{16}O-trajectory among a population of CAIs corroborating the recent suggestion by Young and Russell (1998) for a "primary" ^{16}O-line of slope exactly equal to unity.

The CH CAIs are generally devoid of nucleosynthetic isotope anomalies in Ca and Ti, yet they have the same maximum ^{16}O enrichments (–50 ÷ –40‰) as the vast majority of all other CAIs (Clayton, 1993; McKeegan *et al.*, 1996, 1998; Hiyagon and Hashimoto, 1999). This lack of correlation, as well as magnitude and ubiquity of the oxygen anomaly tends to support a local, solar nebula, origin for isotopically light oxygen (Scott and Krot, 2001; McKeegan *et al.*, 2002).

The overall data set for the CH CAIs is characterized by a bimodal distribution with no overlap between ^{16}O-rich and ^{16}O-poor inclusions (Fig. 10a,b). The HH 237 and QUE 94411 CAIs have O-isotopic compositions similar to the ^{16}O-poor inclusions from the CH chondrites (Fig. 10c). CAIs in CR chondrites have ^{16}O-rich and ^{16}O-poor compositions without any gap between them (Fig. 10d). The CR CAIs with igneous textures tend to be less ^{16}O-enriched than the other CAIs and AOAs (Aléon *et al.*, 2002). Since oxygen isotope heterogeneity within individual CR chondrite clan CAIs is very limited, and mineralogy and chemistry of the CAIs or proto-CAIs are consistent with condensation origin (Weber *et al.*, 1995a; Krot *et al.*, 2001c; McKeegan *et al.*, 2002; Aléon *et al.*, 2002; Weisberg *et al.*, 2002, unpubl. data), we infer that the ^{16}O-rich and ^{16}O-poor CAIs reflect either temporal variations in O-isotopic compositions of the nebular gas in the CAI-forming region(s) or radial transport of some CAI precursors into an ^{16}O-poor gas prior to their melting (see also McKeegan *et al.*, 2002; Scott and Krot, 2001; Aléon *et al.*, 2002).

Implications for Aluminum-Magnesium Isotope Systematics–The general lack of $^{26}Mg^*$ in the hibonite-rich and grossite-rich inclusions in CH chondrites could be explained by four possible scenarios (*e.g.*, Weber *et al.*, 1995a): (1) they formed after ^{26}Al decayed; (2) they incorporated live ^{26}Al, which decayed *in situ*, but $^{26}Mg^*$ was erased by subsequent thermal processing; (3) they formed before ^{26}Al was injected into and homogenized in the solar nebula; and (4) ^{26}Al was heterogeneously distributed (*i.e.*, locally produced) in the CAI-forming region(s) and did not get incorporated into all CAIs.

A late formation scenario for the hibonite-rich and grossite-rich CH CAIs, ~5 Ma after Allende CAIs with a canonical $(^{26}Al/^{27}Al)_0$ ratio of ~5 × 10^{-5}, is inconsistent with their refractory nature, in comparison to Allende CAIs (Weber *et al.*, 1995a).

Late-stage re-equilibration of Mg isotopes in the CH CAIs is inconsistent with petrographic observations that show no evidence for either secondary alteration or reheating that would suggest any thermal processing. It is expected that this thermal processing would not completely erase evidence for $^{26}Mg^*$

(*e.g.*, Podosek *et al.*, 1991; Caillet *et al.*, 1993; MacPherson and Davis, 1993), which is generally not the case for the CH CAIs. The primitive nature of the CH CAIs is also supported by their pristine O-isotopic compositions (Kimura *et al.*, 1993; Sahijpal *et al.*, 1999; McKeegan *et al.*, 2002).

Based on the correlated occurrences of the short-lived radionuclides ^{41}Ca and ^{26}Al in the CAIs in CM and CV chondrites, it was suggested that these nuclides have a nucleosynthetic origin, and that CAIs lacking ^{26}Mg* may have formed prior to the injection of ^{26}Al into the CAI-forming regions within the collapsing protosolar cloud (Sahijpal *et al.*, 1998; Sahijpal and Goswami, 1998). This model excludes an heterogeneous distribution of ^{26}Al in the solar nebula (*e.g.*, Goswami and Vanhala, 2000). The ^{26}Al-free CAIs, including FUN (fractionated and unknown nuclear effect) inclusions, platy crystals (PLACs) and rare pyroxene-hibonite spherules in CO and CM chondrites (Ireland *et al.*, 1991; Russell *et al.*, 1998), are generally characterized by a highly refractory mineralogy and large non-radiogenic isotope anomalies (^{48}Ca, ^{50}Ti), indicating that they are incompletely vaporized presolar material (Ireland and Fegley, 2001). In contrast, the ^{26}Al-free CAIs from CH chondrites have group-II REE patterns and isotopically normal Ca and Ti, which is consistent with their condensation origin (a natural way to erase neutron-rich nucleosynthetic anomalies). If ^{26}Al has a nucleosynthetic origin, its absence in the CH CAIs may indicate their early formation by condensation (Krot *et al.*, 1999a).

It was suggested recently that ^{26}Al was produced locally, in the solar nebula, by cosmic-ray irradiation (Gounelle *et al.*, 2001; Shu *et al.*, 2001). The absence of ^{26}Al in the CH CAIs does not negate this model and may simply indicate that the CH CAI-forming region escaped production of short-lived radionuclides by irradiation.

Chondrules

Magnesian (type I) chondrules are the dominant chondrule type in the CR chondrite clan. Rare ferrous (type II) chondrules occur in CH and CR chondrites, but have not been yet systematically studied and are not described in this section. A subset of ferrous chondrules with euhedral metal grains occur in CH chondrites, described below, are the only exception (Krot *et al.*, 2000a). No type II chondrules were found in the CB chondrites HH 237, QUE 94411, Bencubbin, Gujba, and Weatherford.

Another rare chondrule type reported in the CR chondrite clan are Al-rich chondrules (Weber and Bischoff, 1997; Weisberg *et al.*, 2001, 2002a, unpubl. data; Krot and Keil, 2001; Krot *et al.*, 2001d). Based on their mineralogy, the Al-rich chondrules can be divided into anorthite-rich and Al-diopside-rich subtypes; the latter are exceptionally rare and were observed only in HH 237, QUE 94411, CH chondrites, and in the unique carbonaceous chondrite Adelaide (Krot *et al.*, 2001b,e).

Anorthite-Rich Chondrules in CR and CH Chondrites

Mineralogy and Petrography–Anorthite-rich chondrules (ARCs) are fairly common in CR chondrites (about 3–5 per thin section) and very rare (only one ARC was found) in CH chondrites (Weber and Bischoff, 1997; Hutcheon *et al.*, 2000; Krot, 2000; Krot and Keil, 2001; Weisberg *et al.*, 2002, unpubl. data). These chondrules consist of low-Ca and high-Ca pyroxenes, Mg-rich anorthitic plagioclase (An_{90-100}, 0.5–1.2 wt% MgO), Cr-rich olivine (Fa_{1-3}, 0.3–0.8 wt% Cr_2O_3), Cr-bearing spinel, FeNi-metal, and crystalline mesostasis composed of silica, anorthitic plagioclase, and high-Ca pyroxenes (Fig. 14a,b). The low-Ca and high-Ca pyroxenes have high contents of Al_2O_3, Cr_2O_3, and TiO_2 (Fig. 15). Several ARCs contain regions which are mineralogically similar to type I chondrules and composed of forsterite, Al_2O_3-poor (<0.5 wt%) low-Ca-pyroxene, and abundant FeNi-metal nodules. Igneous rims around ARCs are very rare. Several ARCs are associated with refractory inclusions which are FeNi-metal-free and composed of anorthite, spinel, ±Al-diopside, and ±olivine (Fig. 14c–h).

Trace Element and Isotope Chemistry–Trace element studies of ARCs in CR chondrites are virtually absent. REE abundances in plagioclase of the only analyzed ARC in Renazzo exhibit an essentially flat pattern (~20 × CI); no evidence for ^{26}Mg* was found in the plagioclase ($(^{26}Al/^{27}Al)_0 < 1.8 \times 10^{-5}$) (Weisberg *et al.*, 2002, unpubl. data). Only 1 of the 11 ARCs in CR chondrites analyzed by Marhas *et al.* (2000) showed clearly resolvable ^{26}Mg* corresponding to the $(^{26}Al/^{27}Al)_0$ of $(6.0 \pm 2.8) \times 10^{-6}$; two chondrules showed barely resolvable ^{26}Mg* corresponding to the $(^{26}Al/^{27}Al)_0$ of approximately $(4–5) \times 10^{-6}$; eight ARCs are devoid of radiogenic ^{26}Mg* ($(^{26}Al/^{27}Al)_0 < 10^{-6}$).

No ^{26}Mg* was found in anorthite of both the relic CAI and the host chondrule in the CH chondrite Acfer 182 shown in Fig. 14f–h; the estimated upper limits for $(^{26}Al/^{27}Al)_0$ are 6×10^{-6} and 4×10^{-6}, respectively (Krot *et al.*, 1999c,d). Spinel of the relic CAI in Acfer 182 chondrules is enriched in ^{16}O ($\delta^{18}O$, –37‰, $\delta^{17}O$, –40‰) relative to anorthite ($\delta^{18}O$, –13‰, $\delta^{17}O$, –15‰); chondrule pyroxenes have heavy oxygen-isotopic compositions ($\delta^{18}O$, +8‰, $\delta^{17}O$, +4‰). No oxygen isotope studies of ARCs in CR chondrites have been reported yet.

Magnesian Chondrules in Bencubbin, Weatherford, and Gujba

The silicates in Bencubbin occur as angular-to-subrounded millimeter-to-centimeter-sized clasts that appear to be chondrules or chondrule fragments (Weisberg *et al.*, 1987, 1990). Some silicates occur in clusters of millimeter-to-submillimeter-sized angular fragments intermixed with FeNi-metal. Texturally, the silicate fragments have BO and CC textures (Fig. 3d). The BO fragments consist of a single, or multiple, optically continuous olivine bars in parallel growth ($Fa_{3.5}$, 0.3–0.6 wt% Cr_2O_3) with a feldspathic mesostasis in between. In some fragments, low-Ca pyroxene (Fs_2Wo_1) occurs as large (millimeter-sized) crystals in between olivine bars.

Gujba is petrologically similar to Bencubbin and Weatherford (Rubin *et al.*, 2001; Weisberg *et al.*, 2002). However, the majority of chondrules are complete spheres, with a slight elongation. This is in contrast to Bencubbin and

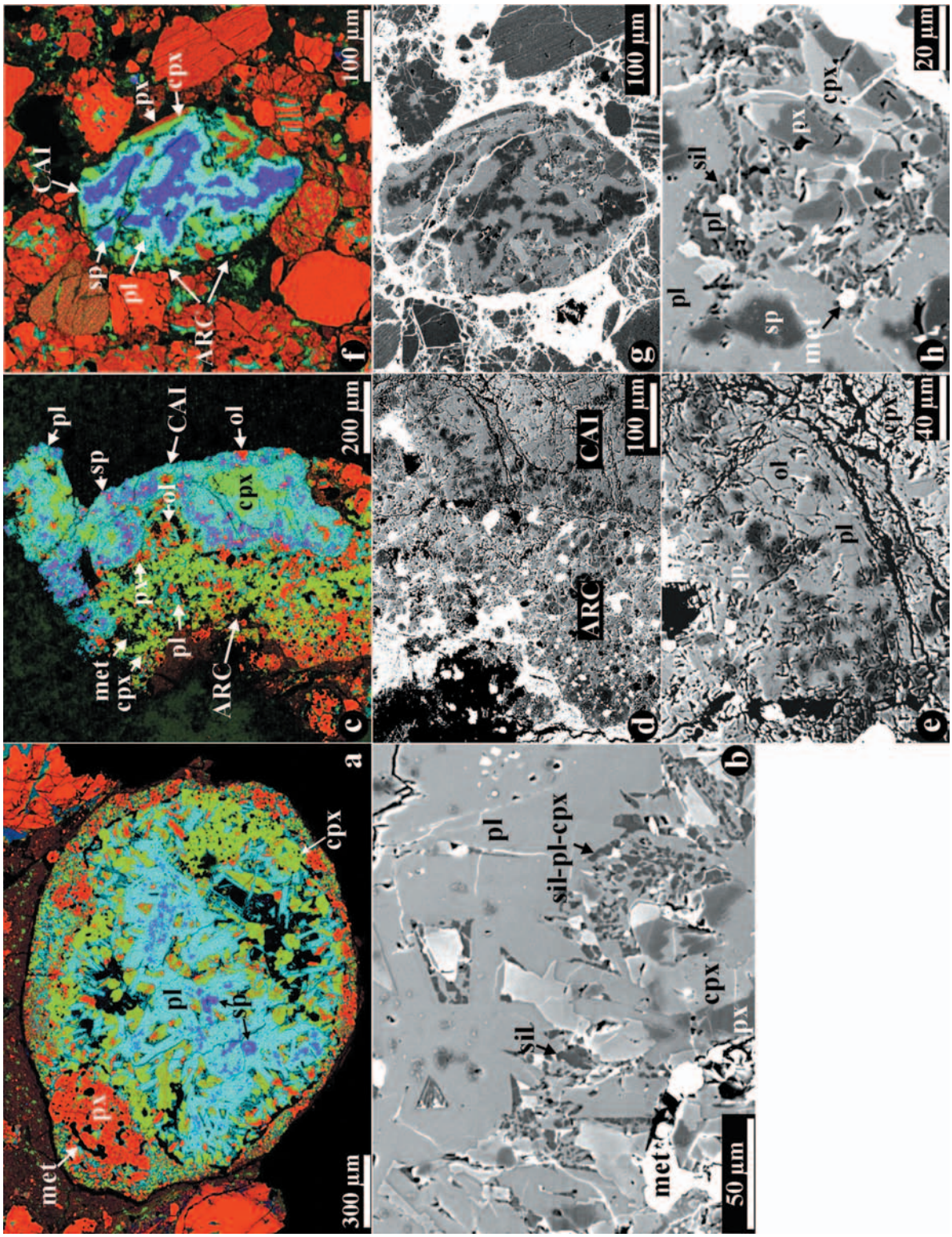

FIG. 14. Combined x-ray elemental maps (a, c, f) and BSE images (b, d, e, g, h) of the anorthite-rich chondrules from the CR chondrites EET 92042 (a, b) and Acfer 087 (c–e) and CH chondrite Acfer 182 (f–h). The chondrules consist of low-Ca pyroxene (px) overgrown by high-Ca pyroxene (cpx), forsteritic olivine (ol), anorthitic plagioclase (pl), FeNi-metal nodules, ±spinel (sp) and crystalline mesostasis composed of plagioclase, silica (sil) and high-Ca pyroxene. The Acfer 087 chondrule is associated with a CAI composed of anorthite, spinel, forsterite and Al-diopside. The Acfer 182 chondrule contains a relic CAI composed of spinel and anorthitic plagioclase.

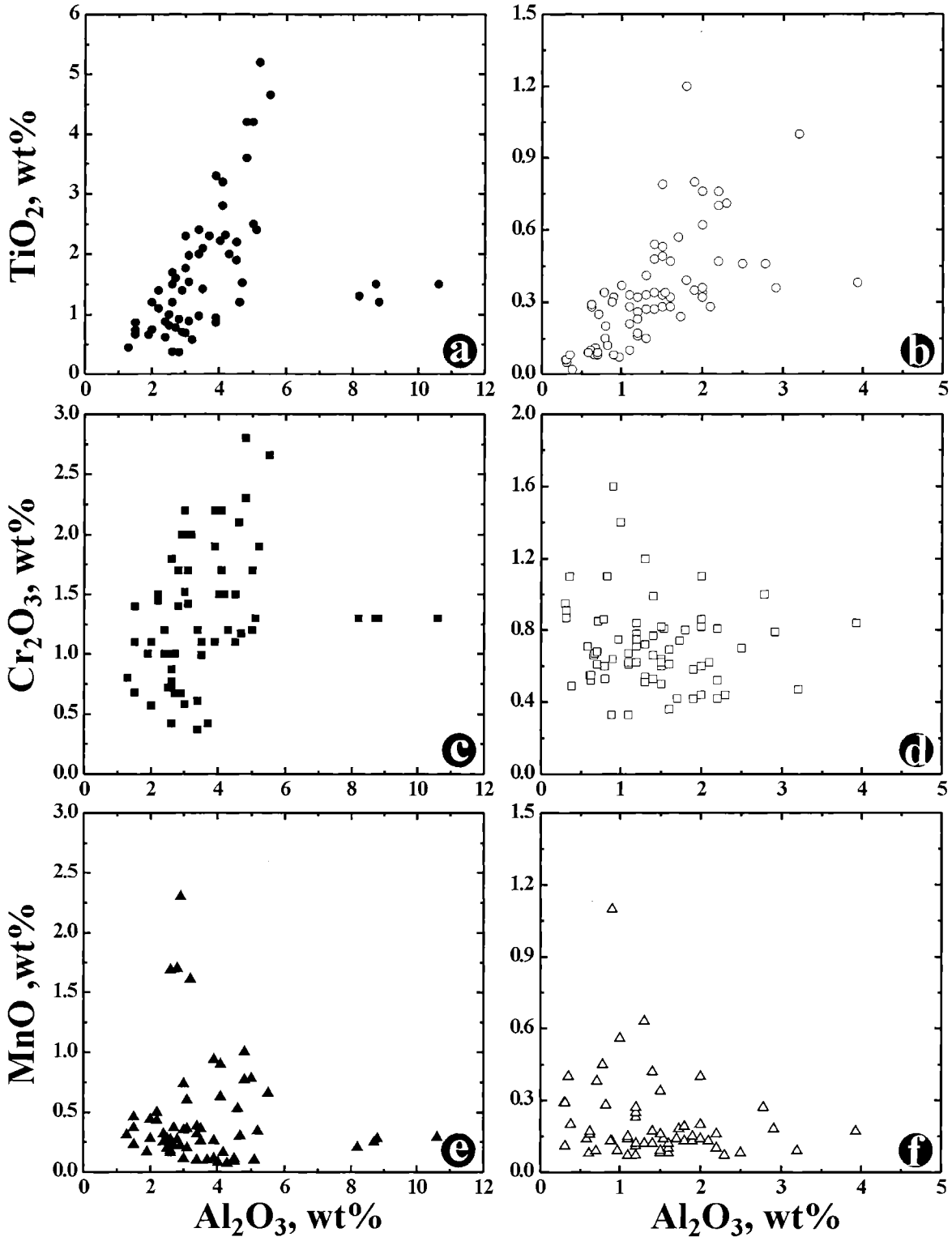

FIG. 15. Concentrations (in wt%) of TiO_2 (a, b), Cr_2O_3 (c, d) and MnO (e, f) *vs.* Al_2O_3 in high-Ca pyroxene (a, c, e) and low-Ca pyroxene (b, d, f) in anorthite-rich chondrules in CR chondrites.

Weatherford in which most chondrules are fragmented and highly deformed. Some BO chondrules contain micrometer-sized subhedral spinel grains. As in other CB chondrites, chondrules are FeNi-metal and sulfide-free.

Magnesian Chondrules in Hammadah al Hamra 237 and Queen Alexandra Range 94411

Chondrules in HH 237 and QUE 94411 have BO and CC textures; chondrules with porphyritic textures are absent (Figs. 3c and 16). BO chondrules are generally larger than CC chondrules (25–250 *vs.* 20–100 μm, respectively) and consist of Cr-rich forsteritic olivine (Fa_{2-4}; 0.2–0.6 wt% Cr_2O_3), low-Ca pyroxene ($Fs_{1-5}Wo_{4-7}$; 0.5–0.9 wt% Cr_2O_3), high-Ca pyroxene ($Fs_{2-4}Wo_{40-50}$; 0.6–1.2 wt% Cr_2O_3) and anorthitic mesostasis (Table 3; Fig. 16a–f). Both low-Ca and high-Ca pyroxenes contain high contents of Al_2O_3 (2–10 and 11–17 wt%) and TiO_2 (0.2–0.5 and 0.7–1.4 wt%, respectively). CC chondrules are poor in CaO and Al_2O_3 and have olivine-pyroxene normative compositions (Table 4). FeNi-metal nodules in chondrules are absent, whereas chemically zoned FeNi-metal grains typically contain silicate inclusions which are mineralogically similar to CC chondrules (Fig. 16g–i).

Chondrules are highly depleted in Mn, K, Na, and S (<0.05–0.07 wt%), but have relatively high contents of Cr_2O_3 (BO, 0.45 ± 0.1 wt%; CC, 0.7 ± 0.1 wt%) (Fig. 17a). BO chondrules are enriched (approximately (2–10) × CI) in refractory lithophile elements (such as Ca, Al, Ti, and REEs), whereas the abundance of these elements in CC chondrules varies from ~2 to 0.01 × CI (Fig. 17a,c).

Magnesian Chondrules in CH Chondrites

Two populations of magnesian chondrules were reported in CH chondrites: (1) A dominant population of small (~20 μm; up to 200 μm in Acfer 182), FeNi-metal-free CC and BO

TABLE 3. Microprobe analyses (in wt%) of olivine, pyroxenes and mesostasis in barred olivine chondrules from Queen Alexandra Range 94411.

Mineral	ol	px	px	px	px	px	cpx	cpx	cpx	mes	mes
SiO_2	41.7	55.9	53.5	51.6	54.0	52.7	48.4	48.6	43.9	50.3	51.9
TiO_2	0.06	0.42	0.32	0.37	0.28	0.39	1.1	1.4	0.85	0.27	1.33
Al_2O_3	0.17	3.1	4.6	6.6	8.3	10.0	10.9	11.0	17.1	25.7	21.0
Cr_2O_3	0.55	0.47	0.78	0.73	0.51	0.74	0.88	1.2	0.59	0.09	0.45
FeO	3.3	0.67	1.9	2.7	2.1	1.7	1.5	1.2	0.54	1.0	1.0
MnO	<0.07	<0.07	<0.07	<0.07	<0.07	<0.07	<0.07	0.07	<0.07	<0.07	<0.07
MgO	53.8	36.3	37.5	34.1	33.9	33.7	18.3	17.5	14.5	6.7	8.0
CaO	0.30	2.4	1.9	3.6	2.0	2.1	19.2	20.3	21.8	15.6	17.1
Na_2O	<0.05	<0.05	<0.05	<0.05	<0.05	<0.05	<0.05	0.05	<0.05	<0.05	0.07
K_2O	<0.04	<0.04	<0.04	<0.04	<0.04	<0.04	<0.04	<0.04	<0.04	<0.04	<0.04
Total	99.9	99.2	100.5	99.6	101.1	101.3	100.2	101.2	99.4	99.7	100.9
Fa	3.3	–	–	–	–	–	–	–	–	–	–
Fs	–	1.0	2.7	3.9	3.2	2.6	2.5	2.1	1.0	–	–
Wo	–	4.5	3.4	6.9	3.8	4.2	41.9	44.5	51.4	–	–

Abbreviations: ol = olivine; px = low-Ca pyroxene; cpx = high-Ca pyroxene; mes = mesostasis.

TABLE 4. Representative bulk compositions of CC and BO chondrules from Queen Alexandra Range 94411.

Chondrule	CC	CC	CC	CC	CC	BO	BO	BO	BO	BO	BO
SiO_2	55.1	54.9	55.5	55.2	54.5	49.9	50.3	47.8	47.4	48.3	46.5
TiO_2	<0.04	<0.04	<0.04	0.05	0.07	0.17	0.24	0.30	0.36	0.42	0.46
Al_2O_3	<0.04	0.11	0.15	1.1	1.3	3.7	5.5	7.7	9.3	10.4	13.8
Cr_2O_3	0.77	0.76	0.65	0.85	0.80	0.78	0.75	0.62	0.44	0.48	0.35
FeO	1.0	0.56	0.58	1.0	0.66	3.4	3.5	3.3	3.2	2.2	2.6
MnO	0.07	0.07	<0.07	0.12	0.12	0.14	0.16	<0.07	<0.07	<0.07	<0.07
MgO	44.3	44.7	44.3	42.0	42.9	38.3	36.7	35.3	33.1	32.5	28.0
CaO	<0.04	0.08	0.11	0.95	0.98	2.7	4.0	5.6	7.0	7.6	9.4
Na_2O	<0.05	<0.05	<0.05	<0.05	<0.05	0.07	<0.05	0.06	<0.05	<0.05	<0.05
K_2O	<0.04	<0.04	<0.04	<0.04	<0.04	<0.04	<0.04	<0.04	<0.04	<0.04	<0.04
Total	101.3	101.2	101.4	101.3	101.4	99.2	101.1	100.8	100.8	101.9	101.1

Abbreviations: CC = cryptocrystalline, BO = barred olivine.

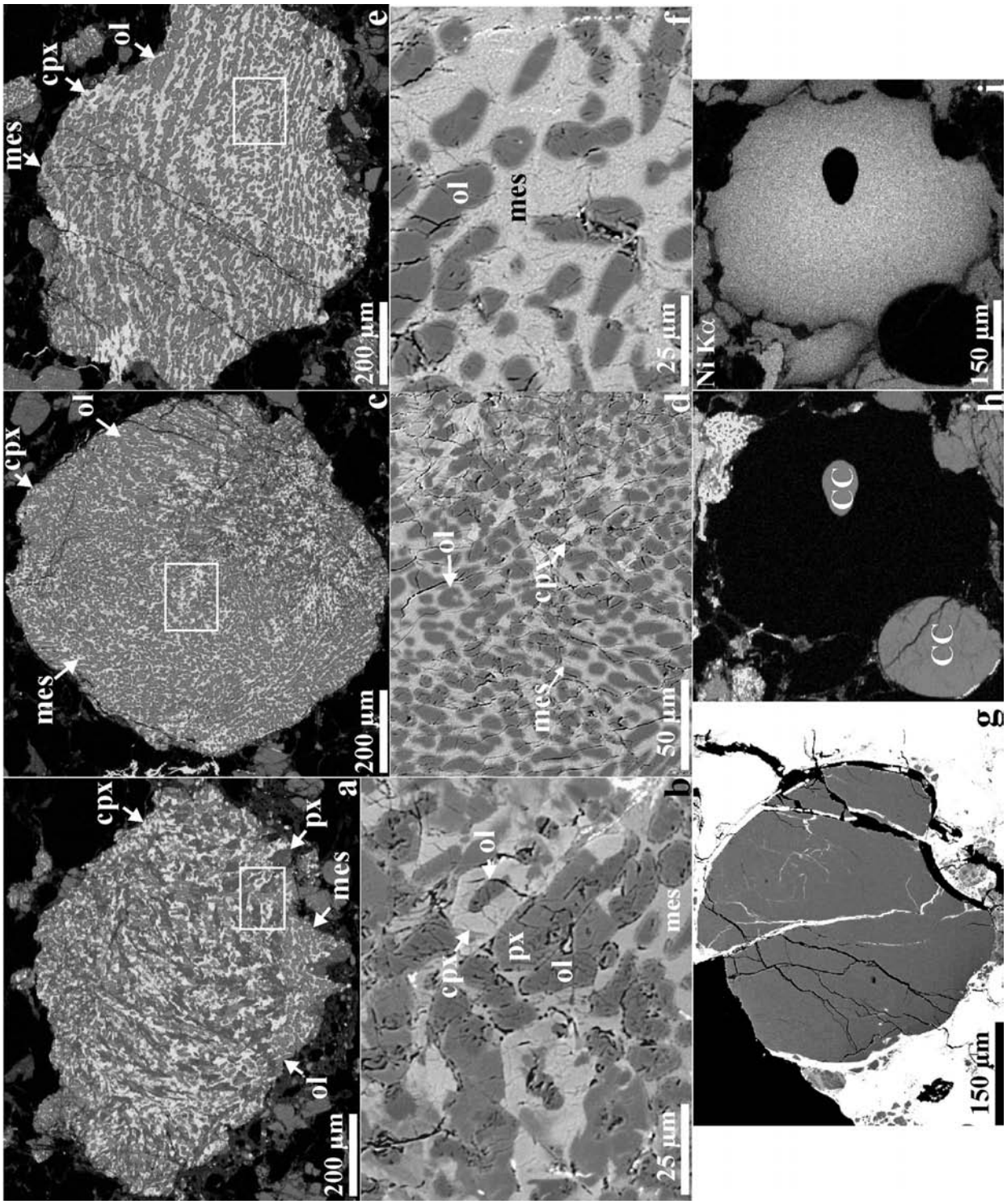

FIG. 16. Combined x-ray elemental maps (a, c, e, h), x-ray elemental map in Ni Kα (i) and BSE images (b, d, f, g) of chondrules from HH 237. (a–f) Barred olivine (BO) chondrules composed of forsteritic olivine (ol), low-Ca pyroxene (px), high-Ca pyroxene (cpx), and glassy mesostasis (mes). The modal abundances of these mineral phases vary in a broad range. (g–i) Cryptocrystalline (CC) chondrules and silicate inclusions inside chemically zoned FeNi-metal grains.

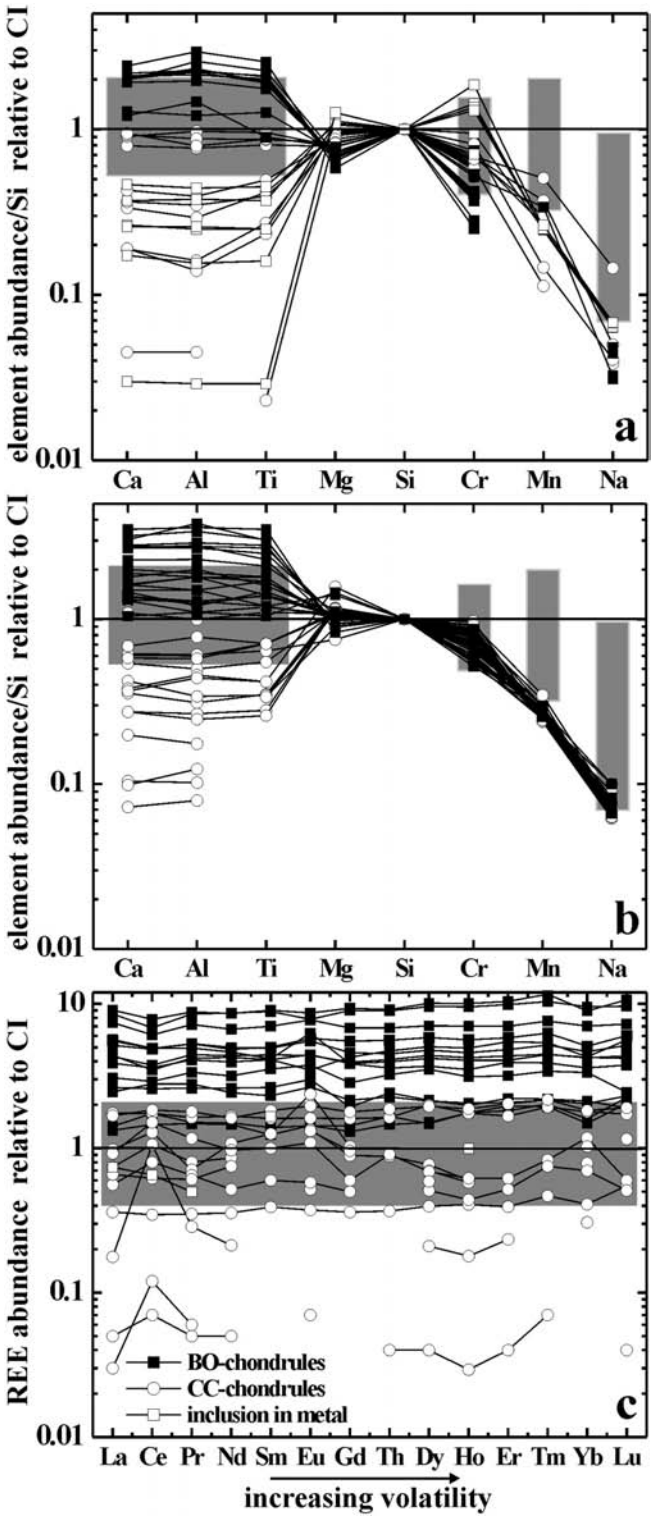

FIG. 17. (a, b) Bulk contents of lithophile elements normalized to Si and CI chondrite abundances in BO and CC chondrules from the HH 237 and QUE 94411 (a, c) and CH (b) chondrites. The chondrules show a large range in abundances of refractory lithophile elements, such as Ca, Al, Ti, and REEs, and are highly depleted in moderately volatile elements, such as Mn and Na. Shadow regions show compositional ranges of chondrules from other carbonaceous chondrites.

chondrules. These chondrules are texturally, mineralogically and chemically similar to BO and CC chondrules in HH 237 and QUE 94411 (Fig. 3b). Bulk Cr, Mn, K, and Na abundances in these chondrules decrease smoothly with increasing volatility; the abundances of refractory lithophile elements range from ~5 to 0.01 × CI (Fig. 17b). (2) A population of "normal" chondrules (>50 μm; >200 μm in Acfer 182), largely present as chondrule fragments, with porphyritic olivine (PO), porphyritic olivine-pyroxene (POP) and radial pyroxene (RP) textures (Fig. 3b) (Scott, 1988; Grossman *et al.*, 1988; Weisberg *et al.*, 1988; Wasson and Kallemeyn, 1990; Bischoff *et al.*, 1993b; Krot *et al.*, 2000b). These chondrules contain FeNi-metal nodules, have approximately CI level of refractory lithophile elements and up to 1 wt% of Na_2O in their mesostases (Grossman *et al.*, 1988). Compositions of the FeNi-metal grains are correlated with their locations: metal grains in chondrule cores have higher Ni and Co contents than those in chondrule peripheries (Krot *et al.*, 2000b).

Magnesian Chondrules in CR Chondrites

Most magnesian chondrules in CR chondrites have PO, POP, and porphyritic pyroxene (PP) textures and contain abundant FeNi-metal nodules; sulfides are generally absent; CC and BO chondrules are rare (Fig. 3a). The magnesian chondrules of porphyritic textures are commonly layered (Mason and Wiik, 1962; McSween, 1977; Prinz *et al.*, 1985a,b; Weisberg *et al.*, 1992, 1993; Krot *et al.*, 2000c). Their cores consist of olivine and/or low-Ca pyroxene phenocrysts and blebs of FeNi-metal set in a feldspathic glassy or phyllosilicate mesostasis. Core olivine and pyroxenes are Mg- and Cr-rich (about 0.5–1 wt% Cr_2O_3, Fa/Fs_{1-4}) (Table 5); metal blebs have up to 14 wt% Ni and a solar Co/Ni ratio (Fig. 4 in Weisberg *et al.*, 1993). The phyllosilicate mesostasis is a mixture of two or more phyllosilicates including serpentine and/or chlorite minerals.

The rim layers consist of olivine and/or pyroxene, feldspathic mesostasis, and FeNi-metal. Some rims appear to be multi-layered with layers of metal followed by an olivine- and/or pyroxene-rich layer; many rims have silica-rich outer layers (Fig. 18). Silica is absent in the rims around Renazzo and Al Rais chondrules, which are among the most heavily altered CR chondrites (Krot *et al.*, 2000c). The absence of silica in Renazzo and Al Rais chondrules could be a result of its replacement by phyllosilicates. In comparison to the cores, the rims have somewhat higher contents of ferrosilite, MnO, and Cr_2O_3 in pyroxenes; mesostasis has higher contents of Ab and Or components (Fig. 19); FeNi-metal has lower concentrations of Ni (<6 wt%) a solar Co/Ni ratio (Fig. 4 in Weisberg *et al.*, 1993).

Oxygen isotope measurements of separated cores and igneous rims from layered chondrules in El Djouf 001 showed that the cores and rims lie on a slope 0.7 CR-mixing line with each rim consistently having heavier oxygen that its core (Fig. 1 in Weisberg *et al.*, 1992). No evidence for evaporative mass fractionation of Si and Mg isotopes were found in pyroxene and olivine of the El Djouf 001 layered chondrules (Fig. 2 in Huss *et al.*, 1996).

TABLE 5. Microprobe analyses (in wt%) of the pyroxenes and olivine a silica-rich igneous rim and host chondrule from the CR chondrite Pecora Escarpment 91082.

	Chondrule			Silica-rich rim				
	ol	px	px	px	px	px	px	px
SiO_2	42.0	59.0	51.6	58.5	56.9	55.3	53.4	51.5
TiO_2	<0.03	0.05	0.72	0.07	0.18	0.22	0.33	0.58
Al_2O_3	0.05	0.26	3.6	0.41	0.91	1.3	2.1	3.3
Cr_2O_3	0.76	0.61	3.3	1.6	2.7	2.9	3.4	3.2
FeO	2.5	1.4	1.5	2.1	2.1	2.4	2.3	1.5
MnO	0.44	0.03	2.0	0.86	2.9	4.2	4.4	4.1
MgO	54.9	38.8	18.5	36.1	33.5	29.2	24.3	18.3
CaO	0.10	0.14	18.1	0.41	1.5	4.5	9.4	16.9
Na_2O	<0.05	<0.05	<0.05	<0.05	<0.05	0.05	0.08	0.22
K_2O	<0.03	<0.03	<0.04	<0.03	<0.03	<0.03	<0.03	<0.03
Total	100.9	100.2	99.49	100.0	100.7	100.1	99.6	99.6
Fs	–	1.9	2.7	3.1	3.3	4.0	3.9	2.6
Wo	–	0.2	40.2	0.8	3.0	9.7	20.9	38.9
Fa	2.5	–	–	–	–	–	–	–

Abbreviations: ol = olivine; px = low-Ca pyroxene.

Ferrous Chondrules with Euhedral to Unhedral FeNi-Metal Grains in CH Chondrites

Ferrous chondrules, 15–30 μm in apparent diameter, with rounded-to-euhedral FeNi-metal grains are found in all CH chondrites (Fig. 1 in Krot *et al.*, 2000a). The silicate portions of the chondrules consist of CC, ferrous (Fe/(Fe + Mg) $\approx$ 0.11–0.35) silicate material and $\pm SiO_2$-rich glasses. Similar to the magnesian CC chondrules, the CC ferrous material has an olivine-pyroxene-normative composition and is highly depleted in CaO, Al_2O_3, and TiO_2 (typically below the detection limits of the electron microprobe: <0.03–0.04 wt%). However, this material is enriched in MnO and Na_2O compared to the magnesian CC chondrules (Fig. 14b). Metal grains in ferrous chondrules are compositionally uniform within the grains, but show significant intergrain compositional variations (about 8–18 wt% Ni, <0.09 wt% Cr) and have subsolar Co/Ni ratio. There is a positive correlation between Fe/(Fe + Mg) in the silicate portions of the spherules and Fe concentration in the metal grains. This is inconsistent with oxidation/reduction of iron ($FeO_{sil} \square Fe_{met}$) during melting of solid precursors, but consistent with condensation origin under highly oxidizing conditions, possibly as liquids (Krot *et al.*, 2000a). The extreme depletion of the ferrous spherules in Ca, Al, and Ti suggests that the condensation occurred in a fractionated system. Although a similar depletion in refractory lithophile elements is observed in some magnesian CC chondrules (Fig. 14b), the genetic relationship between these chondrule types remains unclear. Because liquidus temperatures of the euhedral FeNi-metal grains are systematically lower than those of the coexisting ferrous silicates, it was concluded that the former crystallized from supercooled melts (Krot *et al.*, 2000a).

Silica-Rich Chondrules in CH Chondrites

Silica-rich chondrules, both magnesian and ferrous, are found in all CH chondrites (Kimura and El Goresy, 1989). These chondrules are depleted in Mg and Cr relative to other chondrules in CH chondrites (Fig. 14b). Petaev and Krot (1999) suggested that silica-rich precursors resulted from gas–solid condensation with significant degree of isolation of earlier condensed forsterite.

FeNi-Metal

Meibom *et al.* (2001a) reviewed in detail the mineralogy, petrography, and trace element chemistry of FeNi-metal from the CR chondrite clan. Here, only the most important observations are discussed.

FeNi-Metal in Bencubbin, Gujba, and Weatherford

The Bencubbin, Gujba, and Weatherford meteorites contain about 40–60 vol% FeNi-metal that occurs exclusively outside the silicate nodules as rounded to angular metal–sulfide aggregates with sizes ranging from ~0.1 to ~10 mm (Figs. 4d and 20a) (McCall, 1968; Newsom and Drake, 1979; Dehn and McCoy, 1998; Rubin *et al.*, 2001; Campbell *et al.*, 2002). The aggregates consist of sulfide-free and sulfide-bearing kamacite grains ranging in size from about 10 to 300 μm, which are sintered together, with sulfide blebs frequently occurring at the grain margins.

Metal in individual aggregates is compositionally uniform, but there are compositional differences between the aggregates (in wt%): Ni, about 5–7.5; Co, 0.25–0.35; Cr, 0.07–0.33; P, 0.16–0.35 (Newsom and Drake, 1979). Phosphorous is homogeneously distributed within an aggregate. Chromium is positively correlated with Ni and shows evidence for

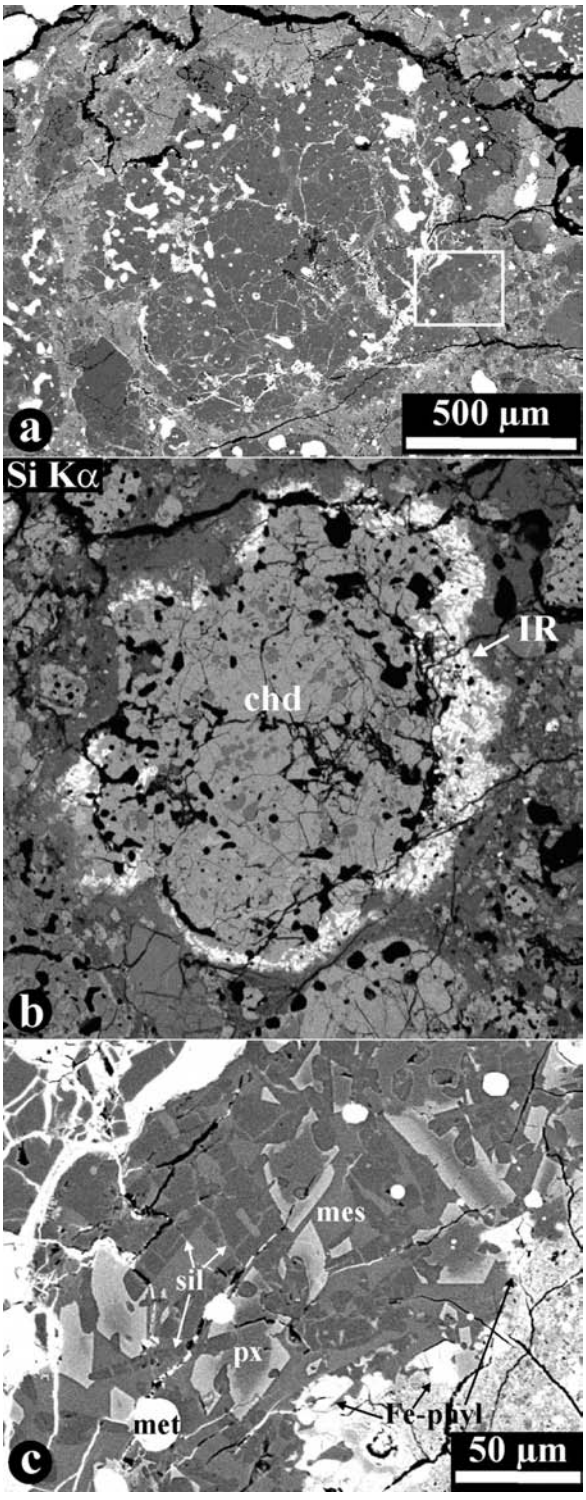

FIG. 18. BSE images (a, c) and x-ray elemental map in Si Kα (b) of a POP chondrule surrounded by a silica-rich igneous rim from the CR chondrite GRA 95229. Region outlined in (a) is shown in detail in (c). The rim consists of rounded and prismatic grains of silica (sil), zoned pyroxene grains (px), glassy mesostasis (mes) and rounded FeNi-metal nodules (met). Silica grains along the peripheral portion of the rim are replaced by Fe-phyllosilicate (Fe-phyl).

redistribution between FeNi-metal and sulfides; Cr is depleted by up to 25% in metal adjacent to sulfide inclusions, which are composed of Cr-rich troilite and daubreelite (Ramdohr, 1973; Newsom and Drake, 1979).

Platinum group elements (PGEs: Os, Ir, Pt, Ru, Rh, Pd) are enriched in the most Ni-rich (~7.5 wt%) metal by about (1.5–2) × CI (Fe normalized) and are present at ~1 × CI levels in low-Ni metal (~5 wt%) grains. All PGEs, including Pd, are positively correlated with Ni (Campbell *et al.*, 2002). Moderately volatile elements, such as Cu, Ga, Ge, As, Sb, and Sn, are depleted by factors of about 10–1000 (normalized to Fe and CI), and these depletions correlate with increasing volatility (Kallemeyn *et al.*, 1978; Campbell *et al.*, 2002).

FeNi-Metal in Hammadah al Hamra 237 and Queen Alexandra Range 94411

The QUE 94411 and HH 237 meteorites contain about 60–75 vol% FeNi-metal (Zipfel *et al.*, 1998; Righter and Chabot, 1998; Weisberg *et al.*, 2001). Metal occurs exclusively outside chondrules in three textural forms: (1) compositionally zoned grains (100–500 μm) comprising 15–25% of the metal grains (Fig. 4c) and often enclosing silicate inclusions (Fig. 16h,i). Sulfides associated with the zoned FeNi-metal grains were not observed. (2) Compositionally homogeneous grains (100–300 μm). (3) Large (millimeter-sized) metal–sulfide aggregates texturally similar to those in Bencubbin, Gujba, and Weatherford consisting of kamacitic metal grains containing micrometer blebs of troilite and, in some cases, displaying triple junctions outlined by troilite (Fig. 20b). A thin rim of high-Ni metal is present around some troilite blebs (Weisberg *et al.*, 2001).

All textural types of metal are characterized by a solar Co/Ni ratio (Fig. 5a). The compositionally zoned grains have Ni and Co concentrations decreasing from high levels (Ni, about 10–15 wt%; Co, about 0.45–0.55 wt%) in the center to lower levels (Ni, about 3–6 wt%; Co, about 0.15–0.2 wt%) at the edge of the grains (Fig. 21a). Chromium is negatively correlated with Ni and Co; its concentration increases from the core (about 0.1–0.15 wt%) towards the periphery (about 0.2–0.35 wt%) of a grain. PGEs (Os, Ir, Ru, Pt, and Rh) are zoned in a manner similar to Ni and Co with Fe-normalized abundances at about (2.5–4) × CI in the center of the grains, dropping off to ~1 × CI at the edge (Fig. 21b,c). Palladium is the exception, displaying essentially flat concentration profiles. Moderately volatile siderophile elements, such as Cu, Ga, As, and Sn, are strongly depleted. Copper is depleted by about a factor of ~500 (normalized to Fe and CI) in the core and displays a very steep increasing gradient close the edge of the zoned grains. Germanium is depleted by a factor of ≥250 in the core and is less depleted at the edge. Gallium, As, and Sn are also depleted by large factors, but fall below the current detection limits by laser inductively coupled plasma-mass spectrometry (Campbell *et al.*, 2001).

FeNi-Metal in CH Chondrites

The CH chondrites contain ~20 vol% FeNi-metal. Most of the metal occurs outside chondrules (Fig. 4b) as irregularly

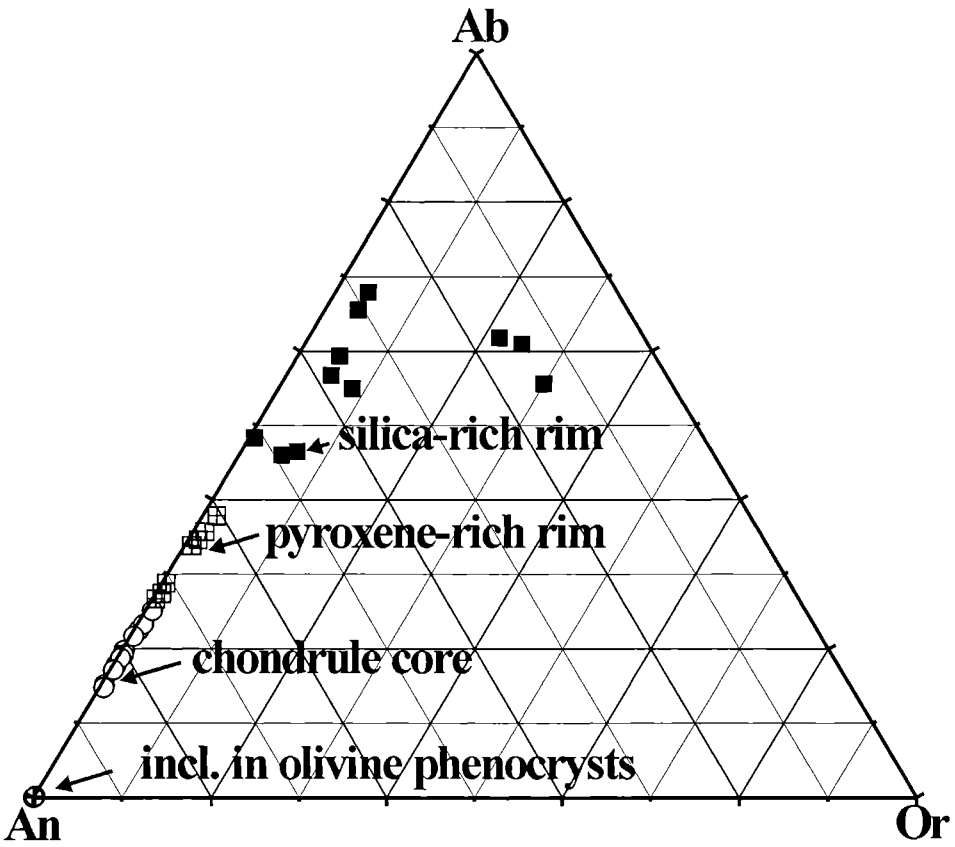

FIG. 19. Compositions of plagioclase in anorthite-rich chondrules and glassy mesostases in type I chondrules and silica-rich igneous rims around them in CR chondrites, in terms of mol% An (anorthite, $CaAl_2Si_2O_8$), Or (orthoclase, $KAlSi_3O_8$) and Ab (albite, $NaAlSi_3O_8$).

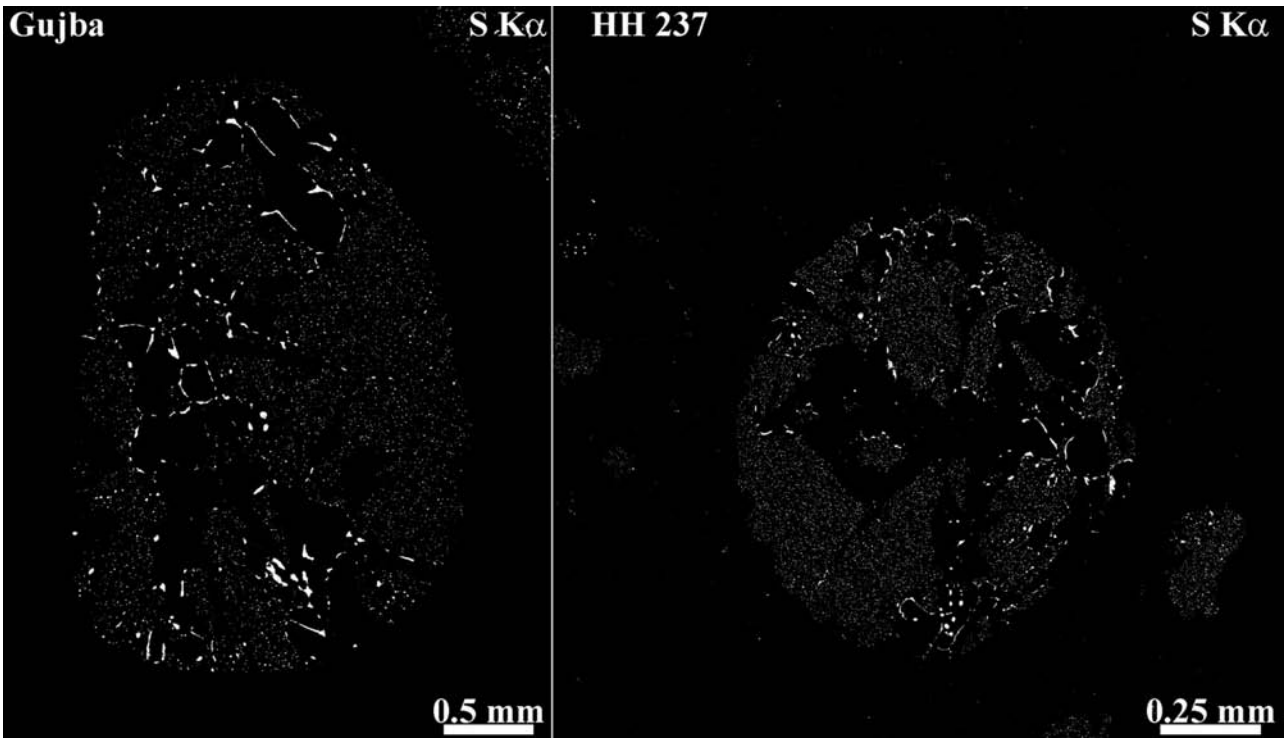

FIG. 20. X-ray elemental maps in S Kα of metal–sulfide aggregates in Gujba (a) and HH 237 (b).

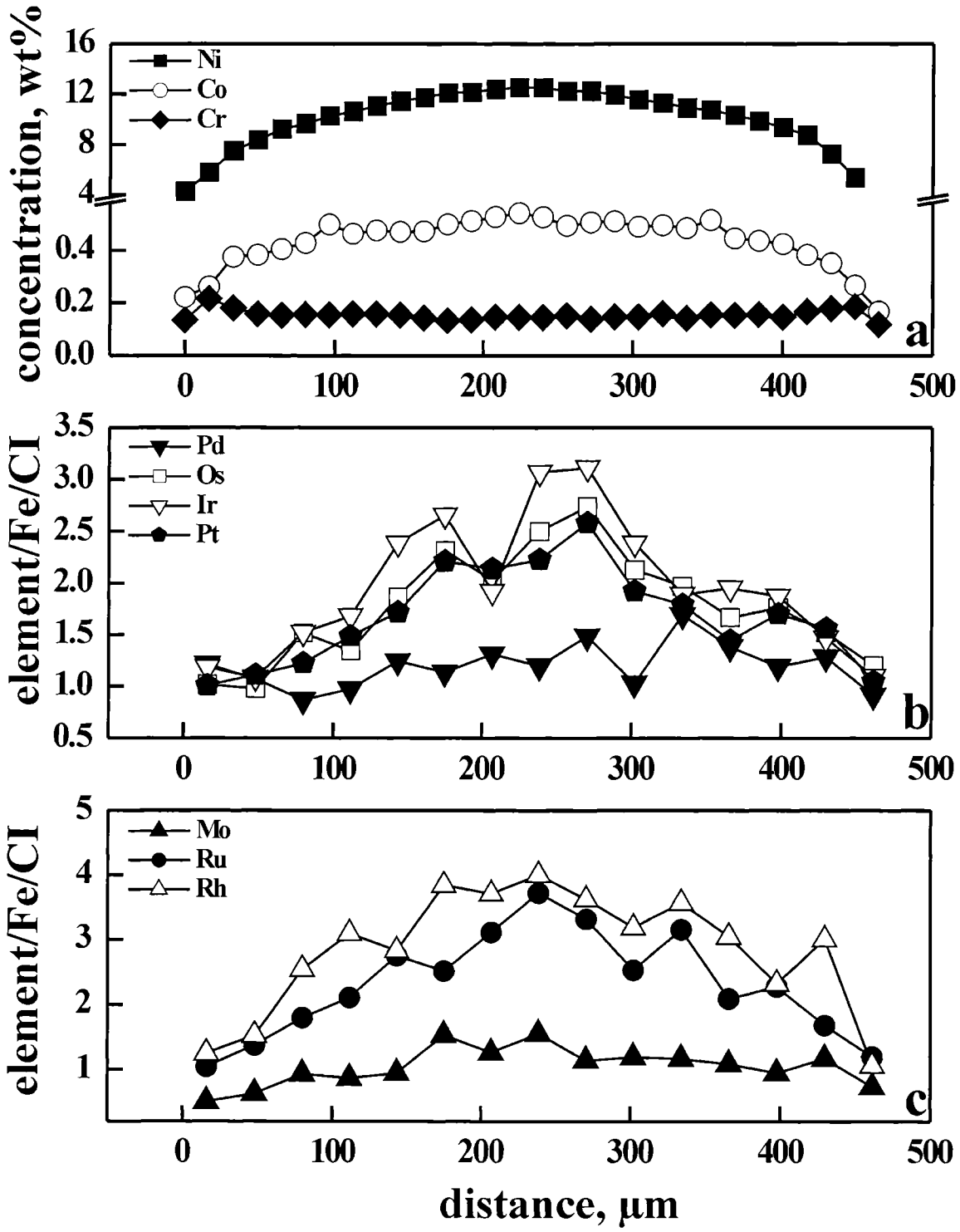

FIG. 21. (a) Compositional profiles across a chemically zoned FeNi-metal grain in QUE 94411. Ni and Co are positively correlated; the Co/Ni ratios is solar. (b, c) Concentrations of PGEs in the zoned FeNi-metal grain (data from Campbell *et al.*, 2002). The highly refractory PGEs (Os, Ir, Pt, Ru, Rh) show Fe-normalized abundances enriched by a factor of (2.5–3) × CI in the center of the grain and decreasing to roughly CI levels at the edge. Palladium, which has a condensation temperature similar to Fe and Ni, is not zoned.

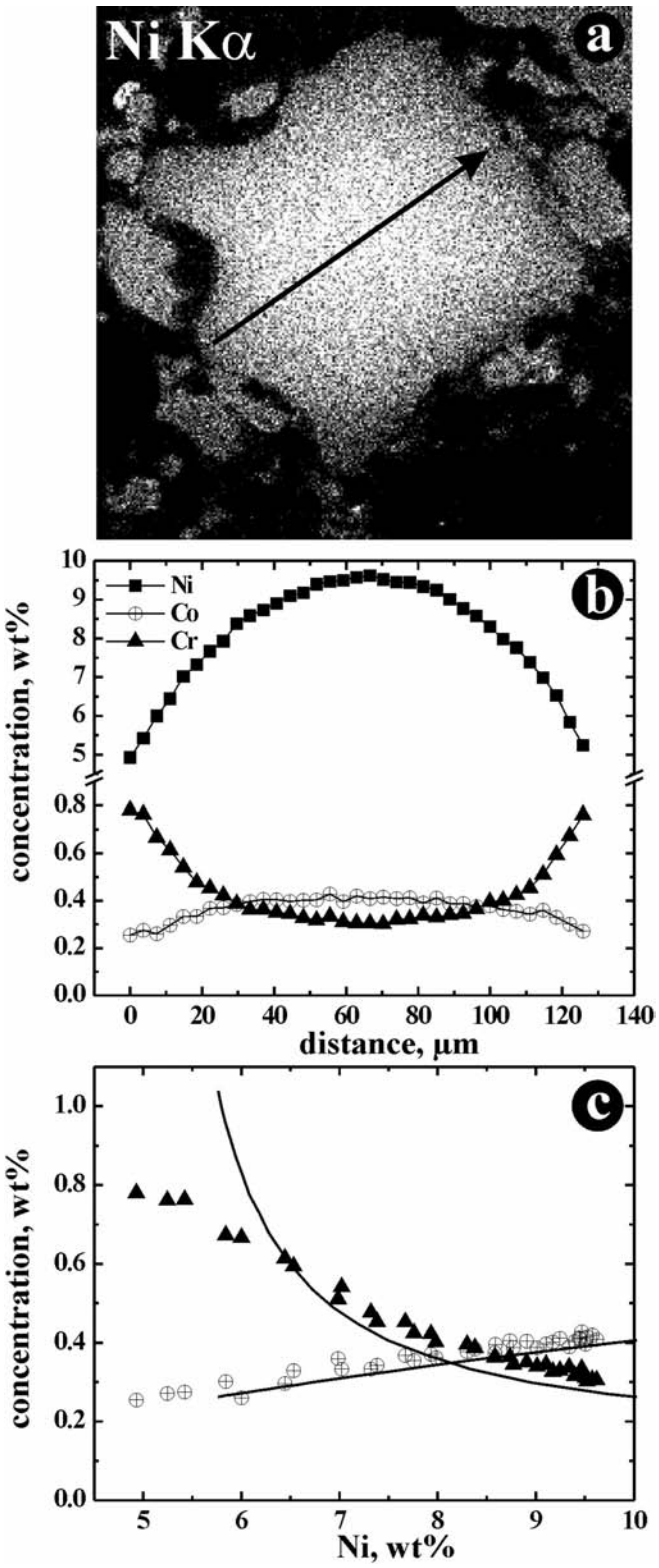

FIG. 22. *(right)* (a) X-ray elemental map in Ni Kα of a compositionally zoned FeNi metal grain in the CH chondrite PAT 91546. The Ni concentration is highest in the center of the grain and decreases smoothly towards the edges. The arrow (~130 μm) indicates the path of the electron microprobe traverse shown in (b). (b) Ni and Co are positively correlated with a roughly solar Co/Ni ratio; Cr is anti-correlated with Ni and Co and increases from center to edge. (c) Concentrations of Cr and Co *vs.* Ni. Solid lines represent thermodynamically calculated equilibrium condensation paths of non-ideal metal solutions from a gas of solar composition (dust/gas ratio = 1) at a total gas pressure of 10^{-4} bar (Meibom *et al.*, 1999a).

shaped grains ranging in size from a few to several hundred micrometers (Bischoff *et al.*, 1993b; Grossman *et al.*, 1988; Scott, 1988; Wasson and Kallemeyn, 1990; Weisberg *et al.*, 1988; Meibom *et al.*, 1999a). Metal inside chondrules is rare and largely associated with magnesian (type I) porphyritic chondrules (Meibom *et al.*, 2001, unpubl. data). Ferrous CC chondrules with rounded-to-euhedral metal grains are rare, but found in all CH chondrites (Krot *et al.*, 2000a).

Most metal grains have compositions within the following ranges: Ni, about 4–12 wt%, Co, about 0.2–0.5 wt%, Cr, about 0.05–0.8 wt%, P, about 0.05–0.35 wt% and have a solar Co/Ni ratio (Fig. 5b) (Scott, 1988; Weisberg *et al.*, 1988; Meibom *et al.*, 1999a, 2001, unpubl. data). A small fraction of the larger (>50 μm) individual metal grains display smooth compositional zoning with decreasing Ni (about 4–10 wt%) and Co (about 0.3–0.5 wt%) and increasing Cr (about 0.3–0.8 wt%) from core to edge (Fig. 22). Metal grains inside chondrules are compositionally uniform with Ni and Co systematically decreasing from the core towards the edge of the chondrules (Ni, about 4–9 wt%; Co, about 0.2–0.4 wt%) (Fig. 1 in Krot *et al.*, 2000b).

FeNi-Metal in CR Chondrites

The CR chondrites contain about 7–9 vol% FeNi-metal primarily associated with chondrules (Fig. 4a) (Weisberg *et al.*, 1993, 1995). It occurs as rounded to subrounded nodules in four textural settings: (1) inside chondrules, with sizes ranging from about 1 to 1000 μm, ~45 vol% of the metal; (2) at chondrule margins, with sizes ranging from about 1 to 600 μm, ~15% of the metal; (3) in coarse-grained igneous rims around chondrules, with sizes from about 5–25 μm, ~20% of the metal; and (4) in fine-grained matrix, with sizes ranging from about 10 to 1000 μm, ~20% of the metal (Lee *et al.*, 1992). The largest metal objects in the matrix are sometimes referred to as metallic chondrules (Wood, 1962; Lee *et al.*, 1992; Weisberg *et al.*, 1993).

Most FeNi-metal grains are characterized by a solar Co/Ni ratio. Metal compositions fall within the ranges: Ni, about 4–15 wt%; Co, about 0.1–0.5 wt%; Cr, about 0–1.8 wt%; P, about 0–1.1 wt% (Weisberg *et al.*, 1993). Metal grains inside chondrules are characterized by higher Ni and Co concentrations (Ni > about 5 wt%, Co > about 0.2 wt%) and a wider compositional range than grains at the chondrule margins and rims (Ni < about 6 wt%, Co < about 0.3 wt%) (Weisberg *et al.*, 1993). Metal inside individual chondrules is fairly similar in composition, but there are substantial variations between chondrules (*e.g.*, Lee *et al.*, 1992; Zanda *et al.*, 1994; Weisberg *et al.*, 1993).

Moderately volatile siderophile elements (such as Au, As, Cu, Sb, and Ga) are depleted in the metal (Fe-nomalized)

relative to CI by up to an order of magnitude and the depletions correlate with increasing volatility (Kong *et al.*, 1999; Kallemeyn *et al.*, 1994). Volatility controlled depletions are also observed among PGEs. Metal in chondrule interiors generally have Os, Ir, and Pt (Fe-normalized) abundances at ~1.5 × CI and Au depleted by approximately an order of magnitude (Connolly *et al.*, 2001). Metal in igneous rims has Os, Ir, and Pt (Fe-normalized) abundances at ~0.2 × CI and Au at about (0.05–0.5) × CI (Connolly *et al.*, 2001). Metal grains occurring in matrix are chemically similar to metal in chondrules and are believed to have been derived from them.

Discussion (II)

Existing Models for the Origin of FeNi-Metal and Chondrules in the CR Clan–There is no consensus on the origin of the FeNi-metal grains in the CR clan. Proposed models for the origin of different types of FeNi-metal in CR clan described above include: (1) metal–silicate equilibration during chondrule formation (FeNi-metal in CRs) (Zanda *et al.*, 1994); (2) reduction from silicates followed by evaporation and partial recondensation during chondrule formation (FeNi-metal in CRs) (Connolly *et al.*, 2001); (3) gas–solid condensation prior to and/or during chondrule formation (FeNi-metal in CRs, CHs, HH 237 and QUE 94411) (Weisberg *et al.*, 1993; Meibom *et al.*, 1999a, 2001, unpubl. data); and (4) condensation from an impact produced gas highly enriched in siderophile elements (up to 10^7 × CI) gas (FeNi-metal–sulfide aggregates in Bencubbin, Gujba, Weatherford, HH 237, and QUE 94411) (Wasson and Kallemeyn, 1990; Campbell *et al.*, 2002).

The origin of chondrules in CHs, QUE 94411, and HH 237 and silicate nodules in Bencubbin, Gujba, and Weatherford is also controversial (*e.g.*, Wasson and Kallemeyn, 1990; Wasson, 2000, pers. comm.; Scott, 1988; Weisberg *et al.*, 1988; Grossman *et al.*, 1988; Bischoff *et al.*, 1993b; Rubin *et al.*, 2001; Campbell *et al.*, 2002). Wasson and Kallemeyn (1990) hypothesized that a large impact on a CR-like asteroid resulted in devolatilization, reduction, and formation of small CC chondrules in CH chondrites by gas–liquid condensation in the vapor cloud. A similar origin was proposed for the silicate nodules in Bencubbin, Gujba, and Weatherford by Rubin *et al.* (2001) and Campbell *et al.* (2002). Other authors (Scott, 1988; Weisberg *et al.*, 1988; Grossman *et al.*, 1988) have concluded that CC chondrules in CH chondrites formed by nebular processes and suggested that their low concentrations of moderately volatile elements are due to prolonged heating above the liquidus temperature. Based on the observed negative correlation between refractory Be and volatile B, Brearley and Layne (1995) concluded that the low abundance of moderately volatile elements in the CH CC chondrules is a condensation signature of their precursors.

We argue below that FeNi-metal grains in CR clan formed by gas–solid condensation; indeed most chondrules in CR clan formed at high ambient nebular temperatures. Metal–silicate equilibration, evaporation and recondensation during chondrule formation could have modified the primary condensation signatures of the CR and some CH metal grains, but did not entirely erase them. The origin of FeNi-metal–sulfide aggregates and silicate nodules in Bencubbin, Gujba, Weatherford, HH 237 and QUE 94411 remains unclear.

Origin of Compositionally Zoned Metal Grains in Hammadah al Hamra 237, Queen Alexandra Range 94411, and CH Chondrites–Thermodynamic calculations of equilibrium FeNi-metal condensation from a gas of solar composition (Fig. 22c) provide a reasonable match to the measured interelement correlations in the zoned CH metal grains at temperatures from about 1370 to 1270 K (Meibom *et al.*, 1999a, Petaev *et al.*, 1999). However, the very presence of compositional zoning and the observation of subsolar Ni/Fe ratios at the edge of some zoned CH metal grains imply that equilibrium between the gas and the growing metal grains was not attained (Meibom *et al.*, 1999a; Petaev *et al.*, 1999). Disequilibrium condensation, in which earlier formed metal is partially isolated from reactions with the nebular gas, conceivably as a result of grain-overgrowth, allow for the condensation of metal with subsolar Ni/Fe ratio and such calculations provide a much improved match to the compositional data (Meibom *et al.*, 1999a; Petaev *et al.*, 1999).

Similar conclusions were reached for a suite of compositionally zoned grains from QUE 94411 and HH 237 (Petaev *et al.*, 2000, 2001). However, the Cr concentrations in these metal grains are lower by a factor of about 3–4 compared with the CH zoned metal grains (Weisberg and Prinz, 1999; Meibom *et al.*, 1999a; Petaev *et al.*, 2001). This could have been accomplished if some Cr was incorporated into silicates condensing from a relatively oxidizing gas before FeNi-metal (Petaev and Wood, 2001; Petaev *et al.*, 2001). Several observations in QUE 94411, HH 237, and CHs are consistent with this model: (1) enrichment of chondrule silicates in Cr_2O_3 (about 0.4–0.7 wt%) and FeO (about 1–4 wt%), (2) the absence of metal grains inside chondrules, and (3) the presence of CC chondrules inside chemically zoned metal grains (Krot *et al.*, 2001a). Oxidizing conditions could have been achieved by vaporization of a nebular region with initially enhanced (about 10–50 × solar) dust/gas ratio (Krot *et al.*, 2001a; Petaev *et al.*, 2001; Petaev and Wood, 2001). (The term "dust" is defined here as a solid phase containing all elements in cosmic proportion, with the exception of H and the noble gases (Anders and Grevesse, 1989). The dust/gas ratio is the atomic Si/H ratio normalized to the solar Si/H ratio of 3.58×10^{-5}.) Under these conditions the zoned metal grains in QUE 94411 and HH 237 are inferred to have condensed in the temperature interval from 1500 to 1400 K, at 10^{-4} atm (Petaev *et al.*, 2001).

The PGE distributions in the zoned metal grains from QUE 94411 and HH 237 refine these conclusions (Fig. 21b,c). Equilibrium condensation models predict that the refractory PGEs condense from the nebular gas at temperatures hundreds of degrees above the condensation temperature of FeNi-metal. This would lead to extreme enrichments in refractory PGEs in the earliest formed metal, noticeable as a spike in refractory PGE concentrations in the core of the metal grains; later formed

metal surrounding the core region would contain virtually no refractory PGEs (Campbell *et al.*, 2001). Conversely, the moderately high PGE abundances and their smooth distributions indicate that the PGEs were not sequestered in earlier formed nuggets, but were continuously accessible in the nebular gas to be incorporated into the zoned grains. At the temperature of FeNi-metal condensation, the nebula was highly supersaturated in refractory PGEs (Campbell *et al.*, 2001). These observations call for a condensation model for the formation of the zoned FeNi metal grains in QUE 94411 and HH 237 in which the condensation at high temperature of refractory PGEs was kinetically inhibited by the combined effects of (1) a lack of nucleation sites, (2) the low density of PGEs in the nebular gas, and (3) a relatively fast cooling rate of the nebular gas (discussed below) (Campbell *et al.*, 2001; Meibom *et al.*, 2001, unpubl. data).

Other processes have been considered for the formation of the zoned FeNi-metal grains, including fractional crystallization and reduction of FeO in silicates to metallic Fe followed by diffusion of Fe (and Cr) into initially homogeneous, high-Ni metal grains (Lee *et al.*, 1992; Zanda *et al.*, 1994). However, fractional crystallization can be ruled out because Os, Ir, Pt, Ru, and Rh correlate positively with Ni, opposite to the trends produced by fractional crystallization (Wasson, 1985; Campbell *et al.*, 2001). Reduction of FeO in silicates and diffusion into FeNi-metal can also be ruled out because Pd does not display zonation (Fig. 21b). If the zoning pattern was established by the addition of Fe (and Cr) diffusing into the grains from the edge all elements with condensation temperature higher than or similar to Fe, including Pd, would show compositional zoning similar to Ni (Campbell *et al.*, 2001).

Origin of Barred Olivine and Cryptocrystalline Chondrules in Hammadah al Hamra 237, Queen Alexandra Range 94411, and CH Chondrites–Chondrules in HH 237 and QUE are metal-free (Figs. 3c, 4c, and 16a–g), whereas silicate inclusions, texturally and compositionally similar to CC chondrules, are commonly observed inside chemically zoned FeNi-metal condensates (Figs. 16h,i, and 17a). Krot *et al.* (2001a) inferred that chondrules formed in the same nebular region as the zoned FeNi-metal grains, but above the metal condensation temperature (~1500 K). The complementary behavior of refractory lithophile elements (Ca, Al, Ti, REEs) in BO and CC chondrules suggests that these chondrules formed in a chemically closed system (Krot *et al.*, 2001a). Furthermore, the high Cr_2O_3 (0.4–0.7 wt%) and FeO (1–4 wt%) contents in the chondrules and complementary depletions in the FeNi-metal grains suggests formation in a closed system under relatively oxidizing conditions; complete evaporation of a nebula region with enhanced dust/gas ratio of about 10–50× solar seems required (Krot *et al.*, 2001a; Petaev *et al.*, 2001).

The absence of fine-grained rims and chondrules with porphyritic textures suggests that chondrules in HH 237 and QUE crystallized in a dust-free environment from melts completely free of nuclei (Connolly and Hewins, 1995). The absence of dust is consistent with the conclusion, derived from the PGE distributions in zoned FeNi-metal grains, that initially all solids were vaporized. This requires sustained temperatures in excess of ~1800 K (Campbell *et al.*, 2001).

Two formation scenarios for the BO and CC chondrules can be considered. Either these chondrules formed by direct gas–liquid condensation or by prolonged heating of the gas–solid condensates above their liquidus temperatures, which destroyed all solid nuclei. In both scenarios, chondrule formation must have taken place at high temperatures before metal condensation. The inferred enhanced initial dust/gas ratios favor a gas–liquid condensation scenario (Ebel and Grossman, 2000).

The observed continuous range of refractory lithophile element abundances (from ~10 × CI to <0.01 × CI) and flat element patterns (Fig. 17a,c) are explained by fractional condensation of chondrules or chondrule precursors in a closed system. The refractory lithophile elements were preferentially sequestered in the earlier formed BO chondrules and the CC chondrules formed at lower temperatures when the gas was increasingly depleted in these elements.

The depletion of chondrules in moderately volatile elements (Mn, Na, K, S, Cu, Zn, Ga) suggests that they were efficiently isolated from the hot nebula gas before condensation of these elements (Russell *et al.*, 2000a). This requires fast transport of chondrules into colder (<650 K) nebula regions, where accretion took place.

In contrast to typical chondrules with porphyritic textures, BO and CC in HH 237, QUE 94411, and CH chondrites appear to have escaped re-melting by repetitive flash-heating in a region with low ambient nebular temperatures. Such recycling would have caused melting and homogenization of the zoned FeNi-metal grains, formation of metal-bearing chondrules, porphyritic textures, relic grains, and enrichment of chondrules in moderately volatile elements, which are not observed. Based on these observations, Krot *et al.* (2001a) inferred that the BO and CC chondrules in HH 237, QUE 94411, and CH chondrites formed in a single stage process.

Origin of Metal–Sulfide Aggregates and Silicate Nodules in Bencubbin, Gujba, and Weatherford–Recent measurements of PGEs in metal–sulfide aggregates in Bencubbin, Gujba and Weatherford by Campbell *et al.* (2002) eliminate several proposed models for their origin, such as (1) oxidation of FeNi-metal with an initially chondritic abundances of PGEs (Weisberg *et al.*, 1990), (2) crystallization from impact-generated magma (Kallemeyn *et al.*, 1978), (3) metal–sulfide equilibration during partial melting, and (4) condensation from solar nebula gas (Newsom and Drake, 1979). Volatility controlled depletions in moderately volatile siderophile elements (Cu, Ga, Ge, Sn) and positive correlations between the most refractory PGEs (Os, Ir, Pt, Ru, Rh) and Ni are generally consistent with a condensation origin. However, the observed steep positive correlation between Pd and Ni (Fe and CI-normalized) implies that condensation could not have taken

place from gas of solar composition under plausible nebular conditions and requires gas with extremely high partial pressures of the siderophile elements (up to ~10^7 × CI) (Campbell *et al.*, 2002). Under these conditions, metallic alloy condenses as liquid at ~2500 K (Campbell *et al.*, 2001) and direct condensation of sulfide liquids is expected (Ebel and Grossman, 2000). Campbell *et al.* (2002) concluded that metal–sulfide aggregates and silicate nodules in Bencubbin, Gujba, and Weatherford condensed as liquids in a vapor cloud generated in a protoplanetary impact involving a metal-rich body and a reduced-silicate body.

Based on experimental studies of FeNiS-alloys (Ma *et al.*, 1998) and textural observations (*i.e.*, presence of ubiquitous rounded troilite inclusions and fine rims of high-Ni metal surrounding many of these inclusions) of metal–sulfide aggregates in Bencubbin, Gujba and Weatherford, Meibom *et al.* (2001, unpubl. data) concluded that the aggregates experienced prolonged annealing at temperatures about 700–500 K, most likely in an asteroidal setting.

Origin of Magnesian Chondrules and FeNi-Metal in CR Chondrites–The presence of igneous rims around many magnesian chondrules in CR chondrites provides important constraints on their origin. Weisberg *et al.* (1993) concluded that the cores and igneous rims of the CR chondrules were derived from the same reservoir of materials; the rim materials accreted onto solidified cores and were subsequently melted. The higher moderately volatile element (Mn, Cr, Na, K) abundances in the rims compared to the cores was explained either by lesser volatile element loss from the rims or their formation from more volatile-rich precursors (Weisberg *et al.*, 1993). The presence of abundant silica in some of the igneous rims and their higher pyroxene/olivine ratios compared to the host chondrules (Fig. 18) suggest the rims formed from a material enriched in Si compared to the host chondrules (Krot *et al.*, 2000c). Because the silica-normative rim compositions cannot be produced from a gas of solar composition, which is characterized by atomic Mg/Si ratio of ~1, the rim materials must have formed from a fractionated solar nebula gas (Mg/Si < 1). The required fractionation could be due to isolation of forsteritic olivines at high temperatures during chondrule formation in the cooling solar nebula or preferential evaporation–recondensation of Si relative to Mg during chondrule remelting. The lack of difference in Mg and Si isotope mass-dependent fractionation between core and rim olivine/pyroxene in the layered CR chondrules is consistent with isolation of olivine at high temperatures, but not with an evaporation/recondensation scenario (Huss *et al.*, 1996). It is also supported by the enrichment of mesostases in igneous rims in Na and K relative to those in the host chondrules (Fig. 19). Based on these observations, we infer that the magnesian chondrules in CR chondrites formed at high ambient nebular temperatures when condensation of the major chondrule-forming elements (Mg, Si, Na, K) was still incomplete.

Most FeNi-metal grains in CR chondrites occur as rounded, compositionally uniform nodules inside chondrules and in igneous chondrule rims suggesting solidification from chondrule melt. A negative correlation between Cr concentrations in the chondrule metal and FeO concentration in the adjacent olivine phenocrysts suggests that chondrule formation may have resulted in metal–silicate equilibration (Zanda *et al.*, 1994). However, the relatively high Ni and Co concentrations in FeNi-metal in chondrule interiors relative to metal in igneous rims and a solar Co/Ni ratio might reflect a condensation signature imprinted on the metal component of the chondrule precursor material, that has not been completely erased during chondrule formation (*e.g.*, Weisberg *et al.*, 1993; Meibom *et al.*, 2001, unpubl. data). This interpretation is consistent with volatility controlled abundances of moderately volatile elements in FeNi-metal nodules in CR chondrites (Kong *et al.*, 1999; Meibom *et al.*, 2001, unpubl. data); however, evaporation and partial recondensation of moderately siderophile elements during chondrule formation could have resulted in similar effects (Connolly *et al.*, 2001). The absence of sulfides in the igneous rims and host chondrules suggests that the metal-rich CR chondrules were isolated from the nebular gas prior to sulfur condensation.

Origin of Anorthite-Rich Chondrules: Genetic Link to Calcium-Aluminum-Rich Inclusions–Anorthite-rich chondrules is a subset of Al-rich chondrules as defined by Bischoff and Keil (1984). It was recently suggested that Al-rich chondrules formed from precursors that formed by partial evaporation of ferromagnesian chondrule precursors (MacPherson and Huss, 2000). A genetic relationship between ARCs and ferromagnesian chondrules is supported by the presence of type I chondrule-like regions in ARCs. Relatively high abundances of moderately-volatile elements such as Cr, Mn and Si in the ARCs, however, suggest that these chondrules could not have been produced by volatilization of the ferromagnesian chondrule precursors or by melting of the refractory materials only. Krot and Keil (2001) inferred instead that ARCs in CR and CH chondrites formed by melting of the reduced chondrule precursors (olivine, pyroxenes, FeNi-metal) mixed with the refractory materials, including relic CAIs, composed of anorthite, spinel, high-Ca pyroxene, and forsterite. Based on the mineralogical, chemical and textural similarities of the ARCs in several carbonaceous chondrite groups (CV, CO, CH, CR), common presence of relic CAIs and reported enrichment of ARCs in ^{16}O relative to ferromagnesian chondrules in ordinary chondrites (Russell *et al.*, 2000b), Krot *et al.* (2001d,e, 2002c) suggested that ARCs formed in the region(s) intermediate between the regions where CAIs and ferromagnesian chondrules originated.

Implications for Nebular Processes from Zoned FeNi-Metal Grains in Hammadah al Hamra 237, Queen Alexandra Range 94411, and CH Chondrites

Large-Scale Thermal Events in the Solar Nebula–The zoned FeNi-metal grains in QUE 94411, HH 237, and CH chondrites

formed by disequilibrium gas–solid condensation from a nebular gas of variable composition at a total pressure of ~10^{-4} bar in the temperature range from 1500 to 1300 K; the gas formed by complete evaporation of nebular region with enhanced dust/gas ratio (1–50 × CI) (Meibom *et al.*, 2000a,b; Petaev *et al.*, 2001). Using kinetic growth modeling, a timescale for the growth of zoned FeNi-metal grains has been estimated to be on the order of about 1–20 days (for details see Meibom *et al.*, 1999a, 2000a, 2001; Petaev *et al.*, 2001). Although the obtained growth timescales are short enough to avoid complete redistribution of Fe, Ni, Co, Cr and PGEs within the zoned grains by solid-state diffusion (Meibom *et al.*, 2001; 2001, unpubl. data; Campbell *et al.*, 2001), the effects of solid-state diffusion cannot be entirely neglected and can potentially provide improved estimates of the growth timescales and the thermal histories of the zoned metal grains (*e.g.*, Petaev *et al.*, 2001).

Combining the growth time with the inferred condensation temperature interval of the zoned FeNi-metal grains (~100 K in CH chondrites and about 30–70 K in HH 237/QUE 94411), the cooling rates for the nebular gas has been estimated to be about 0.2–2 K/h (Meibom *et al.*, 1999a, 2000a, 2001; Petaev *et al.*, 2001). These cooling rates are orders of magnitude slower than the cooling rate estimates for typical (type I and type II) porphyritic chondrules (>100 K/h) and comparable to those for type B CAIs (about 5–10 K/h) (Davis and MacPherson, 1996). In order for a region of the solar nebula to cool on a timescale comparable to the growth timescale of the zoned metal grains (days to weeks), the size of the region has to be millions of kilometers, comparable to the scale height of the nebula disk (Meibom *et al.*, 2000a; Desch, 2000). This astrophysical setting is inconsistent with localized and brief thermal events generally considered for the origin of typical porphyritic chondrules (*e.g.*, Connolly and Love, 1998).

Isolation of FeNi-Metal Condensates from Nebular Gas at High Temperatures–The zoned FeNi-metal grains in QUE 94411, HH 237, and CH chondrites are highly depleted in moderately volatile siderophile elements such as Au, As, Cu, Sb, Ga, and Ge and show no evidence of sulfurization (Campbell *et al.*, 2001; Herzog *et al.*, 2000; Meibom *et al.*, 1999a, 2001, unpubl. data; Weisberg *et al.*, 2001). This indicates that they must have been effectively isolated from the cooling nebula gas before the temperature dropped significantly below ~1200 K; as result the elements condensing at lower temperatures were not incorporated into the metal in substantial quantities (Campbell *et al.*, 2001; Herzog *et al.*, 2000). Although fast accretion into planetesimals at high ambient temperatures could have prevented condensation of moderately volatile elements (*e.g.*, Grossman *et al.*, 1988), the metastable nature of the zoned metal grains indicates fast cooling (>>1 K h^{-1}; R. Riesener, pers. comm., 2001) through the martensite transition (~1050 K), which is inconsistent with this scenario (Meibom *et al.*, 2001, unpubl. data). It was suggested that the stellar wind operating in conjunction with the large-scale convective updrafts may have played an important role in separating the newly formed, zoned metal grains at high temperature (*e.g.*, Liffman and Brown, 1996; Shu *et al.*, 1996, 1997, 2001; Meibom *et al.*, 2000a, 2001, unpubl. data; Krot *et al.*, 2001a).

Fine-Grained Matrix Material

Matrix Lumps in Hammadah al Hamra 237, Queen Alexandra Range 94411, and CH Chondrites

Mineralogy and Petrography–Fine-grained matrix material associated with CAIs, chondrules, and FeNi-metal grains is absent in QUE 94411, HH 237, and CH chondrites; instead it occurs as isolated, heavily hydrated matrix lumps (often referred to as "lithic clasts" or "dark inclusions") (Grossman *et al.*, 1988; Scott, 1988; Weisberg *et al.*, 1988; Greshake *et al.*, 2002). The matrix lumps are composed of magnetite, pyrrhotite, pentlandite, and Ca-carbonates set in a phyllosilicate matrix (Fig. 23a,b). They contain no chondrules or chondrule fragments. Magnetites occur as large spherules, clusters of tiny crystals, platelets, and as framboids.

Most phyllosilicates are poorly crystalline and occur as very small, sometimes only 1–2 layers thick, randomly orientated crystals; many areas appear to be almost totally amorphous. Ubiquitous 100–150 nm sized rounded inclusions of magnetite and sulfides are present. In several places more coarse-grained phyllosilicates occur in irregularly shaped clusters. They consist of two types of phyllosilicates: (1) blocky up to 0.3 μm wide and 1 μm long crystals with lattice spacing of 0.7 nm typical for serpentine and (2) about 0.1 to 0.2 μm wide and up to 0.4 μm long flake-like smectite grains with basal spacings of 1.1–1.2 nm. Intergrowths of typically straight parallel serpentine layers and more curved wavy smectites frequently occur at the rim of the compact serpentine crystals (Fig. 23c).

The bulk compositions of the matrix lumps are similar to the FeNi-metal-sulfide-ferrous silicate impact melts between chondrules, CAIs, and FeNi-metal grains of QUE 94411 and HH 237 (Meibom *et al.*, 2000c). Based on this similarity, it was suggested that fine-grained, porous material compositionally similar to the matrix lump was present between the FeNi metal grains and chondrules in QUE 94411 and HH 237, but was preferentially heated in a shock event and melted.

Genetic Relationship to Chondrules; Place of Hydration–The bulk compositions of the matrix lumps and ferrous silicate shock melts in CH chondrites and QUE 94411/HH 237 are not complementary to chondrules in these meteorites, suggesting no genetic relationship between these components (Meibom *et al.*, 2000c; Greshake *et al.*, 2002). This conclusion is consistent with the condensation origin of the QUE 94411/HH 237 chondrules and zoned FeNi-metal grains in the region that experienced complete evaporation (Krot *et al.*, 2001a; Petaev *et al.*, 2001).

The absence of aqueous alteration of chondrules and metal grains in the QUE 94411, HH 237, and CH chondrites indicates that the matrix lumps experienced hydration prior to

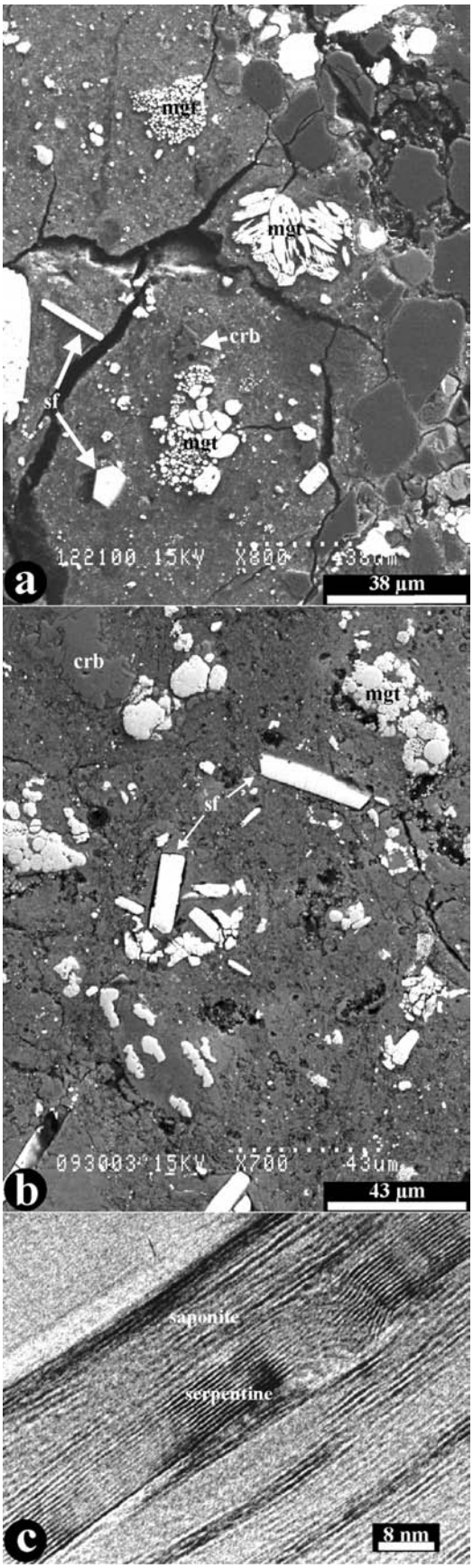

FIG. 23. *(left)* (a, b) BSE images of matrix lumps from the CH chondrite PAT 91546 (a) and CB chondrite QUE 94411 (b). The lumps consist of framboidal and platelet magnetite (mgt), prismatic sulfides (sf), and carbonates (crb) embedded in heavily hydrated material composed of serpentine and saponite. (c) High-resolution TEM image of serpentine with basal spacing of ~7 Å and saponite with basal spacing of ~11 Å in the matrix lump from QUE 94411.

incorporation into the CH and QUE 94411/HH 237 parent bodies. The matrix lumps were incorporated into the CH and QUE 94411/HH 237 parent bodies either during regolith gardening or they accreted together with chondrules and FeNi-metal grains after these high-temperature components had been transported from their hot formation region to a much colder region of the solar nebula (Greshake *et al.*, 2002; Meibom *et al.*, 2000c).

Fine-Grained Matrix Materials in CR Chondrites

Mineralogy and Petrography; Place, Time, and Conditions of Aqueous Alteration–Fine-grained matrix materials in CR chondrites occur in two textural types: (1) matrix lumps or "dark inclusions", and (2) matrix material interstitial to the chondrules and CAIs (Fredriksson *et al.*, 1981; Weisberg *et al.*, 1991, 1993; Bischoff *et al.*, 1993a). Both textural types of matrix materials are heavily hydrated and have similar mineralogy and bulk chemistry. They consist of framboidal and platelet magnetites, calcite, prismatic sulfides, and phyllosilicates (serpentine-saponite intergrowths). Calcite ranges in composition from pure $CaCO_3$ to having up to 7 wt% FeO, 3 wt% MgO and 3 wt% MnO; no dolomite was found. Isolated olivine grains, microchondrules, and micro-CAIs are present in some matrix areas and in some matrix lumps; these components experienced aqueous alteration of varying degrees (Zolensky, 1991; Zolensky *et al.*, 1992, 1996; Endreβ *et al.*, 1994). Based on the similarities in mineralogy and bulk chemistry, it was suggested that the interstitial matrix was derived from the matrix lumps (Prinz and Weisberg, 1992; Weisberg *et al.*, 1993). However, within each CR chondrite, the matrix lumps are generally more phyllosilicate-rich than the interstitial matrix, suggesting these components experienced different alteration history before accretion (Zolensky *et al.*, 1992).

Weisberg *et al.* (1994) reported carbonates in chondrules, CAIs, mineral fragments and in veins in several lithologies of the polymict chondrite breccia Kaidun and inferred that carbonates formed after the assemblage of the Kaidun breccia. Radiogenic ^{53}Cr, the decay product of ^{53}Mn with $t_{1/2} \approx 3.7$ Ma, was found in carbonates from three different carbonaceous chondrite lithologies (CM1, CI, and CR) of Kaidun (Hutcheon *et al.*, 1999). The inferred initial $^{53}Mn/^{55}Mn$ ratio is $(9.4 \pm 1.6) \times 10^{-6}$ and requires a very early onset of aqueous activity, within ~1 Ma of CAI formation (Lugmair and Shukolyukov, 1998).

There is no agreement on the temperature of aqueous alteration of CR chondrites. Based on the calcite compositions in Kaidun meteorite, the temperature of calcite precipitation was estimated to be >250 °C (Weisberg *et al.*, 1994). Based

on the presence of serpentine-saponite intergrowths and absence of tochilinite, a maximum temperature of the CR aqueous alteration was estimated to be 150 °C (Zolensky, 1991). Even lower temperature (~100 °C) of aqueous alteration was inferred from the oxygen-isotopic studies (Clayton and Mayeda, 1999).

Genetic Relationship between Chondrules and Matrix– Klerner and Palme (1999, 2000) reported that Mg/Si and Ti/Al ratios in the Renazzo chondrules and matrix appear to be complementary and concluded that both components formed from a single gaseous reservoir with a solar Mg/Si and Ti/Al ratios. Palme and Klerner (2000) suggested "that high-temperature formation of perovskite and subsequent incorporation into chondrule-forming material depleted the gas in Ti and led to low Ti/Al ratios in matrix that formed at lower temperatures from the same batch of solar gas". The observed enrichment in Si content (decrease in Mg/Si ratio) from the forsterite-rich cores to the silica-rich igneous rims around many magnesian chondrules in CR chondrites, which requires high-temperature fractionation of Mg and Si during chondrule formation (Krot *et al.*, 2000c), is in a general agreement with this model. We note however, that Renazzo experienced relatively extensive aqueous alteration (Weisberg *et al.*, 1993; Clayton and Mayeda, 1999), which could have resulted in redistribution of Si and Al between chondrules and matrix materials.

Kong *et al.* (1999) inferred that moderately volatile siderophile element (*e.g.*, Au, As, Sb, Ga) abundances (CR-normalized) in chondrules and matrices of CR chondrites are complementary to each other, with matrix being enriched in these elements. It has been concluded that this complementarity resulted from evaporation–recondensation of moderately volatile elements during chondrule formation (Kong *et al.*, 1999; Connolly *et al.*, 2001).

Presolar Grains and Nitrogen Isotope Anomaly in the CR Chondrite Clan

Newton *et al.* (1995) reported a correlation between between C and $\delta^{15}N$ in the CH chondrite Reckling Peak (RKP) 92435 and suggested that the majority of the ^{15}N-rich nitrogen is in a carbonaceous phase. Based on the observed variation of $\delta^{15}N$ to ^{14}N values at ~500 °C during the stepped combustion extraction of N, Newton *et al.* (1995) inferred the presence of Cδ nanometer-sized diamonds. Sugiura (2000) found that the ultimate source of heavy N ($\delta^{15}N$ > 1500‰) in the CH chondrite PCA 91467 are carbon–silicate aggregates of interstellar origin.

Franchi *et al.* (1986) found two N components in Bencubbin: (1) Nα, released at 900–1050 °C, and (2) Nβ, released at 600–800 °C; Nα is 10× more abundant than Nβ; all the N is enriched in ^{15}N. The heavy N is thought to be carried by presolar grains or by materials derived from presolar grains largely located in the shock melt areas (Franchi *et al.*, 1986; Keeling *et al.*, 1987). Mostefaoui *et al.* (2001) reported large ^{15}N (up to 1100‰) enrichments in silicon carbide (SiC) and fluffy type carbon grains found in acid-resistant residues of Bencubbin; $\delta^{13}C$ values vary between –160 and +60‰. Recently, Mostefaoui *et al.* (2002) reported *in situ* nitrogen isotope measurements of diamonds and graphitic carbon grains in Bencubbin. The diamonds have relatively low N concentrations (several 100 ppm) and are slightly depleted in ^{15}N with an average $\delta^{15}N$ of 87 ± 24‰. The graphitic carbon grains associated with the diamonds have similar nitrogen concentrations and isotopic compositions, whereas most of the isolated graphitic carbon grains are characterized by high N concentrations of several weight percent and $\delta^{15}N \approx 1000$‰. Mostefaoui *et al.* (2002) concluded that if diamonds in Bencubbin were formed by shock, the ^{15}N-rich component must have been added in a later event.

Sugiura *et al.* (2000) found that isotopically heavy N in QUE 94411 and HH 237 is largely located around sulfide in metal grains and in impact melt areas. The N carriers in the former appear to be taenite and/or carbide, whereas those in the latter are molten metal, tiny graphitic carbon in metal and/or oxi-nitride glass. Nitrogen in the various N carriers is isotopically equilibrated, and therefore, the carriers are not pristine presolar grains. Sugiura *et al.* (2000) suggested that (1) the ulimate source of N in QUE 94411 and HH 237 may be organic in nature and (2) the carrier of isopically heavy N ($\delta^{15}N \approx 170$‰) in CR chondrites (Ash and Pillinger, 1992) may be derived from similar interstellar organic materials in the CR parent body and/or in the solar nebula.

FINAL DISCUSSION

Major Constraints on the Solar Nebula Models from the CR Clan Chondritic Components

In this section, we summarize the major constraints on solar nebula models from the CR clan chondritic components as discussed above ("Discussion (I)" and "Discussion (II)"). Because the origin of metal–sulfide aggregates and silicate nodules in Bencubbin, Gujba, and Weatherford remains enigmatic and may be related to asteroidal processing, they are not discussed in this section.

(1) The CR, CH, and QUE 94411/HH 237 chondrites contain mineralogically and isotopically distinct populations of refractory inclusions, suggesting that there were multiple episodes of CAI formation.

(2) The observed differences in mineralogy of the CAIs from the CR, CH, and QUE 94411/HH 237 chondrites suggest that they were isolated from the nebular gas at various temperatures.

(3) The presence of isotopically uniform ^{16}O-rich and ^{16}O-poor CAIs in the CH, CR and QUE 94411/HH 237 chondrites, which are mineralogically pristine, devoid of nucleosynthetic isotope anomalies, and preserve condensation signatures (*e.g.*, group II REE patterns), indicate primary variations in O-isotopic compositions of the nebular gas in the CAI-forming region(s). The existence of ^{16}O-rich nebular gas is supported

by the discoveries of ^{16}O-rich forsterite condensates (AOAs and forsterite-rich accretionary rims around CAIs) associated with refractory inclusions in CV and CR chondrites (Hiyagon and Hashimoto, 1999; Krot *et al.*, 2002b; Aléon *et al.*, 2002).

(4) The absence of ^{26}Al in most grossite-rich and hibonite-rich CAIs in CH chondrites suggests that either these CAIs formed before injection of interstellar ^{26}Al into the solar nebula or that ^{26}Al was produced locally (in the solar nebula) by irradiation and that the CH CAI-forming region largely escaped its production.

(5) It appears that CAIs and ferromagnesian chondrules formed in isotopically and chemically distinct reservoirs, separated spatially or temporally. Most CAIs show no evidence for being present in the region(s) of ferromagnesian chondrule formation at the time of chondrule formation. In contrast, many anorthite-rich chondrules in carbonaceous chondrites contain relic spinel-anorthite ± pyroxene CAIs, possibly indicating that they formed in a region overlapping both the CAI- and chondrule-forming regions (Krot *et al.*, 2001b, 2002c).

(6) Zoned FeNi-metal grains in CHs and QUE 94411/HH 237 formed by gas–solid condensation in a solar nebula region with an initially enhanced dust/gas ratio (about 1–50 × solar) that experienced complete evaporation during large-scale thermal event. The metal-free BO and CC chondrules in these meteorites formed in the same nebular region before condensation of FeNi-metal (*i.e.*, at high ambient nebular temperatures) and escaped subsequent remelting. Both chondritic components were efficiently isolated from the cooling nebula gas before the temperature dropped below ~1200 K; as a result the elements condensing at lower temperatures were not incorporated into the metal and chondrules in substantial quantities. The metastable nature of zoned metal grains excludes fast accretion into planetesimals at high ambient temperatures as a mechanism for preventing condensation of moderately volatile elements.

(7) The metal-rich magnesian (type I) chondrules in CR chondrites could have formed at high ambient temperature, when condensation of the major chondrule-forming elements, such as Mg, Si, Na, and K, was still incomplete. FeNi-metal nodules in these chondrules experienced melting, metal–silicate reequilibration and could have been affected by evaporation and partial recondensation during chondrule formation, but they still retain the condensation signature of their initial formation. The absence of sulfides in the magnesian chondrules in CR chondrites suggests that these chondrules were isolated from the cooling nebula gas prior to S condensation. The metastable nature of Ni-rich metal nodules in these chondrules excludes fast accretion into planetesimals at high ambient temperatures as a mechanism for this isolation.

(8) Fine-grained matrix materials in CHs and QUE 94411/HH 237 are heavily hydrated and show no compositional complementarity to chondrules in these meteorites, which escaped aqueous alteration. This suggests that (1) the matrix materials were absent from the CH and QUE 94411/HH 237 chondrule-forming regions, and (2) they experienced hydration prior to incorporation into the CH and QUE 94411/HH 237 parent bodies.

(9) Aqueous alteration of the CR chondrites affected all chondritic components, probably indicating that it occurred *in situ*, at least partly. Mn-Cr dating of carbonates in the Kaidun breccia suggests a very early onset of the aqueous alteration, within ~1 Ma of CAI formation.

(10) The CR chondrules and matrices appear to be compositionally complementary (Kong *et al.*, 1999; Klerner and Palme, 2000; Palme and Klerner, 2000) possibly indicating formation from a single reservoir. However, because CR chondrites experienced relatively extensive aqueous alteration, which could have resulted in redistribution of elements between their chondrules and matrices, a genetic relationship between these components remains unclear.

Acknowledgments–The authors are grateful to I. Lyon, C. Perron, H. Palme, and J. Zipfel for detailed constructive reviews, which led to improvement of the paper. This work was supported by NASA Grants NAG5-10610 (A. N. Krot, P. I.), NAG5-1159 (K. Keil, P. I.), and NAG5-11546 (M. K. Weisberg, P. I.).

Editorial handling: I. C. Lyon

REFERENCES

ALÉON J., KROT A. N. AND MCKEEGAN K. D. (2002) Calcium-aluminum-rich inclusions and amoeboid olivine aggregates from the CR carbonaceous chondrites. *Meteorit. Planet. Sci.* **37** (in press).

ANDERS E. AND GREVASSE N. (1989) Abundances of the elements: Meteoritic and solar. *Geochim. Cosmochim. Acta* **53**, 197–214.

ASH R. D. AND PILLINGER C. T. (1992) Carbon and nitrogen isotopes in CR chondrites; evidence for a single parent body? (abstract). *Lunar Planet. Sci.* **23**, 41–42.

BISCHOFF A. AND KEIL K. (1984) Al-rich objects in ordinary chondrites: Related origin of carbonaceous and ordinary chondrites and their constituents. *Geochim. Cosmochim. Acta* **48**, 693–709.

BISCHOFF A., KEIL K. AND STÖFFLER D. (1985) Perovskite-hibonite-spinel-bearing inclusions and Al-rich chondrules and fragments in enstatite chondrites. *Chemie Erde* **44**, 97–106.

BISCHOFF A. *ET AL.* (1993a) Paired Renazzo-type (CR) carbonaceous chondrites from the Sahara. *Geochim. Cosmochim. Acta* **57**, 1587–1603.

BISCHOFF A., PALME H., SCHULTZ L., WEBER D., WEBER H. AND SPETTEL B. (1993b) Acfer 182 and paired samples, an iron-rich carbonaceous chondrite: Similarities with ALH 85085 and relationship to CR chondrites. *Geochim. Cosmochim. Acta* **57**, 2631–2648.

BREARLEY A. J. (1997) Phyllosilicates in the matrix of the unique carbonaceous chondrite, LEW 85332 and possible implications for the aqueous alteration of CI chondrites. *Meteorit. Planet. Sci.* **32**, 377–388.

BREARLEY A. J. AND LAYNE G. D. (1995) Light lithophile element (Li, Be, B) abundance in microchondrules in CH chondrites: Insights into volatile behavior during chondrule formation (abstract). *Lunar Planet. Sci.* **26**, 167–168.

CAILLET C., MACPHERSON G. J. AND ZINNER E. K. (1993) Petrologic and Al-Mg isotopic clues to the accretion of two refractory inclusions onto the Leoville parent body; one was hot, the other wasn't. *Geochim. Cosmochim. Acta* **57**, 4725–4743.

CAMPBELL A. J., HUMAYUN M., MEIBOM A., KROT A. N. AND KEIL K. (2001) Origin of zoned metal in the QUE 94411 chondrite. *Geochim. Cosmochim. Acta* **65**, 163–180.

CAMPBELL A. J., HUMAYN M. AND WEISBERG M. K. (2002) Siderophile element constraints on the formation of metal in the metal-rich chondrites Bencubbin, Weatherford, and Gujba. *Geochim. Cosmochim. Acta* **66**, 647–660.

CLAYTON R. N. (1993) Oxygen isotopes in meteorites. *Ann. Rev. Earth Planet. Sci.* **21**, 115–149.

CLAYTON R. N. AND MAYEDA T. K. (1999) Oxygen isotope studies of carbonaceous chondrites. *Geochim. Cosmochim. Acta* **63**, 2089–2104.

CLAYTON R. N., ONUMA N., GROSSMAN L. AND MAYEDA T. K. (1977) Distribution of the pre-solar component in Allende and other carbonaceous chondrites. *Earth Planet. Sci. Lett.* **34**, 209–224.

CLAYTON R. N., MAYEDA T. K., IVANOV A. V. AND MACPHERSON G. J. (1994) Oxygen isotopes in Kaidun (abstract). *Lunar Planet. Sci.* **25**, 269–270.

CONNOLLY H., JR. AND HEWINS R. (1995) Chondrules as products of dust collisions with totally molten droplets within a dust-rich nebular environment; an experimental investigation. *Geochim. Cosmochim. Acta* **59**, 3231–3246.

CONNOLLY H., JR. AND LOVE S. G. (1998) The formation of chondrules; petrologic tests of the shock wave model. *Science* **280**, 62–67.

CONNOLLY H. C., JR., HUSS G. R. AND WASSERBURG G. J. (2001) On the formation of metal in CR2 meteorites: *In situ* determination of PGE distributions and bulk chondrule compositions. *Geochim. Cosmcohim. Acta* **65**, 4528–4567.

DAVIS A. M. AND MACPHERSON G. J. (1996) Thermal processing in the solar nebula; constraints from refractory inclusions. In *Chondrules and the Protoplanetary Disk* (eds. R. H. Hewins, R. H. Jones and E. R. D. Scott), pp. 71–76. Cambridge Univ. Press, Cambridge, U.K.

DEHN G. A. AND MCCOY T. J. (1998) The formational history of the Bencubbin meteorite: A macroscopic analysis (abstract). *Lunar Planet. Sci.* **29**, #1193, Lunar and Planetary Institute, Houston, Texas, USA (CD-ROM).

DESCH S. J. (2000) Astrophysical constraints on chondrule formation models (abstract). *Lunar Planet Sci.* **31**, #1923, Lunar and Planetary Institute, Houston, Texas, USA (CD-ROM).

EBEL D. S. AND GROSSMAN L. (2000) Condensation in dust-enriched sustems. *Geochim. Cosmochim. Acta* **64**, 339–366.

ENDREß M., KEIL K., BISCHOFF A., SPETTEL B., CLAYTON R. N. AND MAYEDA T. K. (1994) Origin of dark clasts in the Acfer 059/El Djouf 001 CR2 chondrite. *Meteoritics* **29**, 26–40.

FAGAN T. J., KROT A. N. AND KEIL K. (2000) Calcium, aluminum-rich inclusions in enstatite chondrites. *Meteorit. Planet. Sci.* **35**, 771–783.

FRANCHI I. A., WRIGHT I. P. AND PILLINGER C. T. (1986) Heavy nitrogen in Bencubbin—A light-element isotopic anomaly in a stony-iron meteorite. *Nature* **323**, 138–140.

FREDRIKSSON K., MASON B., BEAUCHAMP R. AND KURAT G. (1981) Carbonates and magnetites in the Renazzo chondrite (abstract). *Meteoritics* **16**, 316.

GOSWAMI J. N. AND VANHALA H. A. T. (2000) Extinct radionuclides and the origin of the solar system. In *Protostars and Planets IV* (eds. V. Mannings, A. P. Boss and S. S. Russell), pp. 963–995. Univ. Arizona Press, Tucson, Arizona, USA.

GOUNELLE M., SHU F. H., SHANG H., GLASSGOLD A. E., REHM K. E. AND LEE T. (2001) Extinct radioactivities and protosolar cosmic-rays: Self-shielding and light elements. *Astrophys. J.* **548**, 1051–1070.

GRADY M. M. AND PILLINGER C. T. (1990) ALH 85085: Nitrogen isotope analysis of a highly unusual primitive chondrite. *Earth Planet. Sci. Lett.* **97**, 29–40.

GREENWOOD R. C., HUTCHISON R., HUSS G. R. AND HUTCHEON I. D. (1992) CAIs in CO3 meteorites; parent body or nebular alteration? (abstract). *Meteoritics* **27**, 229.

GRESHAKE A., KROT A. N., MEIBOM A., WEISBERG M. K. AND KEIL K. (2002) Heavily-hydrated matrix lumps in the CH and metal-rich chondrites QUE 94411 and Hammadah al Hamra 237. *Meteorit. Planet. Sci.* **37**, 281–293.

GROSSMAN J. N., RUBIN A. E. AND MACPHERSON G. J. (1988) ALH 85085; a unique volatile-poor carbonaceous chondrite with possible implications for nebular fractionation processes. *Earth Planet. Sci. Lett.* **91**, 33–54.

GUAN Y., HUSS G. R., MACPHERSON G. J. AND WASSERBURG G. J. (2000) Calcium-aluminum-rich inclusions from enstatite chondrites; indigenous or foreign? *Science* **289**, 1330–1333.

HERZOG G. F., FLYNN G. J., SUTTON S. R., DELANEY J. S., KROT A. N. AND MEIBOM A. (2000) Low gallium and germanium contents in metal grains from the Bencubbin/CH-like meteorite QUE 94411 determined by synchrotron XRF (abstract). *Meteorit. Planet. Sci.* **35 (Suppl.)**, A71.

HIYAGON H. AND HASHIMOTO A. (1999) ^{16}O excesses in olivine inclusions in Yamato 86009 and Murchison chondrites and their relation to CAIs. *Science* **283**, 828–831.

HUSS G. R., WEISBERG M. K. AND WASSERBURG G. J. (1996) Magnesium and silicon isotopes in layered chondrules from El Djouf (CR2) (abstract). *Lunar Planet. Sci.* **27**, 575–576.

HUTCHEON I. D., WEISBERG M. K., PHINNEY D. L., ZOLENSKY M. E., PRINZ M. AND IVANOV A. V. (1999) Radiogenic ^{53}Cr in Kaidun carbonates: Evidence for very early aqueous activity (abstract). *Lunar Planet. Sci.* **30**, #1722, Lunar and Planetary Institute, Houston, Texas, USA (CD-ROM).

HUTCHEON I. D., KROT A. N. AND ULYANOV A. A. (2000) ^{26}Al in anorthite-rich chondrules in primitive carbonaceous chondrites: Evidence chondrules post-date CAI (abstract). *Lunar Planet. Sci.* **31**, #1869, Lunar and Planetary Institute, Houston, Texas, USA (CD-ROM).

ICHIKAWA O. AND IKEDA Y. (1994) Petrology of Yamato-8449 chondrite (CR) (abstract). *Symp. Antarct. Meteorites* **19**, 18–19.

IVANOV A. V. (1989) The meteorite Kaidun: Composition and history of formation. *Geokhimiya* **2**, 259–266.

IRELAND T. R. AND FEGLEY B., JR. (2001) The solar system's earliest chemistry: Systematics of refractory inclusions. *Int. Geol. Rev.* **42**, 865–894.

IRELAND T. R., FAHEY A. J. AND ZINNER E. K. (1991) Hibonite-bearing microspherules: A new type of refractory inclusions with large isotopic anomalies. *Geochim. Cosmochim. Acta* **55**, 367–379.

KALLEMEYN G. W. AND WASSON J. T. (1981) The compositional classification of chondrites: I. The carbonaceous chondrite groups. *Geochim. Cosmochim. Acta* **45**, 1217–1230.

KALLEMEYN G. W. AND WASSON J. T. (1982) The compositional classification of chondrites: III. Ungrouped carbonaceous chondrites. *Geochim. Cosmochim. Acta* **46**, 2217–2228.

KALLEMEYN G. W. AND WASSON J. T. (1985) The compositional classification of chondrites: IV. Ungrouped chondritic meteorites and clasts. *Geochim. Cosmochim. Acta* **49**, 261–270.

KALLEMEYN G. W., BOYNTON W. V., WILLIS J. AND WASSON J. T. (1978) Formation of the Bencubbin polymict meteoritic breccia. *Geochim. Cosmochim. Acta* **42**, 507–515.

KALLEMEYN G. W., RUBIN A. E. AND WASSON J. T. (1991) The compositional classification of chondrites: V. The Karoonda (CK) group of carbonaceous chondrites. *Geochim. Cosmochim. Acta* **55**, 881–892.

KALLEMEYN G. W., RUBIN A. E. AND WASSON J. T. (1994) The compositional classification of chondrite VI: The CR carbonaceous chondrite group. *Geochim. Cosmochim. Acta* **58**, 2873–2888.

KEELING D. L., MARTI K. AND NEWSOM H. E. (1987) Nitrogen anomalies in Weatherford metal clasts (abstract). *Meteoritics* **22**, 426–427.

KELLER L. P. (1992) Petrography and mineral chemistry of calcium- and aluminum-rich inclusions in the Maralinga CK4 chondrite (abstract). *Lunar Planet. Sci.* **23**, 671–672.

KERRIDGE J. F. (1985) Carbon, hydrogen, and nitrogen in carbonaceous chondrites: Abundances and isotopic compositions in bulk samples. *Geochim. Cosmochim. Acta* **49**, 1707–1714.

KIMURA M. AND EL GORESY A. (1989) Discovery of E-chondrite assemblages, SiC, and silica-bearing objects in ALH 85085: Link between E- and C-chondrite (abstract). *Meteoritics* **24**, 286.

KIMURA M., EL GORESY A., PALME H. AND ZINNER E. (1993) Ca-, Al-rich inclusions in the unique chondrite ALH 85085: Petrology, chemistry, and isotopic compositions. *Geochim. Cosmochim. Acta* **57**, 2329–2359.

KLERNER S. AND PALME H. (1999) Origin of chondrules and matrix in the Renazzo meteorite (abstract). *Meteorit. Planet. Sci.* **34 (Suppl.)**, A64–A65.

KLERNER S. AND PALME H. (2000) Large titanium/aluminum fractionation between chondrules and matrix in Renazzo and other carbonaceous chondrites (abstract). *Meteorit. Planet. Sci.* **35 (Suppl.)**, A89.

KONG P., EBIHARA M. AND PALME H. (1999) Siderophile elements in martian meteorites and implications for core formation in Mars. *Geochim. Cosmochim. Acta* **63**, 1865–1875.

KROT A. N. (2000) Anorthite-rich chondrules from primitive carbonaceous chondrites: Genetic links between CAI and chondrules (abstract). *Meteorit. Planet. Sci.* **35 (Suppl.)**, A93.

KROT A. N. AND KEIL K. (2001) Anorthite-rich chondrules in CR and CH carbonaceous chondrites: Genetic link between Ca, Al-rich inclusions and ferromagnesian chondrules. *Meteorit. Planet. Sci.* **37**, 91–111.

KROT A. N., SAHIJPAL S., MCKEEGAN K. D., WEBER D., ULYANOV A. A., PETAEV M. I., MEIBOM A. AND KEIL K. (1999a) Unique mineralogy and isotopic signatures of calcium-aluminum-rich inclusions from the CH chondrite Acfer 182 (abstract). *Meteorit. Planet. Sci.* **34 (Suppl.)**, A69.

KROT A. N., ULYANOV A. A. AND WEBER D. (1999b) Al-diopside-rich refractory inclusions in the CH chondrite Acfer 182 (abstract). *Lunar Planet. Sci.* **30**, #2018, Lunar and Planetary Institute, Houston, Texas, USA (CD-ROM).

KROT A. N., WEBER D., GRESHAKE A., ULYANOV A. A., MCKEEGAN K. D., HUTCHEON I. D., SAHIJPAL S. AND KEIL K. (1999c) Relic Ca,Al-rich inclusions in chondrules from the carbonaceous chondrites Acfer 182 and Acfer 094 (abstract). *Lunar Planet. Sci.* **30**, #1511, Lunar and Planetary Institute, Houston, Texas, USA (CD-ROM).

KROT A. N., SAHIJPAL S., MCKEEGAN K. D., WEBER D., GRESHAKE A., ULYANOV A. A., HUTCHEON I. D. AND KEIL K. (1999d) Mineralogy, aluminum-magnesium and oxygen isotope studies of the relic calcium-aluminum-rich inclusions in chondrules (abstract). *Meteorit. Planet. Sci.* **34 (Suppl.)**, A68–A69.

KROT A. N., MEIBOM A., PETAEV M. I., KEIL K., ZOLENSKY M. E., SAITO A., MUKAI M. AND OHSUMI K. (2000a) Ferrous silicate spherules with euhedral Fe,Ni-metal grains from CH carbonaceous chondrites: Evidence for supercooling and condensation under oxidizing conditions. *Meteorit. Planet. Sci.* **35**, 1249–1259.

KROT A. N., MEIBOM A. AND KEIL K. (2000b) Volatile-poor chondrules in CH carbonaceous chondrites: Formation at high ambient nebular temperature (abstract). *Lunar Planet. Sci.* **31**, #1481, Lunar and Planetary Institute, Houston, Texas, USA (CD-ROM).

KROT A. N., WEISBERG M. K., PETAEV M. I., KEIL K. AND SCOTT E. R. D. (2000c) High-temperature condensation signatures in type I chondrules from CR carbonaceous chondrites (abstract). *Lunar Planet. Sci.* **31**, #1470, Lunar and Planetary Institute, Houston, Texas, USA (CD-ROM).

KROT A. N., MEIBOM A., RUSSELL S. S., ALEXANDER C. M. O'D., JEFFRIES T. E. AND KEIL K. (2001a) A new astrophysical setting for chondrule formation. *Science* **291**, 1776–1779.

KROT A. N., MCKEEGAN K. D., RUSSELL S. S., MEIBOM A., WEISBERG M. K., ZIPFEL J., KROT T. V., FAGAN T. J. AND KEIL K. (2001b) Refractory Ca, Al-rich inclusions and Al-diopside-rich chondrules in the metal-rich chondrites Hammadah al Hamra 237 and QUE 94411. *Meteorit. Planet. Sci.* **36**, 1189–1217.

KROT A. N., MCKEEGAN K. D., RUSSELL S. S., MEIBOM A., WEISBERG M. K., ZIPFEL J. AND KEIL K. (2001c) ^{16}O-poor refractory inclusions in CB chondrites (abstract). *Lunar Planet. Sci.* **32**, #1229, Lunar and Planetary Institute, Houston, Texas, USA (CD-ROM).

KROT A. N., PETAEV M. I., KEIL K. AND RUSSELL S. S. (2001d) Anorthite-rich chondrules in carbonaceous chondrites: Significance for understanding the astrophysical setting of CAI and chondrule formation (abstract). *Meteorit. Planet. Sci.* **36 (Suppl.)**, A107.

KROT A. N., HUTCHEON I. D. AND HUSS G. R. (2001e) Aluminum-rich chondrules and associated refractory inclusions in the unique carbonaceous chondrite Adelaide (abstract). *Meteorit. Planet. Sci.* **36 (Suppl.)**, A105–A107.

KROT A. N., ALEON J. AND MCKEEGAN K. D. (2002a) Mineralogy, petrography and oxygen-isotopic compositions of Ca, Al-rich inclusions and amoeboid olivine aggregates in the CR carbonaceous chondrites (abstract). *Lunar Planet. Sci.* **33**, #1412, Lunar and Planetary Institute, Houston, Texas, USA (CD-ROM).

KROT A. N., MCKEEGAN K. D., LESHIN L. A., MACPHERSON G. J. AND SCOTT E. R. D. (2002b) Existence of an ^{16}O-rich gaseous reservoir in the solar nebula. *Science* **295**, 1051–1054.

KROT A. N., HUTCHEON I. D. AND KEIL K. (2002c) Anorthite-rich chondrules in the reduced CV chondrites: Evidence for complex formation history and genetic links between CAIs and ferromagnesian chondrules. *Meteorit. Planet. Sci.* **37**, 155–182.

LEE M-S., RUBIN A. E. AND WASSON J. T. (1992) Origin of metallic Fe-Ni in Renazzo and related meteorites. *Geochim. Cosmochim. Acta* **56**, 2521–2533.

LIFFMAN K. AND BROWN M. J. I. (1996) The protostellar jet model of chondrule formation. In *Chondrules and the Protoplanetary Disk* (eds. R. H. Hewins, R. H. Jones and E. R. D. Scott), pp. 285–302. Cambridge Univ. Press, Cambridge, U.K.

LOVERING J. F. (1962) The evolution of the meteorites—Evidence for the co-existence of chondritic, achondritic and iron meteorites in a typical parent meteorite body. In *Researches on Meteorites* (ed. C. B. Moore), pp. 179–197. Wiley, New York, New York, USA.

LUGMAIR G. W. AND SHUKOLYUKOV A. (1998) Early solar system timescales according to ^{53}Mn-^{53}Cr systematics. *Geochim. Cosmochim. Acta* **62**, 2863–2886.

MA L., WILLIAMS D. B. AND GOLDSTEIN J. I. (1998) Determination of the Fe-rich portion of the Fe-Ni-S phase diagram. *J. Phase Equil.* **19**, 299–309.

MACPHERSON G. AND DAVIS A. M. (1993) A petrologic and ion microprobe study of a Vigarano type B refractory inclusion; evolution by multiple stages of alteration and melting. *Geochim. Cosmochim. Acta* **57**, 231–243.

MACPHERSON G. J. AND DELANEY J. S. (1985) A fassaite-two olivine-pleonaste-bearing refractory inclusion from Karoonda (abstract). *Lunar Planet. Sci.* **16**, 515–516.

MACPHERSON G. J. AND HUSS G. R. (2000) Convergent evolution of CAIs and chondrules: Evidence from bulk compositions and a cosmochemical phase diagram (abstract). *Lunar Planet. Sci.* **31**, #1796, Lunar and Planetary Institute, Houston, Texas, USA (CD-ROM).

MACPHERSON G. J., BAR-MATTHEWS M., TANAKA T., OLSEN E. AND GROSSMAN L. (1983) Refractory inclusions in the Murchison meteorite. *Geochim. Cosmochim. Acta* **47**, 823–840.

MACPHERSON G. J., GROSSMAN L., HASHIMOTO A., BAR-MATTHEWS M. AND TANAKA T. (1984) Petrographic studies of refractory inclusions from the Murchison meteorite. *J. Geophys. Res.* **89**, C299–C312.

MACPHERSON G. J., WARK D. A. AND ARMSTRONG J. T. (1988) Primitive material surviving in chondrites: Refractory inclusions. In *Meteorites and the Early Solar System* (eds. J. F. Kerridge and M. S. Matthews), pp. 746–807. Univ. Arizona Press, Tucson, Arizona, USA.

MACPHERSON G. J., DAVIS A. M. AND GROSSMAN J. N. (1989) Refractory inclusions in the unique chondrite ALH 85085 (abstract). *Meteoritics* **24**, 297.

MARHAS K. K., HUTCHEON I. D., KROT A. N. AND GOSWAMI J. N. (2000) ^{26}Al in carbonaceous chondrite chondrules (abstract). *Meteorit. Planet. Sci.* **35 (Suppl.)**, A102.

MARHAS K. K., KROT A. N. AND GOSWAMI J. N. (2001) Al-Mg isotopic systematics in CAIs from CR chondrites (abstract). *Meteorit. Planet. Sci.* **36 (Suppl.)**, A121–A122.

MASON B. AND NELEN J. (1968) The Weatherford meteorite. *Geochim. Cosmochim. Acta* **32**, 661–664.

MASON B. AND WIIK H. B. (1962) The Renazzo meteorite. *Am. Museum Novitates* **2106**, 11.

MCCALL G. J. H. (1968) The Bencubbin meteorite: Further details, including microscopic character of the host material and two chondrite enclaves. *Mineral. Mag.* **36**, 726–739.

MCKEEGAN K. D., LESHIN L. A., RUSSELL S. S. AND MACPHERSON G. J. (1996) *In situ* measurement of O isotopic anomalies in a type B Allende CAI (abstract). *Meteorit. Planet. Sci.* **31 (Suppl.)**, A86–A87.

MCKEEGAN K. D., LESHIN L. A., RUSSELL S. S. AND MACPHERSON G. J. (1998) Oxygen isotopic abundances in calcium-aluminum-rich inclusions from ordinary chondrites: Implications for nebular heterogeneity. *Science* **280**, 414–418.

MCKEEGAN K. D., SAHIJPAL S., KROT A. N., WEBER D. AND ULYANOV A. A. (2002) Preservation of primary oxygen-isotopic compositions in Ca,Al-rich inclusions from CH chondrites. *Earth Planet. Sci. Lett.* (submitted).

MCSWEEN H. Y., JR. (1977) Petrographic variations among carbonaceous chondrites of the Vigarano type. *Geochim. Cosmochim. Acta* **41**, 1777–1790.

MEIBOM A., PETAEV M. I., KROT A. N., WOOD J. A. AND KEIL K. (1999a) Primitive FeNi metal grains in CH carbonaceous chondrites formed by condensation from a gas of solar composition. *J. Geophys. Res.* **104**, 22 053–22 059.

MEIBOM A. *ET AL.* (1999b) Metal condensates in CH and Bencubbin-like chondrites: Evidence for localized nebula heating events and variations in gas composition (abstract). *Meteorit. Planet. Sci.* **34 (Suppl.)**, A80.

MEIBOM A., DESCH S. J., KROT A. N., CUZZI J. N., PETAEV M. I., WILSON L. AND KEIL K. (2000a) Large-scale thermal events in the solar nebula: Evidence from FeNi metal grains in primitive meteorites. *Science* **288**, 839–841.

MEIBOM A., DESCH S. J., PETAEV M. I., KROT A. N., CUZZI J. N., WOOD J. A. AND KEIL K. (2000b) An astrophysical model for the formation of zoned Fe,Ni-metal grains in the Bencubbin/CH-like chondrites QUE 94411 and Hammadah al Hamra 237 (abstract). *Meteorit. Planet. Sci.* **35 (Suppl.)**, A107.

MEIBOM A., KROT A. N., KEIL K., RIGHTER K. AND CHABOT N. (2000c) FeNi-metal/sulfide—Ferrous silicate shock melts in QUE 94411 and Hammadah al Hamra 237: Remains of the missing matrix? (abstract). *Lunar Planet. Sci.* **31**, #1420, Lunar and Planetary Institute, Houston, Texas, USA (CD-ROM).

MEIBOM A., PETAEV M. I., KROT A. N., KEIL K. AND WOOD J. A. (2001) Growth mechanism and additional constraints on FeNi-metal condensation in the solar nebula. *J. Geophys. Res.* **106**, 32 797–32 801.

MOSTEFAOUI S., EL GORESY A., HOPPE P., GILLET P. AND OTT U. (2001) *In situ* discovery of diamond in Bencubbin: Evidence from Raman spectroscopy and cathodoluminescence (abstract). *Meteorit. Planet. Sci.* **36 (Suppl.)**, A141–A142.

MOSTEFAOUI S., EL GORESY A., HOPPE P., GILLET P. AND OTT U. (2002) Nitrogen-isotopic compositions of *in situ* diamonds and graphitic carbon grains in the Bencubbin meteorite: A nanoSIMS study (abstract). *Lunar Planet. Sci.* **33**, #1487, Lunar and Planetary Institute, Houston, Texas, USA (CD-ROM).

NEWSOM H. E. AND DRAKE M. J. (1979) The origin of metal clasts in the Bencubbin meteoritic breccia. *Geochim. Cosmochim. Acta* **43**, 689–707.

NEWTON J., GRADY M. M. AND PILLINGER C. T. (1995) A new member of the "CH" chondrite group of meteorites: Nitrogen and carbon stable isotope geochemistry of RKP 92435 (abstract). *Lunar Planet. Sci.* **26**, 1045–1046.

NOGUCHI T. (1993) Petrology and mineralogy of CK chondrites; implications for the metamorphism of the CK chondrite parent body. *Proc. NIPR Symp. Antarct. Meteorites* **6**, 204–233.

NOGUCHI T. (1994) Petrology and mineralogy of the PCA 91082 chondrite and its comparison with the Yamato-793495 (CR) chondrite. *Proc. NIPR Symp. Antarct. Meteorites* **8**, 33–62.

PALME H. AND KLERNER S. (2000) Formation of chondrules and matrix in carbonaceous chondrites (abstract). *Meteorit. Planet. Sci.* **35 (Suppl.)**, A124.

PETAEV M. I. AND KROT A. N. (1999) Condensation of CH chondrite materials: Inferences from the CWPI model (abstract). *Lunar Planet. Sci.* **30**, #1775, Lunar and Planetary Institute, Houston, Texas, USA (CD-ROM).

PETAEV M. I. AND WOOD J. A. (2001) Chromium condensation in the solar nebula: Insights from the upgraded CWPI code (abstract). *Lunar Planet. Sci.* **32**, #1424, Lunar and Planetary Institute, Houston, Texas, USA (CD-ROM).

PETAEV M. I., MEIBOM A., KROT A. N. AND WOOD J. A. (1999) The condensation origin of some metal in CH chondrites: A thermodynamic model (abstract). *Lunar Planet. Sci.* **30**, #1613, Lunar and Planetary Institute, Houston, Texas, USA (CD-ROM).

PETAEV M. I., MEIBOM A., KROT A. N., WOOD J. A. AND KEIL K. (2000) The condensation origin of zoned metal grains in QUE 94411: Implications for the formation of Bencubbin/CH-like chondrites (abstract). *Lunar Planet. Sci.* **31**, #1606, Lunar and Planetary Institute, Houston, Texas, USA (CD-ROM).

PETAEV M. I., MEIBOM A., KROT A. N., WOOD J. A. AND KEIL K. (2001) The condensation origin of zoned grains in QUE 94411: Implications for the formation of the Bencubbin-like chondrites. *Meteorit. Planet. Sci.* **36 (Suppl.)**, 93–107.

PODOSEK F. A., ZINNER E. K., MACPHERSON G. J., LUNDBERG L. L., BRANNON J. C. AND FAHEY A. J. (1991) Correlated study of initial ^{87}Sr/^{86}Sr and Al-Mg isotopic systematics and petrologic properties in a suite of refractory inclusions from the Allende meteorite. *Geochim. Cosmochim. Acta* **55**, 1083–1110.

PRINZ M. AND WEISBERG M. K. (1992) Acfer 182/207: A new ALH 85085-type chondrite and its implications (abstract). *Lunar Planet. Sci.* **23**, 1109–1110.

PRINZ M., WEISBERG M. K., NEHRU C. E. AND DELANEY J. S. (1985a) Layered chondrules; evidence for multistage histories during chondrule formation (abstract). *Meteoritics* **20**, 732–733.

PRINZ M., WEISBERG M. K., NEHRU C. E. AND DELANEY J. S. (1985b) Chondrules of the Renazzo and Al Rais carbonaceous chondrites: Layering and accretionary growth as part of the chondrule-forming process (abstract). *Lunar Planet. Sci.* **16**, 677–678.

PRINZ M., WEISBERG M. K., BREARLEY A. J., GRADY M. M., PILLINGER C. T. AND CLAYTON R. N. (1992) LEW 85332; a C2 chondrite in the CR clan (abstract). *Meteoritics* **27**, 278–279.

PRINZ M., WEISBERG M. K., CLAYTON R. N. AND MAYEDA T. K. (1993a) Ordinary and Carlisle Lakes-like clasts in the Weatherford chondrite breccia (abstract). *Meteoritics* **28**, 419–420.

PRINZ M., WEISBERG M. K., CLAYTON R. N. AND MAYEDA T. K. (1993b) Oxygen isotopic relationships between the LEW 85332 carbonaceous chondrite and CR chondrites (abstract). *Lunar Planet. Sci.* **24**, 1185–1186.

PRINZ M., WEISBERG M. K., CLAYTON R. N. AND MAYEDA T. K. (1994) Petrologic and oxygen isotopic study of ALH 85085-like chondrites (abstract). *Meteoritics* **29**, 519–520.

RAMDOHR P. (1973) *The Opaque Minerals in Stony Meteorites*. Elsevier, Amsterdam, The Netherlands. 245 pp.

RIGHTER K. AND CHABOT N. L. (1998) Silicate and metal phases in the Queen Alexandra Range 94411 iron meteorite (abstract). *Meteorit. Planet. Sci.* **33 (Suppl.)**, A129.

RUBIN A. E. AND KALLEMEYN G. W. (1990) Lewis Cliff 85332; a unique carbonaceous chondrite. *Meteoritics* **25**, 215–225.

RUBIN A. E., KALLEMEYN G. W., WASSON J. T., CLAYTON R. N., MAYEDA T. K., GRADY M. M. AND VERCHOVKY A. B. (2001) Cujba: A new Bencubbin-like meteorite fall from Nigeria (abstract). *Lunar Planet. Sci.* **32**, #1779, Lunar and Planetary Institute, Houston, Texas, USA (CD-ROM).

RUSSELL S. S., HUSS G. R., FAHEY A. J., GREENWOOD R. C., HUTCHISON R. AND WASSERBURG G. J. (1998) An isotopic and petrologic study of calcium-aluminum-rich inclusions from CO3 meteorites. *Geochim. Cosmochim. Acta* **62**, 689–714.

RUSSELL S. S., KROT A. N., MEIBOM A., ALEXANDER C. M. O'D. AND JEFFRIES T. E. (2000a) Chondrules of the first generation? Trace element geochemistry of silicate from Bencubbin/CH-like meteorites (abstract). *Meteorit. Planet. Sci.* **35 (Suppl.)**, A139.

RUSSELL S. S., MACPHERSON G. J., LESHIN L. A. AND MCKEEGAN K. D. (2000b) ^{16}O enrichments in aluminum-rich chondrules from ordinary chondrites. *Earth Planet. Sci. Lett.* **184**, 57–74.

SAHIJPAL S. AND GOSWAMI J. N. (1998) Refractory phases in primitive meteorites devoid of ^{26}Al and ^{41}Ca: Representative samples of first solar system solids? *Astrophys. J.* **539**, L137–L140.

SAHIJPAL S., GOSWAMI J. N., DAVIS A. M., GROSSMAN L. AND LEWIS R. S. (1998) A stellar origin for the short-lived nuclides in the early solar system. *Nature* **391**, 559–561.

SAHIJPAL S., MCKEEGAN K. D., KROT A. N., WEBER D. AND ULYANOV A. A. (1999) Oxygen isotopic compositions of calcium-aluminum-rich inclusions from the CH chondrites, Acfer 182 and PAT 91546 (abstract). *Meteorit. Planet. Sci.* **34 (Suppl.)**, A101.

SCOTT E. R. D. (1988) A new kind of primitive chondrite, Allan Hills 85085. *Earth Planet. Sci. Lett.* **91**, 1–18.

SCOTT E. R. D. AND KROT A. N. (2001) Oxygen isotopic compositions and origins of Ca-Al-rich inclusions and chondrules. *Meteorit. Planet. Sci.* **36**, 1307–1319.

SHU F. H., SHANG H. AND LEE T. (1996) Toward an astrophysical theory of chondrites. *Science* **271**, 1545–1552.

SHU F. H., SHANG H., GLASSGOLD A. E. AND LEE T. (1997) X-rays and fluctuating x-winds from protostars. *Science* **277**, 1475–1479.

SHU F. H., SHANG H., GOUNELLE M., GLASSGOLD A. E. AND LEE T. (2001) The origin of chondrules and refractory inclusions in chondritic meteorites. *Astrophys. J.* **548**, 1029–1070.

SIMON S. B., YONEDA S., GROSSMAN L. AND DAVIS A. M. (1994) A $CaAl_4O_7$-bearing refractory spherule from Murchison; evidence for very high-temperature melting in the solar nebula. *Geochim. Cosmochim. Acta* **58**, 1937–1949.

SIMPSON E. S. AND MURRAY D. G. (1932) A new siderolite from Bencubbin, Western Australia. *Mineral. Mag.* **23**, 33–37.

SUGIURA N. (2000) Petrographic evidence for *in situ* hydration of the CH chondrite PCA 91467 (abstract). *Lunar Planet. Sci.* **31**, #1503, Lunar and Planetary Institute, Houston, Texas, USA (CD-ROM).

SUGIURA N., ZASHU S., WEISBERG M. K. AND PRINZ M. (2000) A nitrogen isotope study of Bencubbinites. *Meteorit. Planet. Sci.* **35**, 987–996.

WASSON J. T. (1985) *Meteorites: Their Record of Early Solar-System History*. W. H. Freeman and Co., New York, New York, USA. 267 pp.

WASSON J. T. AND KALLEMEYN G. W. (1990) Allan Hills 85085: A subchondritic meteorite of mixed nebular and regolithic heritage. *Earth Planet. Sci. Lett.* **101**, 148–161.

WEBER D. (1996) Petrography of refractory inclusions from the CR chondrite Acfer 059–El Djouf 001 and relationship to other inclusion populations (abstract). *Meteorit. Planet. Sci.* **31 (Suppl.)**, A147–A148.

WEBER D. AND BISCHOFF A. (1994) The occurrence of grossite ($CaAl_4O_7$) in chondrites. *Geochim. Cosmochim. Acta* **18**, 3855–3877.

WEBER D. AND BISCHOFF A. (1997) Refractory inclusions in the CR chondrite Acfer 059–El Djouf 001: Petrology, chemical composition, and relationship to inclusion populations in other types of carbonaceous chondrites. *Chem. Erde* **57**, 1–24.

WEBER D., ZINNER E. AND BISCHOFF A. (1995a) Trace element abundances and magnesium, calcium, and titanium isotopic compositions of grossite-containing inclusions from the carbonaceous chondrite Acfer 182. *Geochim. Cosmochim. Acta* **59**, 803–823.

WEBER D., SCHIRMEYER S. AND BISCHOFF A. (1995b) Refractory inclusions from the CH-chondrite PCA 91467: Similarities with and relationship to inclusions from ALH 85085 and Acfer 182 (abstract). *Lunar Planet. Sci.* **26**, 1475–1476.

WEISBERG M. K. AND PRINZ M. (1990) Refractory inclusions in CR2 (Renazzo-type) chondrites (abstract). *Lunar Planet. Sci.* **21**, 1315–1316.

WEISBERG M. K. AND PRINZ M. (1991) Aqueous alteration in CR2 chondrites (abstract). *Lunar Planet. Sci.* **22**, 1483–1484.

WEISBERG M. K. AND PRINZ M. (1999) Zoned metal in the CR clan chondrites (abstract). *Symp. Antarct. Meteorites* **24**, 187–189.

WEISBERG M. K. AND PRINZ M. (2000) The Grosvenor Mountains 95577 CR1 chondrite and hydration of the CR chondrites (abstract). *Meteorit. Planet. Sci.* **35 (Suppl.)**, A168.

WEISBERG M. K., PRINZ M. AND NEHRU C. E. (1987) Barred olivine-textured Bencubbin major silicates; a ureilite connection? (abstract). *Meteoritics* **22**, 526–527.

WEISBERG M. K., PRINZ M. AND NEHRU C. E. (1988) Petrology of ALH 85085: A chondrite with unique characteristics. *Earth Planet. Sci. Lett.* **91**, 19–32.

WEISBERG M. K., PRINZ M. AND NEHRU C. E. (1990) The Bencubbin chondrite breccia and its relationship to CR chondrites and the ALH 85085 chondrite. *Meteoritics* **25**, 269–279.

WEISBERG M. K., PRINZ M., CHATTERJEE N., CLAYTON R. N. AND MAYEDA T. K. (1991) Dark inclusions in CR2 chondrites (abstract). *Meteoritics* **26**, 407.

WEISBERG M. K., PRINZ M., CLAYTON R. N. AND MAYEDA T. K. (1992) Formation of layered chondrules in CR2 chondrites: A petrologic and oxygen isotopis study (abstract). *Meteoritics* **27**, 306.

WEISBERG M. K., PRINZ M., CLAYTON R. N. AND MAYEDA T. K. (1993) The CR (Renazzo-type) carbonaceous chondrite group and its implications. *Geochim. Cosmochim. Acta* **57**, 1567–1586.

WEISBERG M. K., PRINZ M. AND ZOLENSKY M. E. (1994) Carbonates in the Kaidun chondrite (abstract). *Meteoritics* **29**, 549–550.

WEISBERG M. K., PRINZ M., CLAYTON R. N., MAYEDA T. K., GRADY M. M. AND PILLINGER C. T. (1995) The CR chondrite clan. *Proc. NIPR Symp. Antarct. Meteorites* **8**, 11–32.

WEISBERG M. K., PRINZ M., CLAYTON R. N., MAYEDA T. K., SUGIURA N., ZASHU S. AND EBIHARA M. (2001) A new metal-rich chondrite grouplet. *Meteorit. Planet. Sci.* **36**, 401–418.

WEISBERG M. K., BOESENBERG J. S. AND EBEL D. S. (2002) Gujba and origin of the Bencubbin-like (CB) chondrites (abstract). *Lunar Planet. Sci.* **33**, #1551, Lunar and Planetary Institute, Houston, Texas, USA (CD-ROM).

WOOD J. A. (1962) Chondrules and the origin of the terrestrial planets. *Nature* **194**, 127–130.

YOUNG E. D. AND RUSSELL S. S. (1998) Oxygen reservoirs in the early solar nebula inferred from an Allende CAI. *Science* **282**, 452–455.

YURIMOTO H., ITO M. AND NAGASAWA H. (1998) Oxygen isotope exchange between refractory inclusion in Allende and solar nebula gas. *Science* **282**, 1874–1877.

ZANDA B., BOUROT-DENISE M., PERRON C. AND HEWINS R. (1994) Origin and metamorphic redistribution of silicon, chromium, and phosphorous in the metal of chondrites. *Science* **265**, 1846–1849.

ZIPFEL J., WLOTZKA F. AND SPETTEL B. (1998) Bulk chemistry and mineralogy of a new "unique" metal-rich chondritic breccia, Hammadah al Hamra 237 (abstract). *Lunar Planet. Sci.* **29**, #1417, Lunar and Planetary Institute, Houston, Texas, USA (CD-ROM).

ZOLENSKY M. E. (1991) Mineralogy and matrix composition of "CR" chondrites Renazzo and EET 87770, and ungrouped chondrites Essebi and MAC 87300 (abstract). *Meteoritics* **26**, 414.

ZOLENSKY M. E., WEISBERG M. K., BUCHANAN P. C., PRINZ M., REID A. AND BARRETT R. A. (1992) Mineralogy of dark clasts in CR chondrites, eucrites and howardites (abstract). *Lunar Planet. Sci.* **23**, 1587–1588.

ZOLENSKY M. E., HYMAN M., ROWE M. W. AND WEISBERG M. K. (1996) The origin of round phyllosilicate aggregates in CR2 and CI1 chondrites (abstract). *Lunar Planet. Sci.* **27**, 1505–1506.